SCHEDULING CHARGING FOR FLEETS OF BATTERY ELECTRIC VEHICLES: TECHNIQUES FOR MODELING AND REAL-TIME OPERATION

by

Justin J. Whitaker

A dissertation submitted in partial fulfillment
of the requirements for the degree

of

DOCTOR OF PHILOSOPHY

in

Electrical Engineering

Approved:

Greg Droge, Ph.D. Major Professor	Jake Gunther, Ph.D. Committee Member
Donald Cripps, Ph.D. Committee Member	Hongjie Wang, Ph.D. Committee Member
Mario Harper, Ph.D. Committee Member	D. Richard Cutler, Ph.D. Vice Provost of Graduate Studies

UTAH STATE UNIVERSITY
Logan, Utah

2024

ABSTRACT

Scheduling Charging for Fleets of Battery Electric Vehicles: Techniques for Modeling and Real-time Operation

by

Justin J. Whitaker, Doctor of Philosophy

Utah State University, 2024

Major Professor: Greg Droge, Ph.D.
Department: Electrical and Computer Engineering

Battery-electric vehicles are becoming increasingly popular in both consumer and business usage. These vehicles differ from traditional internal combustion engine vehicles in many ways, with some significant differences being lower capacity energy storage and longer refueling times. Within the context of vehicle fleets, such as public transport buses or delivery vehicles, these differences necessitate more careful planning of routes and charging than is required for traditional vehicles to ensure continued operation. Additionally, the refueling costs for electric vehicles are typically significantly more complex than for traditional vehicles, with costs varying based on the time of day, the amount of energy consumed, and the power drawn from the grid. This complexity in cost structure also requires sophisticated planning to minimize costs in addition to ensuring feasible operation. The objective of this research is to explore methods to schedule the charging for a fleet of electric vehicles to ensure that the vehicles can complete their routes while minimizing the cost of charging.

This objective is achieved by developing optimization models that account for the complex costs and constraints of electric vehicle charging for two types of fleet vehicles. Some vehicles in fleets will have a fixed or known schedule, such as public transport buses, while others will have more flexible schedules where assignments and/or timing of routes

are to be determined as part of the optimization, such as delivery vehicles. A network-flow-based method is formulated for the fixed-schedule vehicles that accounts for the time-varying costs of charging and uses a high-fidelity, non-linear charging profile to model the charging process. The modelling techniques to account for the costs and the non-linear charging profile are then applied to a bin-packing-based model that allows scheduling and assigning routes in addition to scheduling charging. Finally, a receding-horizon control technique is presented for adjusting these models to account for the uncertainties in real-time operation, arising from factors such as traffic congestion, weather, and battery degradation.

(72 pages)

PUBLIC ABSTRACT

Scheduling Charging for Fleets of Battery Electric Vehicles: Techniques for Modeling and Real-time Operation

Justin J. Whitaker

While electric vehicles (EVs) are becoming increasingly popular and can provide cost, maintenance, and environmental benefits, they present unique challenges for regular operation, especially in fleets of vehicles. The limited range, long charging times, and high power requirements of EVs complicate the operations of fleets comprised of EVs. Additionally, the charging costs of EVs can be complex, depending on the time of charging, the energy charged, and the power level of the charging session. These complex charging costs can be significantly affected by the presence of uncontrolled loads. These challenges are further complicated by the inevitable variations in the real world, caused by conditions such as traffic congestion, weather, and equipment malfunctions.

Accordingly, the scheduling of EV charging in fleets is a complex, but necessary, problem to address. This research develops methods to schedule the charging of fleets of EVs that are cost-effective, robust, and scalable. Exact, but computationally expensive, approaches are developed to schedule when and how much each vehicle should charge to minimize the cost of charging while maintaining the operational constraints of the fleet. A technique for adjusting the schedules based on up-to-date arrival time, battery level, and other feedback is demonstrated. These developments are significant steps towards addressing the challenges of scheduling the charging of EVs in fleets and enabling the further adoption of EVs in vehicle fleets.

For my wife, Macy, and my children, Kai and Chloe, whom I love with my whole soul.

ACKNOWLEDGMENTS

In considering all those without whom this research would not be what it is, I must first thank my advisor, Dr. Greg Droge for not only shaping this research and what I have achieved, but for shaping me into the student, researcher, academic, and professional that I am today. I must also thank my committee members for their time and effort in reviewing my work, providing valuable feedback, imparting a fraction of their extensive knowledge, and ensuring that I become the best I could be.

Even more so, however, I must thank my family for their unwavering support, encouragement, and love throughout my academic career. I want to thank my parents for teaching me dedication and perseverance, for supporting me through my academic endeavors, and for helping me see my potential throughout my life. I thank my son Kai for his patience with a father that sometimes had to "do work downstairs on the computer" instead of racing cars or building with LEGOs. I thank my daughter Chloe for coming to meet me at the door when I got home every day since she could crawl. Both Kai and Chloe have provided light and joy to me through this journey and have provided me with motivation to keep going through difficult times.

Most of all, I must thank my wife, Macy, who has been my partner in this endeavor every step of the way. It is no exaggeration to say that she deserves the recognition for the work I have done as much as I do. She has loved me through the late nights of homework, the long hours of conference deadlines, the days of stress when results were not as expected, and the years that have constituted this marathon we call getting a Ph.D. When I felt to quit, she reminded me where and why I was going. When I needed strength she lifted me up. When I ran headlong into failure she helped me dust myself off. And, when I uncovered successes she forced me to celebrate. She has done all that I could not.

Justin J. Whitaker

CONTENTS

CHAPTER 1

INTRODUCTION

Electric vehicles are quickly gaining widespread use. Reduced energy and maintenance costs [1] provide motivation to vehicle fleet operators to adopt electric vehicles. The additional environmental and societal benefits of electric vehicles [2] provide further motivation for some fleet operators, such as transportation agencies. There are, however, several factors that contribute complexity and difficulty to adopting electric vehicles. For example, electric vehicles typically have lower ranges than comparable internal combustion engine vehicles, and often take much longer to refuel/charge [3]. Additionally, the cost of charging infrastructure can be high [4], and the rate structures for electricity can be complex [5]. Within fleet operations, these complexities typically require scheduling charging events to enable cost-effective operation [3].

The Problem

Scheduling the charging of a fleet of electric vehicles is more complex than simply pulling in to charge when the battery charge level is low; charging infrastructure is expensive, energy and power rate structures often are complicated, other electrical loads can affect the energy and power usages, individual vehicles typically have scheduling constraints, and real-world operations will inevitably require dynamic adaptation of any plan. Due to the high up-front cost of charging infrastructure [4], fleet operators have strong incentives to only install as many chargers as necessary. As a result, there are almost always fewer chargers than vehicles needing to charge, and conflicts over chargers must be resolved.

The operational costs of charging the vehicles are due to the energy provider's rate structures and can be dependent on both the energy consumed (often termed *consumption* costs) and the peak power drawn over a billing period (often termed *demand* costs). These rates can have time-dependent aspects, referred to as *time-of-use (TOU)* components, as

well. There can be electric loads on the same meters as the chargers that are outside the direct control of the fleet operator, called *uncontrolled loads* herein, that affect the demand costs incurred by the vehicle charging schedule. These uncontrolled loads could come from vehicles whose charging events cannot be directly scheduled, building loads like HVAC, or any other significant loads not easily controlled within the same context as the charging schedule. These uncontrolled loads are particularly likely to be present when considering scenarios such as meter aggregation, where multiple meters for one organization are aggregated into a single billing account as if they are one meter, or when the organization operates with a micro-grid, i.e., its own energy generation and storage capabilities, that allows additional aggregation of loads in physical meters.

In addition to the cost considerations, the charging dynamics of the batteries in electric vehicles are non-linear and can have a significant impact on the time to charge. Furthermore, many commercially available chargers have the ability to adjust the power level at which they charge. Accurately modeling the non-linear charging dynamics can ensure that vehicles are charged sufficiently in the time available and ensure that operations continue as planned. Utilizing the ability to adjust the charging power level is beneficial for minimizing demand costs, as the power drawn from the grid can be controlled to avoid high peak power draws. This control of the power level can also be used to minimize consumption costs by only scheduling the exact amount necessary for operations during higher cost times.

In many cases, fleet vehicles can have a wide range of scheduling constraints. Some vehicles may have little flexibility in charge scheduling (referred to as *fixed-schedule* vehicles) due to having predetermined route or task scheduling. Other vehicles have a wider range of flexibility (referred to as *flexible-schedule* vehicles), with tasks already grouped into full routes, but with the ability to determine the assignment of vehicles to routes, and sometimes even the timing of the routes. For some vehicles, there is near complete flexibility of scheduling, where each individual task can be scheduled with a vehicle alongside the charging events (termed *open-schedule* vehicles). Considering these groups of vehicles separately could quickly lead to high peak power draw and/or congestion at limited chargers as the

schedules of the different vehicle types inadvertently overlap. The higher peak power draw would result in higher demand costs than anticipated, while congestion at chargers would incur delays as vehicles wait for the next opportunity to charge. Similarly, if other loads on the system, such as an electric train, building HVAC, hot water pumps, etc., are ignored, demand costs are likely to be much higher than when taking those loads into consideration.

Real-world operations introduce delays, variations, and mismatches in models, that can significantly affect operating costs. Relying on a *static*, i.e., precomputed, charging schedule in spite of any variations of real-world operation may often result in higher costs. Introducing real-world data as feedback into a *dynamic* scheduling method allows for adapting to the ever-changing status of operations. The problem of dynamically scheduling fixed-, flexible-, and open-schedule vehicles to charge at a limited number of chargers while accounting for a complicated rate structure and uncontrolled loads is difficult, but necessary for the cost-effective deployment of fleets of electric vehicles.

Previous Works

In the literature, there is a split between methods that address open-schedule problems, and those that address fixed- and flexible-schedule problems. Those that address open-schedule problems typically simplify the charging aspects of the problem to focus on the assignment of tasks to vehicles [6–8]. On the other hand, works that address fixed- and flexible-schedule problems utilize the corresponding simplifications in the task assignment to enable more in-depth charging considerations. Open-schedule methods rarely consider a limited number of chargers, with only a few, such as [9, 10], accounting for the number of available chargers. In contrast, the fixed- and flexible-schedule works almost always account for limited chargers, with only a few exceptions, e.g., [11]. The rate structure of charging costs has primarily been addressed as a non-TOU consumption cost with open-schedule methods, with only a few open-schedule approaches additionally accounting for TOU consumption [12, 13]. On the other hand, fixed- and flexible-schedule methods have addressed the rate structure in varying levels of complexity. For example, of fixed- and flexible-schedule methods, [14–16] only consider consumption costs, [17] only demand costs,

while [11] considers both demand and consumption costs. Of these works, [11, 14, 15, 17] additionally consider TOU in the cost model. Almost no works, whether open-, flexible-, or fixed-schedule, consider the effects of uncontrolled loads on the charge scheduling, except [18], and very recently [19–21]. The charging dynamics of the vehicles are typically simplified in open-, flexible-, and fixed-schedule methods such that a vehicle is assumed to charge to full charge within one time step. Only a handful of fixed-schedule works consider non-linear partial charging profiles, e.g., [16,19] or variable rate charging, e.g., [11,19]. Accounting for real-world conditions is done almost exclusively in the fixed- and flexible-schedule approaches; [22] uses dynamic solution methods and [23, 24] use Markov Decision Process techniques, among others, e.g., [25, 26].

Additionally, one barrier to real-world operation for all variations of the problem is the computation time required to solve the problem. Many works utilize a mixed-integer linear program (MILP) or other optimal solution techniques to solve the problem, which are excellent for small- and sometimes medium-sized instances (typically tens of vehicle or tasks), but may struggle with large-sized instances (hundreds of vehicles or tasks) [27]. To reduce the computational requirements, problem-specific optimal solution techniques can be used (e.g., decomposition [14, 28] or branch-and-price methods [16, 29]). Due to the underlying complexity of the problem, however, these techniques still can only scale so far, inspiring the use of other techniques, most prominently meta-heuristic methods. Some of the most common meta-heuristic methods used include genetic algorithms [27,30], neighborhood search methods [15, 28, 31] and tabu searches [32]. Additionally, various types and classes of rule-based techniques including thresholding [33], queuing [34], and others [28, 31, 35] provide rapid, suboptimal solutions.

The Gap

There are, however, notable gaps in the current literature in accounting for important aspects of the problem together in one formulation. These gaps in the literature can be divided into two main categories: fleets with mixed types of scheduling constraints, and high-fidelity modeling. Both of these categories has room for improved treatment in the

literature in its own right, but considering both aspects together is particularly lacking.

The first category in the literature that is to consider fleets with a mixture of open- flexible- or fixed-schedule vehicles, as well as uncontrolled loads, in the same formulation. It is worth noting that some flexible-schedule formulations, such as [14], are capable of representing fixed-schedule vehicles as a special case of flexible-schedule vehicles, but none of these works perform any experiments or analysis that includes vehicles with both types of scheduling constraints. Additionally, [18–21] consider uncontrolled loads, but only in the context of a fixed-schedule problem. Otherwise, no other works were found that consider any combination of scheduling constraints in the same formulation.

Formulating high-fidelity models has received some attention, but is similarly lacking in considering both the full utility rate schedule and non-linear, variable-rate partial charging. Some fixed-schedule methods, e.g., [11,19] do consider both demand and consumption costs with TOU, alongside non-linear, variable-rate charging, but no open- or flexible-schedule method could be found that does so. Additionally, these works that do consider higher fidelity costs and charging often have other limitations, such as not limiting the number of chargers, as in the case of [11], or only considering a discrete set of charging levels, as in [19].

As these two gaps exist in the literature, there is also a natural gap in the literature for considering mixed scheduling constraints and high-fidelity modeling together. As more fleets get converted to electric vehicles, the need for a method that can handle these complexities will only increase. Additionally, any method bridging these two gaps should be applied to important other considerations of the problem, such as real-world operations considering stochasticity and computational efficiency for large-scale problems.

The Contributions

This gap in the literature is significant, and so the scope of the contributions of this work are limited for the sake of feasibility. Due to the natural split in the literature between open-schedule methods and fixed- and flexible-schedule methods, the primary focus of this work is on the latter. This work bridges a portion of the gap in the literature by providing

1. A mixed integer linear program formulation that provides minimum-cost solutions to problems with complex costs, high-fidelity non-linear charging profiles, flexible- and fixed-schedule vehicles, and uncontrolled loads.

2. A technique to react to real-time feedback and real-world variations within a charge scheduling framework.

The remainder of this document begins with a more detailed exploration of the literature in chapter 2. This is followed by the chapters that accomplish the contributions outlined above. Chapters 3 and 4 build a network-flow-based mixed integer linear program for fixed-schedule vehicles that accounts for uncontrolled loads and complex rate structures. Additionally, chapter 4 introduces a receding-horizon technique to enable real-time feedback under real-world variations. The formulations for the complex costs, uncontrolled loads, and high-fidelity non-linear charging profiles from chapters 3 and 4 are then applied to a bin-packing method in chapter 5 to enable scheduling of flexible-schedule vehicles together with fixed-schedule vehicles. This manuscript concludes with a summary of the contributions and a discussion of future work in chapter 6.

CHAPTER 2

BACKGROUND

As highlighted by the introduction, the problem of scheduling charging for fleets of electric vehicles is complex and multi-faceted. There are several key challenges that must be addressed to develop a comprehensive solution to the problem. The primary challenges are the modeling and consideration of the complex cost structure with time-of-use (TOU) rates for both consumption and demand costs, the modeling of high-fidelity partial charging profiles, the consideration of stochasticity in the problem, and the scalability of the solutions. The following review of the literature in section 2.1 will explore the extent to which these challenges have been addressed in the existing literature for scheduling charging for fleets of electric vehicles. In doing so, the review will provide a foundation for the research contributions of this work, which are outlined in section 2.2.

2.1 Literature Review

To help contextualize the contained work within the state-of-the-art, a classification system is used, based on the type and flexibility of the schedule of the vehicles in a fleet. This classification system is presented, followed by an overview of the treatment of the problem in the literature. The overview is followed by in-depth discussions of the treatment of the complexities of the problem in the literature, including cost considerations, charging models, stochasticity, and scalability.

2.1.1 Vehicle Scheduling Constraints Classification

The classification system used herein uses the term *task* to refer to performing an action at a specific location, and the term *route* to refer to performing a series of tasks starting and ending from a location, such as a station. Vehicles are categorized as uncontrolled, fixed-schedule, flexible-schedule, and open-schedule.

Uncontrolled loads are vehicles (or other electrical loads) for which there is little or no direct control over when and how the charging (or electricity usage) occurs. For example, electric trains that run on a predetermined schedule and use electricity as needed without outside input would be classified as uncontrolled loads. These kinds of vehicles or other loads are at one extreme of the spectrum.

Fixed-schedule vehicles consists of vehicles that have a fixed schedule of routes or tasks, but that are free to schedule when they charge. An example of this is a fleet of electric buses for which the assignment of buses to fixed routes is predetermined (perhaps for operational convenience), but buses may be scheduled to charge whenever they are in a station with charging infrastructure.

Flexible-schedule vehicles also have predefined routes, but allow the timing or assignment of routes to be adjusted to allow for charging at diverse times. These are exemplified by electric mail delivery vehicles that each have some predetermined routes, but have flexibility to adjust the ordering and timing of those routes and the necessary charging sessions between them.

Finally, *open-schedule* vehicles are those that must assign vehicles to tasks and schedule tasks alongside charging sessions. An example of open-schedule vehicles is delivery vehicles that can schedule which vehicle delivers which packages at what times in the day, as well as when and how much they charge amidst their deliveries.

2.1.2 Overview of the Problem in the Literature

The majority of works in the literature for scheduling charging for fleets of electric vehicles address the open- or flexible-schedule variants of the problem, while a few address the fixed-schedule version. The most common approaches to solving these problems utilize an adaptation of the vehicle routing problem (VRP) (also sometimes referred to as the vehicle scheduling problem or VSP). A canonical VRP deals with assigning multiple vehicles to many tasks with spatial relationships (e.g., assigning vehicles to deliver packages) and is often solved in a set-partitioning context [36]. Other methods approach solving the VRP from other contexts, such as network-flow [15, 19, 25, 29], bin-packing [14, 20], Markov

decision processes [23, 24], or rule-based methods [33–35, 37–39].

Methods to approach the open-schedule problem usually differ from flexible- and fixed-schedule approaches in that they simplify the energy consumption, costs, and charging models to focus on the complexities of task assignment and scheduling. In the open-schedule literature, the adaptation of the VRP to consider electric vehicles is often referred to as the electric vehicle routing problem (EVRP) [6–8]. The survey papers of [6–8] give an extensive overview of the state-of-the-art for the EVRP; the assessment of the open-schedule vehicle literature herein relies primarily on their analysis as this dissertation leaves the treatment of open-schedule problems to future work. A significant portion of the literature for the fixed- and flexible-schedule problems focuses on battery electric bus (BEB) fleets, where buses are scheduled for charging and, in the flexible-schedule case, assigned to routes.

The introduction highlights that a main gap in the literature as a whole is the consideration of a fleet of vehicles with more than one type of scheduling constraint. For example, while there are many works that consider vehicle fleets with either flexible-schedule constraints or fixed-schedule constraints, there are none that consider a fleet with both fixed- and flexible-schedule constraints. While some of the more flexible methods could consider vehicles with less flexible scheduling constraints as a special case (those that can be directly scheduled, not uncontrolled loads), none of the works in the literature discuss this explicitly, nor do they analyze the effects on the formulation and solution of the problem that would arise from considering multiple types of scheduling constraints. For example, the flexible-schedule method of [14] could consider fixed-schedule vehicles by fixing a number of the decision variables, but the authors do not discuss or analyze this possibility. This is a significant gap in the literature and holds across all combinations of scheduling constraint types (i.e., uncontrolled loads, and fixed-, flexible-, and open-schedule), except for a few methods that consider fixed-schedule constrained vehicles in combination with uncontrolled loads [18–21].

As outlined in the introduction, the main complexities of the problem are: the modeling and consideration of the complex cost structure with TOU rates for both consumption and

demand costs, the modeling of high-fidelity partial charging profiles, the consideration of stochasticity in the problem, and the scalability of the solutions. While each of these aspects has been addressed in the literature individually, the literature does not address all of these facets simultaneously. The extent to which the literature for fixed-, flexible-, and open-schedule vehicles addresses these complexities is discussed in the following subsections.

2.1.3 Cost Considerations

For fixed- and flexible-schedule problems the seminal work of [29] uses distance as a surrogate for energy consumption. Because of this, the cost of charging is only indirectly considered by minimizing the distance traveled, which minimizes the energy consumed and therefore charged. Accordingly, no TOU consumption nor demand costs are considered in [29].

Several works have extended [29] to directly model the energy used and include consumption in their cost functions [14–16, 22, 25, 26]. Some of these works directly track the battery charge levels of each vehicle [14,22,25], while others track the state-of-charge and assume a one-to-one correspondence between state-of-charge and energy consumed [15,16,26]. In either case, this allows modeling the energy charged and the cost of charging more directly, although several of these methods still do not consider a TOU rate schedule, e.g., [26]. A few of those works, however, do extend the formulations to also consider TOU consumption rate schedules [14, 15]. Most works in the fixed- and flexible-schedule space, such as these works, do not include demand costs in their objective functions. This is despite demand costs typically accounting for a significant percentage of the overall charging costs when they are included in the power provider's rate schedule [19, 20, 33].

However, there are a few works that do consider demand costs in addition to consumption costs [11, 19–21]. The method of [11] directly optimizes over the power draw by a vehicle at each time step, allowing for the consideration of TOU demand costs, and uses slack variables to calculate the corresponding energy and its TOU consumption costs. The authors of [19–21] directly model the energy consumption over time and introduce slack variables to calculate the power usage and demand costs. It is worth noting that, con-

trary to the majority of the literature, [20, 21] both schedule charging in a continuous-time fashion, but still calculate the costs in discrete time steps, as the other methods do. A somewhat unusual case is [17], in which the authors directly model the power grid voltages and currents and introduce slack variables to calculate the power and energy usage, but only consider the TOU demand costs and do not consider any consumption costs.

For open-schedule problems, the simplifications made to the energy consumption models often preclude the direct or accurate consideration of the cost of charging. In many problems, again, distance is used as a surrogate for energy consumption and the cost of charging is not directly considered. Even those methods that do consider the cost of charging often do so in a simplified manner, such as only considering non-TOU consumption costs. Additionally, the open-schedule methods do not account for the power usage of charging, and therefore cannot consider demand costs in any form. Consequently, while these methods usually either directly or indirectly account for non-TOU consumption costs, and a few do account for TOU consumption, no works could be found that accounted for the demand costs of charging for open-schedule vehicles [6–8].

2.1.4 Charging Models

Across the board of open-, flexible-, and fixed-schedule problems, it is almost ubiquitous to assume that a vehicle always charges to full capacity when it is scheduled to charge. This simplification allows disregarding the complexities of partial charging and the nonlinear charging profiles of real-world batteries. In using this simplification, the incoming charge level of a vehicle and the power draw capacity of the charger are not considered, but are assumed to be sufficient that the vehicle can always charge to full capacity within the discretized time step of the formulation (e.g., [14, 15, 26]). While this may be a reasonable assumption for cases where vehicles have small battery capacities and have readily available high-power chargers, it is not a realistic assumption for many real-world scenarios. For example, many electric buses have large battery capacities in the range of 250–660 kWh according to the U.S. Department of Transportation (USDOT) [40]. Even at the low end of the range with 250 kWh of capacity, a 350 kW charger (which USDOT considers to

be a high-power charger [40]) would take 34 minutes to charge to full capacity from a 20% starting charge. Many planning situations require a discretization step size smaller than 30 minutes, and so the assumption of full charging would not be valid under these circumstances.

It is worth noting the fixed-schedule method in [16] that, while utilizing a variation of a full-charge assumption, specifically allows the number of time steps required to reach full charge to vary depending on the charge level of the vehicle. The number of required time steps is calculated using a non-linear function of both the current state-of-charge, and the target state-of-charge, which in this work is always the state-of-charge considered to be full. The non-linear function used by the authors matches a CCCV charging profile, but is not dependent on this profile in particular. Despite this non-linear function, the authors use a set partitioning model and branch and price solution method that allows the non-linearity to be fixed for a given pricing problem. Then, each step of the solution process is a linear program that can be solved rapidly. However, a key aspect of treating the non-linearity as fixed is the assumption to charge to full capacity each charging session, which may not be desired in all scenarios.

In contrast to the full charge assumption, modeling partial charging can allow electric vehicles to share limited chargers more cost-effectively by reducing simultaneous power draw and therefore demand costs, e.g., [11, 19, 20]. Considering partial charging was a key aspect of [11, 17–21] providing models of the energy and power usages and consequently TOU consumption and TOU demand costs. Partial charging can also allow the consideration of non-linear charging profiles [19]. This can further reduce costs and more accurately ensure charge level constraints are enforced as the bus charge levels are more accurately modeled and the charging control can be more precise. As well, partial charging allows [41] to directly model and consider battery health and degradation costs in the optimization problem. As a subset of partial charging, variable rate charging can further reduce costs as the power draw can be more finely adjusted to reduce costs, as in [11, 17, 19].

In the few flexible- and fixed-schedule works that allow partial charging, it is fairly

common to use a "linear" charge profile as do [11, 17, 18, 20, 21, 41]. In these works, the charge gained at a time step, g_k, is modeled a bilinear function of the power draw, p and the discretization step size, δ, as

$$g_k = p\delta.$$

If p is treated as a decision variable, as in [11, 17], the formulation results in a variable rate partial charging method. If p is held constant a corresponding binary decision variable is introduced, x_k, that multiplies g_k and "switches" the energy gained on or off depending on whether the vehicle is charging at time step k, as in [18, 20, 21, 41]. In either case, δ is held constant, resulting in an equation linear in the decision variables and proportional to δ. The "linearity" of this model is in reference to the proportionality of the charge gained to δ, or that the model is linear with respect to time.

The authors of [19] use a linear dynamic system to model a non-linear charging profile that vaguely approximates the constant-current constant-voltage (CCCV) charging profile. This is accomplished by calculating the energy gained at a time step as a function of the current battery charge level, s_k, as

$$g_k = (a - 1)s_k + b$$

where a and b are constants determined by the charging power and charging system specifics. Equivalently, this models the battery charge level over time as the discrete-time linear dynamic system

$$s_{k+1} = as_k + b.$$

As a linear dynamic system, this model can be included in a linear program as a series of linear constraints. Despite this, the model is non-linear with respect to time due to the dependence on s_k, which helps to more closely approximate the exponential decay affects of a non-linear charging profile such as the CCCV profile. However, the approximation from this method is not as accurate over the more linear portions of CCCV and other similar non-linear profiles.

Variable-rate charging, allows further flexibility in charging and a corresponding potential to reduce costs. However, only the fixed-schedule methods [11, 17, 19] were found that consider variable rate partial charging. In [11, 17] the charging rate was continuously variable, but [11] did not consider any limit to the number of simultaneously charging vehicles, while [17] neglects consumption costs entirely. Conversely, [19] considered limited chargers and full TOU consumption and demand costs, but the charging rate could only take on a small set of discrete values.

In the open-schedule literature, if timing is a factor in the problem, for example with the EVRP with time windows (EVRPTW), a full-charge simplification is expanded to calculate the required time to reach full charge, typically with a charge model linear in time, but with some methods employing non-linear charge time models. A few methods allow for partial charging at the station, with both linear and non-linear charging models. No open-schedule methods were found that allow variable-rate charging [6–8].

2.1.5 Stochasticity

A majority of the approaches across all vehicle schedule types in the literature consider the problem from an idealized viewpoint, where all necessary information is known perfectly a priori and the resulting solution can be executed exactly. There are, however, a number of works that account for the stochastic nature of the problem, allowing for the solution approach to be robust to the uncertainties in the system.

For the open-schedule problem, there are a few techniques that use rule-based methods or reinforcement learning techniques to enable real-time solutions that dynamically adapt to feedback, but these do not consider limited chargers or partial charging in their methods [42–44]. Accordingly, despite the existence of these real-time solutions, dynamic solutions for use in real-time scenarios remain substantially unexplored for the open-schedule problem.

In the fixed- and flexible-schedule space, several works take the approach of solving static problems in a manner robust to the possible sources of noise [22, 25, 26]. [22] adds a buffer time to the scheduled end of each route to ensure robustness to traffic delays or higher-than-expected discharge. The approaches in [25, 26] consider stochastic energy

consumption along routes as well as possible traffic delays and formulate an optimization problem that minimizes the expected energy consumption and expected departure delays while providing a robust charging plan. As these methods are solved a priori, they require an estimate of the probability distribution of the energy consumption and traffic delays, which may sometimes be unavailable or inaccurate in some cases.

In contrast, others solve the problem in a dynamic way, allowing the solution to adapt to feedback [22–24]. In [22] the problem is repeatedly solved over a short horizon, applying a portion of each solution before receiving feedback and re-solving in a receding-horizon manner. This enables maintaining sufficient charge levels for the vehicles despite variations in the energy consumption and arrival times while maintaining low operational costs. However, [22] only considers non-TOU consumption costs and is restricted to charging to full capacity, i.e., no partial charging.

The authors of [23, 24] use an optimal policy derived from a Markov decision process (MDP) that models the choices each vehicle can make when in the station. The constructed MDP has four states for a vehicle: full-charge, sufficient charge for the current route, insufficient charge for the current route, and low charge. There are four actions a vehicle can take: wait, perform the current route, perform a different route, or charge. Not all actions are available from every state. Upon arriving at a station, returning to full charge, and regularly while in the waiting state, up-to-date feedback and data are used to create a new instance of the MDP with rewards and transition probabilities that reflect the current status of the vehicle. A policy iteration method is used to solve the MDP, and the resulting policy is used to determine the action the vehicle should take. Due to the low size of the action and state spaces, this policy iteration solution to the MDP can be obtained rapidly. This method, however, requires a large quantity of a priori data to accurately model the MDP, which may not always be available or up-to-date. Additionally, no partial charging or demand costs are considered in the method.

2.1.6 Scalability

A large portion of the methods for all vehicle schedule types solve the problem using classical optimization techniques. This is a good approach for small- and sometimes medium-sized problems, but does not scale to large problem sizes due to the integer constraints on some variables of optimization in nearly all formulations of the problem [27]. The open-schedule problem is particularly susceptible to scalability issues due to the complexity of the problem, and so much of the literature in this field also presents rule-based or meta-heuristic methods to solve the problem rapidly [6–8]. Among the meta-heuristic approaches used for the open-schedule problem, the most common methods are variations of genetic algorithms [12,37,45], tabu searches [32,38,46], and large neighborhood searches [31,39,47].

The fixed- and flexible-schedule problems are somewhat less susceptible to the scalability issues, and so literature in this space present rule-based or meta-heuristic methods less often, but there are still a few notable exceptions split between meta-heuristic [28, 30, 31] and rule-based approaches [27, 33–35, 48].

For the meta-heuristic methods, [30] uses a genetic algorithm to address a fixed-schedule electric vehicle charge scheduling problem where the objective is to "flatten the peaks" of the power draw from the grid. The genetic algorithm plans both power drawn from and supplied to the grid by the electric vehicles to achieve this objective while ensuring vehicles have sufficient charge. Other meta-heuristic methods, [28, 31] perform neighborhood searches based on a MILP formulation of the problem. Both methods address a flexible-schedule problem, and use a neighborhood search that iteratively alters a portion of a feasible solution to explore the neighborhood.

The rule-based methods include [33], which uses a thresholding and queuing technique that determines if a vehicle should charge depending on whether its state of charge is above a certain threshold or not. This allows for a simple and straightforward method to determine when a vehicle should charge, but neglects the complexities of the problem that can be addressed by less straightforward methods. Additionally, [33] determines an optimal threshold value to the nearest whole number percentage, but this value is only applicable

to the specific scenario studied, although it may be used as an informed guess for a good thresholding value in similar scenarios.

Three rule-based approaches were proposed in [34] for fixed-schedule problems that attempt to schedule charging in fixed or variable duration blocks for each vehicle while minimizing the power draw. Each of the three methods iteratively considers each vehicle in turn, and attempts to schedule charging in the available charging windows for that vehicle while avoiding increasing the maximum power drawn over the scheduling period. The three methods differ in how much each scheduled charging session can be adjusted. In the first, the session is set to the entire duration of the available window and the only decision is whether to use a given charge window or not. The second additionally allows adjusting the start time and duration of the charge session. The last method allows scheduling up to two different charge sessions in a single charge window, both of which can be adjusted in start time and duration.

Two rule-based methods derived from optimization formulations are given in [27] for solving a flexible-schedule problem. The first method considers vehicles sequentially and assigns routes to the vehicle using a maximum weight clique problem solution, followed by assigning charging sessions using a greedy scheduling method. The second iteratively solves the assignment of routes to vehicles first using the same approach as the first method, but delays assigning charging sessions until all vehicle charging sessions can be considered together using another maximum weight clique problem formulation.

Additionally, there are two methods that are notable for their computational efficiency while being based on optimization formulations. The work in [11] is a notable fixed-schedule method that utilizes a fully continuous linear program which can be solved rapidly. The authors of [11], however, leveraged the assumption that there is no scarcity of chargers (i.e., a vehicle may charge whenever necessary) in order to eliminate integer variables from the linear program. Similarly, [21] uses a series of smaller mixed-integer linear programs to solve the fixed-schedule problem, scaling to a hundred vehicles effectively. The resulting sub-optimality of [21] is not analyzed in the work, although the authors suggest that the

gap between the optimal and suboptimal solutions is likely to be acceptable.

2.2 Research Contributions

As outlined in the introduction, and further explored in the literature review, the state-of-the-art in electric vehicle charging scheduling is limited in several ways. While some works have individually considered complex costs, high-fidelity models, and stochasticity, few or none have considered all three simultaneously. There is little to no consideration of vehicle fleets with heterogeneous scheduling constraints, with fixed-, flexible-, and open-schedule vehicles being considered in isolation. The state-of-the-art is equally lacking in works that account for uncontrolled loads, which can significantly impact the performance of a charging schedule. Finally, while scalability is commonly addressed, its treatments are inherently lacking in the same ways as stated above.

In addressing these gaps herein, the scope is limited to fixed- and flexible-schedule problems as a first step towards more comprehensive solutions, but many of the methods or techniques are expected to be applicable to open-schedule problems as well. To address the limitations of the state-of-the-art, chapter 3 presents a novel network flow approach for scheduling the charging of fixed-schedule vehicles. This method is capable of simultaneously considering multiple types of chargers with different capabilities in multiple locations. The graph-based network-flow method is flexible enough to accommodate a wide range of constraints and objectives, including logistic or operational considerations. The method forms the basis of considering complex costs and high-fidelity models by considering TOU consumption costs and by incorporating a non-linear charging profile with partial charging.

The method presented in chapter 3 is extended in chapter 4 with the ability to consider TOU demand costs, a more accurate non-linear charging profile and a method to account for uncontrolled loads. The non-linear charging profile is modeled as a piecewise linear dynamic system that closely approximates the commonly used constant-current constant-voltage (CCCV) charging profile. Chapter 4 also introduces a receding-horizon approach to scheduling, which allows considering the stochasticity of vehicle charging, discharging and arrival times. This method is shown to provide significant cost savings over not account-

ing for the full cost structure, and significant robustness benefits over not considering the stochasticity.

Chapter 5 utilizes the formulations for TOU consumption and demand costs, considering uncontrolled loads, and the non-linear charging profile developed in the previous chapters and applies them to the scheduling of flexible-schedule vehicles. An existing flexible scheduling method, from [14], forms the basis of the work in chapter 5, with the addition of the non-linear charging profile, the complex costs and the consideration of uncontrolled loads from chapters 3 and 4. This formulation utilizes a bin-packing method to form the mixed-integer linear program for simultaneously scheduling routes and charging. The method in chapter 5 is shown to provide significant cost savings compared to [14] with similar computational complexity. Additionally, the ability to simultaneously consider fixed- and flexible-schedule vehicles is demonstrated with analysis on the impact on the problem formulation and solution of varying ratios of fixed- to flexible-schedule vehicles.

CHAPTER 3

A NETWORK FLOW APPROACH TO BATTERY ELECTRIC BUS SCHEDULING

Published in *IEEE Transactions on Intelligent Transportation Systems* [49]

A Network Flow Approach to Battery Electric Bus Scheduling

Justin Whitaker, *Graduate Student Member, IEEE*, Greg Droge, *Member, IEEE*, Matthew Hansen, *Graduate Student Member, IEEE*, Daniel Mortensen, and Jacob Gunther, *Senior Member, IEEE*

***Abstract*— A major challenge to adopting battery electric buses into bus fleets is the scheduling of the battery charging while considering route timing constraints and battery charge. This work develops a scheduling framework to balance the use of slow and fast chargers assuming the bus routes and charger locations are fixed. Slow chargers are utilized when possible to lower the cost of charging and fast chargers are used when needed to meet timing constraints and to ensure a sufficient charge for route execution. A directed graph is used to model the available charge times for buses that periodically return to the station to pick up passengers and to recharge its battery. A constrained network flow Mixed-Integer Linear Program (MILP) problem is formulated to optimize the scheduling of chargers as well as to determine the number of chargers required to meet battery state of charge thresholds. Using a randomly generated route schedule for thirty buses, results are presented that demonstrate the ability of the proposed method to find optimal charging plans while considering time-of-use (TOU) costs and allowing for fixed and variable numbers of chargers. These optimal charging plans reduce costs up to 20.9% compared to a thresholding-based plan and up to 12.3% compared to an optimal strategy that does not consider the TOU costs.**

***Index Terms*— Integer linear program, optimization, optimal scheduling, green transportation, batteries, power demand.**

I. Introduction

BATTERY electric buses (BEBs) are being adopted in various markets in an effort to reduce air pollution, decrease vehicle noise, and lower maintenance costs [1], [2], [3], [4]. However, from a "refueling" perspective, energy storage in batteries requires more time than for combustible-fuel energy storage systems. Instead of minutes to fully refill the combustible-fuel energy storage, it can take the better part of an hour for fast charge methods and several hours otherwise [4]. Consideration of bus route schedules and limited numbers of chargers provides additional complexity for determining when and how much to charge each bus. Furthermore, battery health is a concern due to the expense of the battery [5] and is adversely affected by fast-charging [6]. This paper presents a scheduling framework for a BEB fleet that must share a number of slow and fast chargers. It provides the ability to consider first order charging dynamics and fixed bus schedules while ensuring required battery state-of-charge thresholds are met.

Recent research seeks to enable BEB fleet deployment by solving two problems: providing BEB charger scheduling (when to charge, at which charger) and determining BEB infrastructure (charger placement, route design). Much attention has been given to solving both problems simultaneously [7], [8], [9], often using a version of the vehicle scheduling problem [10], [11], [12], [13], [14], [15], [16], [17]. Additional variations in addressing the infrastructure include determining which existing buses should be replaced by a BEB [13], [14], [15], [18], assignments of buses to routes [11], [12], [13], [14], [15], [19], accounting for uncertainty [12], [15], [17], and determining locations of fast wireless chargers along the routes [20], [21]. The added complexity of considering both the BEB charge scheduling and the infrastructure problems necessitates simplifications for sake of computation.

Two such simplifications are common. First, only fast chargers are utilized in planning [7], [8], [9], [11], [13], [14], [15], [16], [17], [18], [19], [20], [21], [22], Second, significant simplifications to the charging models are made. Some approaches assume a bus always charges to full charge [7], [9], [11], [12], [13], [14], [15], [16], [18], [21]. Others have assumed that the charge received is proportional to the time spent charging [17], [19], [20], which can be a valid assumption when the battery state-of-charge (SOC) is below 80% charge [19].

Approaches that account for more than one type of charger (i.e., more than fast chargers), typically only have one type of charger at a location (e.g., slow chargers at a depot and fast chargers at the station) [10], [12]. In [10], this is somewhat mitigated by the capability of the method to charge at variable rates.

Day-to-day operations require higher fidelity charging models to ensure buses have sufficient charge and to better incorporate the monetary cost of charging. In [8] and [22], higher-fidelity, non-linear charge profiles are used at the price of requiring computationally intensive searches; [8] uses a genetic algorithm and [22] uses an exhaustive search strategy.

Manuscript received 31 August 2021; revised 19 April 2022 and 13 January 2023; accepted 25 April 2023. Date of publication 26 May 2023; date of current version 30 August 2023. This work was supported in part by the National Science Foundation through the Advancing Sustainability through Powered Infrastructure for Roadway Electrification (ASPIRE) Engineering Research Center under Grant EEC-1941524, in part by the Department of Energy through a Prime Award with ABB Ltd., under Grant DE-EE0009194, and in part by PacifiCorp under Contract 3590. The Associate Editor for this article was L. Hajibabai. *(Corresponding author: Justin Whitaker.)*

The authors are with the Department of Electrical and Computer Engineering, Utah State University (USU), Logan, UT 84322 USA (e-mail: justin.whitaker@usu.edu; greg.droge@usu.edu; matthew.hansen@usu.edu; daniel.mortensen@usu.edu; jake.gunther@usu.edu).

Digital Object Identifier 10.1109/TITS.2023.3276269

The work in [10] is of note as it formulates a linear program that directly models the charger power use, and thus the battery charge, but must leverage an assumption that there are always enough chargers for the buses at the station to do so.

To the best of our knowledge there is not yet a work that schedules BEB charging that simultaneously addresses multiple charger types, partial charging, non-linear charge profiles, and competition over chargers (less chargers than buses). To address this gap, this paper develops an optimization framework for BEB charger scheduling geared toward day-to-day operations where the infrastructure and route schedule are assumed to be fixed. This focus enables additional essential operational details, including non-linear charge profiles, multiple chargers, and multiple cost considerations, including TOU consumption costs and indirect battery health costs. The following are the contributions of this work:

- Provide a Mixed Integer Linear Program (MILP) for scheduling BEB charging that
  - directly accounts for a non-linear bus charge profile
  - models partial charging of buses
  - considers charger availability (limited chargers)
  - allows for multiple charger types
  - accounts for time-of-use consumption costs
- Develop a first-order dynamic model compatible with the MILP to approximate a non-linear charging profile.

The remainder of the paper proceeds as follows. Preliminaries are presented in Section II. The scheduling problem for a single type of charger is described in Section III, with extensions to multiple types of chargers and optimizing over the number of chargers in Section IV. Examples are then presented in Section V, showing the ability of the MILP framework to reduce charging costs, consider periods of high-cost charging, and determine the number of chargers needed. Section VI provides concluding remarks.

II. Preliminaries

A network is a directed graph whose edges (or arcs) have a defined capacity for moving some quantifiable element [23]. Nodes in the network are represented as vertices of the graph. Source nodes generate flow, sink nodes capture flow, and intermediary nodes serve as branching points for the flow. Network flow formulations have been used to describe a host of problems [24]. In this work, the network is used to determine the actions of chargers in a bus station.

The bus-charging network flow formulation depends upon two components. The first component is the underlying graph representing the network. Thus, graph fundamentals are presented in Section II-A, with the graph to be used described in Section II-B. The second component is the dynamic model of the battery charge, developed in Section II-C. Notation is summarized in Table I.

A. Graph Basics

A directed graph can be used to represent the network where the sources, sinks, and intermediary nodes are vertices of the graph and the arcs consist of directed edges in the graph. A graph G is defined as a set of vertices, V, and edges, $E \subset V \times V$, i.e. $G = \{V, E\}$. Given two vertices in the graph, $v_1, v_2 \in V$, an edge from v_1 to v_2 implies that the ordered pair (v_1, v_2) is in the edge set, i.e., $(v_1, v_2) \in E$. An example directed graph is shown in Fig. 1.

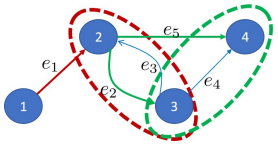

Fig. 1. Sample directed graph with groups where numbered circles show vertices and labeled arrows show directed edges. The colored ovals depict groups as discussed in Section III-B. Edges are colored by the group they enter.

As defined in [25], the incidence matrix can be used to represent the vertices and edges in matrix form and is denoted as D. Given $|V| = n_v$ and $|E| = n_e$, where $|\cdot|$ denotes the cardinality of a set, the incidence matrix is of dimension $n_v \times n_e$. Each column of D is used to represent an edge, while each row of D corresponds to a specific vertex. Using the notation $D = [d_{mn}]$ to denote the matrix such that the element in row m and column n is d_{mn}, the incidence matrix is defined as

$$D = [d_{mn}],\ d_{mn} = \begin{cases} 1 & \text{Edge } n \text{ begins at vertex } m \\ -1 & \text{Edge } n \text{ ends at vertex } m \\ 0 & \text{Otherwise.} \end{cases} \quad (1)$$

The incidence matrix of the graph in Fig. 1 can be written as

$$D = \begin{bmatrix} 1 & 0 & 0 & 0 & 0 \\ -1 & 1 & -1 & 0 & 1 \\ 0 & -1 & 1 & 1 & 0 \\ 0 & 0 & 0 & -1 & -1 \end{bmatrix}. \quad (2)$$

Edge indices are taken directly from the incidence matrix using the notation e_i to represent the edge corresponding to the i^{th} column of D. The edge index set, $\mathcal{I}$, is the set of integers from 1 to n_e.

B. Graph-Based Representation of Charger Action Space

For the purposes of this work, the focus is on a single station scenario where buses perform routes that start and end at the same station. A bus will start at the station, leave for a route, then return to the station for passenger pick-up/drop-off, shift changes, charging opportunities, etc. before leaving on the route again. This work assumes that the bus schedules, i.e., arrival and departure times, are fixed and known a priori.

In this work, the network represents the flow of chargers from one task to another. Each vertex corresponds to a particular charger type either resting or charging a particular bus at a particular point in time. The edges in this scenario denote the possible actions for the chargers. When at a rest vertex, a charger may rest (continue to the next rest vertex) or it may transition to begin charging a bus. When at a charging vertex, a charger may charge the bus for the time step (transition to the next charge vertex of the same bus), or it may transition to a rest vertex. Note that each vertex has an associated time. Thus, charger actions, i.e., charging or not, occur along edges. Only edges between two charging vertices

TABLE I
NOTATION USED THROUGHOUT THE PAPER

Variable	Description	Variable	Description
Counters			
n_c	Number of charger types	n_{c_l}	Number of chargers of type l
n_b	Number of buses	n_v	Number of vertices
n_e	Number of edges	n_t	Number of time steps
n_g	Number of groups		
Indices			
i	Edge index	q	Vertex index
k	Time index	j	Bus index
l	Charger type index	p	Group index
m, n	General matrix indices		
Optimization Auxiliary Variables			
c_i^x	graph edge costs	c_x	Vector of edge costs c_i^x
$c_{j,k}^s$	Charge level costs	c_s	Vector of charge level costs $c_{j,k}^s$
$c_{j,k,l}^g$	Charge gain costs	c_g	Vector of charge gain costs $c_{j,k,l}^g$
Δ	The discretization time step	$\gamma_{j,k}$	Boolean indicating whether vertex for bus j at time k corresponds to a first slot time at the station
Charging variables			
M_j	Maximum charge of bus j	$\delta_{j,k}$	Discharge of bus j on route returning to station at time k
a_l	Charge rate of charger type l	$\bar{a}_l$	Discretized charge rate of charger type l
$\bar{b}_l$	Discretized charge offset of charger type l	$s_j(t)$	The continuous state-of-charge of bus j at time t
Graph variables			
G	A graph	V	A set of vertices
E	A set of edges	$\mathcal{I}$	The index set of edges
v_q	The q^{th} vertex	e_i	The i^{th} edge
D	Incidence matrix for the flow constraint	d_{mn}	Element in row m, column n of D
D_l	Incidence matrix for charger type l		
Decision and Slack variables			
$s_{j,k}$	State-of-charge of bus j at time k	s	Vector of charge variables $s_{j,k}$
$g_{j,k,l}$	Charge gain for bus j at time k from charger type l	g	Vector of gain variables $g_{j,k,l}$
x_i	Binary variable for using edge i	x	Vector of binary decision variables x_i
y	Concatenation of binary (x), charge (s), and gain (g) vectors		
Constraint variables			
b_{f_l}	Flow constraint rhs for charger type l	b_f	Stacked b_{f_l} for multiple-charger types flow constraint
$\mathbb{1}_m$	Vector of ones with m rows	$\mathcal{I}_p$	The index set of edges entering group p
A_g	The group constraint matrix	b_g	The group constraint rhs
A_{gain}^{jkl}	Charging dynamics constraint matrix for bus j at time k with charger type l	b_{gain}^{jkl}	Charging dynamics rhs
		$a_{m,n}^{jkl}$	Element m, n of A_{gain}^{jkl}
A_c^j	The charge constraint matrix of bus j	b_c^j	The charge constraint rhs
$a_{m,n}^{c\ j}$	Element m, n of A_c^j	A_{n_c}	Number of chargers constraint matrix
Index mappings			
$\sigma(j,k,l)$	Index of edge connecting the charging vertices for bus j between times $k-1$ and k using charger type l		
$\eta(j,k)$	Time index corresponding to final interval vertex before time k for bus j		
λ_v	The index of variable v to its index in y		

of a bus correspond to the bus being charged. Due to route schedules, which are assumed to be fixed and known a priori, the buses are not always available to be charged. Vertices for charging a bus are only present when the bus is available. A simplified example of such a graph is shown in Fig. 2.

All chargers of the same type and at the same station can be represented by a single graph in a network flow formulation. Edges corresponding to resting are allowed to have a flow up to the number of chargers, while edges ending at charging vertices are restricted to allow only a unit flow. A separate subgraph is used for each charger type to allow the edges to correspond to different charging rates, costs, availability, etc. Constraints are added to enforce that only one charger can charge a bus at any given time.

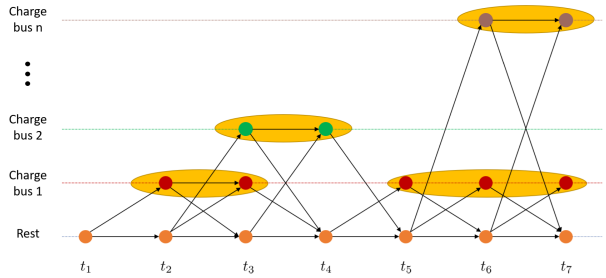

Fig. 2. A graph depicting the possible state and transitions for a single charger type over time for a very simple bus charging example. The bottom row corresponds to the charger at rest while the other rows each correspond to charging a particular bus. Yellow ovals show the vertex groups that are placed around charging windows.

C. Dynamic Charging Model

Modelling the SOC of a battery can be complex as it depends upon both the chemistry of the battery and the charging algorithm to be employed. The battery model alone can vary based upon temperature, current, and cycling [26]. Care must be taken to balance the model accuracy with the

ability to use the model within the optimization framework. A common battery charging control algorithm is CCCV [27], [28]: the charger applies a constant current (CC) to the battery until a battery terminal voltage is reached. The charger then holds that constant voltage (CV) as the charging current decreases. The charging current is approximately proportional to charge rate and so the resulting charging profile transitions from approximately linear at lower charge levels to an exponential decay at higher charge levels. We model this non-linear charge profile using a first order differential system which, when given a step input, approximates the non-linear relationship between time and convergence to the maximum charge.

Index l is used to denote the l^{th} type of charger with a_l being the convergence rate of the charger. It is assumed that bus j has a battery with maximum charge M_j. Expressing the SOC of bus j at time step k as $s_{j,k}$, a discrete-time model is given in the following lemma.

Lemma 1: Assume that the charge will occur over intervals of Δ seconds, the charge at time step $k+1$ for bus j can be related to the charge at time step k using charger l as

$$s_{j,k+1} = \bar{a}_l s_{j,k} - \bar{b}_l M_j, \tag{3}$$

where

$$\bar{a}_l = e^{a_l \Delta}, \quad \bar{b}_l = e^{a_l \Delta} - 1. \tag{4}$$

Proof: A first-order, continuous model converging to M_j at an exponential rate of a_l can be expressed as

$$\dot{s}_j(t) = a_l s_j(t) - a_l M_j. \tag{5}$$

The resulting discrete model in (3) is obtained by using the exact discretization of an LTI system as in [29]. The exact discretization of a general LTI system, represented as $\dot{x}(t) = Ax(t) + Bu(t)$, with discretization time step Δ is given by (assuming $u(t)$ is held constant over the interval)

$$x_{k+1} = \bar{A}x_k + \bar{B}u_k,\ \bar{A} = e^{A\Delta},\ \bar{B} = \int_0^{\Delta} e^{A(\Delta-\tau)} d\tau B. \tag{6}$$

In (5), both a_l and M_l are constants and there is no actual control input. To utilize the general discretization formulation, we write (5) as $\dot{s}_j = a_l s_j(t) + b_l u(t)$ where $b_l = a_l$ and $u(t) = -M_l$. In terms of the general LTI formulation, the state $x(t)$ is replaced with $s_j(t)$ and the matrices A and B are replaced with a_l and b_l, respectively. Employing the discretization formula, the discretized forms of a_l and b_l become

$$\bar{a}_l = e^{a_l \Delta},\ \bar{b}_l = a_l \int_0^{\Delta} e^{a_l(\Delta-\tau)} d\tau. \tag{7}$$

The integral in $\bar{b}_l$ can be solved analytically by taking the anti-derivative as

$$\bar{b}_l = a_l \left(-\frac{1}{a_l} e^{a_l(\Delta-\tau)} |_{\tau=0}^{\tau=\Delta} \right) = e^{a_l \Delta} - 1. \tag{8}$$

□

The charge of bus j will be calculated for each possible vertex that corresponds to charging bus j. While at the station, the charge will be represented using the piecewise dynamics

$$s_{j,k+1} = \begin{cases} \bar{a}_1 s_{j,k} - \bar{b}_1 M_j & \text{Using charger 1} \\ \vdots & \vdots \\ \bar{a}_l s_{j,k} - \bar{b}_l M_j & \text{Using charger } l \\ s_{j,k} & \text{Not being charged.} \end{cases} \tag{9}$$

The update state can be expressed using a summation by introducing the variables $g_{j,k,l}$ as the gain in battery charge for bus j at time step k from charger type l. The gain can be expressed piecewise as

$$g_{j,k,l} = \begin{cases} (\bar{a}_l - 1) s_{j,k} - \bar{b}_l M_j & \text{Using charger } l \\ 0 & \text{otherwise.} \end{cases} \tag{10}$$

Denoting n_c as the number of charger types, the charge while at the station can be expressed as

$$s_{j,k+1} = s_{j,k} + \sum_{l=1}^{n_c} g_{j,k,l}. \tag{11}$$

The amount of charge required for bus j to execute its route and return to the station at time k is denoted as $\delta_{j,k}$. Given that the bus re-enters the station at time k, the mapping $\eta(j,k)$ denotes the time index that bus j was last in the station prior to time k. Recall that bus schedules are assumed to be fixed, and so $\eta(j,k)$ is a constant mapping for a given problem instance. The dynamics across this interval can then be written as

$$s_{j,k} = s_{j,\eta(j,k)} - \delta_{j,k}. \tag{12}$$

III. Network Flow Bus Scheduling Formulation for a Single Charger Type

This section progressively builds to the electric bus charging problem for a single type of charger. A MILP is first presented for the pure network flow problem. This forms the fundamental ability to plan for multiple chargers of the same type. The solution to the MILP determines which edges in the graph will be used as well as the number of chargers that will take a given edge. Constraints on the flow into vertex groups are then introduced to ensure that at most one charger will be assigned to a bus each time it visits the station. The final portion of this section introduces variables and constraints to track the dynamics of each bus charge and constrain the lower limit of the charge.

A. A Network Flow Approach to Graph Search

This section presents a MILP formulation of the graph search problem that allows for simultaneous search of multiple routes through the graph. An integer decision variable is introduced for each edge in the graph. Edge e_i is associated with the decision variable $x_i \geq 0$, where x_i is the amount of flow along the i^{th} edge. To weight the selection of one path over another, a value is assigned to each edge, denoted as c_i^x. As a minimization problem will be formulated, $c_i^x > 0$ denotes an edge cost or penalty. The total path cost can be written as the summation of the incurred costs, $c_1^x x_1 + c_2^x x_2 + \ldots + c_{n_e}^x x_{n_e}$. This can be written more succinctly as $c_x^T x$, where both c_x

and x are column vectors. This cost will be discussed in more detail with the other components of the cost that are introduced in Section III-D

Constraints must be introduced to balance the flow through the network so that the chosen path moves continuously from one vertex to another through the graph. The starting vertices are sources with positive flow, the ending are sinks with negative flow, and all others must have the same outgoing flow as incoming flow. This balance of flow can be represented as a constraint using the incidence matrix. Recall that the edge directionality is encoded into the incidence matrix. Summing across row q of D will give the number of edges originating at vertex v_q minus the number of edges ending at vertex v_q. As x represents the amount of flow along each edge, Dx is a column vector where each row corresponds to the outgoing flow minus the incoming flow for the vertex.

Assuming that a single source vertex is the first vertex and that a single sink vertex is the final vertex (i.e., all chargers start and end at "rest"), the network flow constraint for a single type of charger ($l = 1$) can be written as

$$\begin{aligned} Dx &= b_{f_1} \\ b_{f_1} &= \begin{bmatrix} n_{c_1} & 0 & \dots & 0 & -n_{c_1} \end{bmatrix}^T, \end{aligned} \tag{13}$$

where n_{c_l} is the number of chargers of type l. This enforces the outgoing flow from the source vertex and the incoming flow to the sink vertex to be equal to n_{c_1}, and enforces balanced incoming and outgoing flow for all other vertices.

The optimization problem can then be re-written to include this constraint as

$$\begin{aligned} &\min_x \ c_x^T x \\ &\text{s.t. } Dx = b_{f_1},\ x_i \in \{0, \dots, n_{c_l}\}. \end{aligned} \tag{14}$$

Note that (14) is very similar to the formulation in Chapter 10 of [24], using different notation and expressing the constraint in matrix form using the incidence matrix.

A simple network flow example: Consider the simple example from (2) depicted in Fig. 1. Assuming a source flow of 1, the network flow constraint in (13) can be reduced to

$$Dx = \begin{bmatrix} x_1 \\ -x_1 + x_2 - x_3 + x_5 \\ -x_2 + x_3 + x_4 \\ -x_4 - x_5 \end{bmatrix} = \begin{bmatrix} 1 \\ 0 \\ 0 \\ -1 \end{bmatrix}. \tag{15}$$

A row-by-row overview of the constraint can help to understand the flow constraint. Row 1 indicates that e_1 must be used. This is also obvious from Fig. 1 as it is the only edge coming out of the source vertex. Row four states that either e_4 or e_5 be selected, but not both due to the constraint that x_i be non-negative integers. Rows two and three show the balance of incoming and outgoing edges for vertices v_2 and v_3.

B. Group Constraints

One significant advantage of using the MILP formulation for performing a graph search is the ability to add additional constraints. One constraint of import is that during each stop at the station, a bus may visit at most one charger, with an optional wait before and after charging, as needed. For a group of vertices corresponding to a single visit, there will be at most one edge entering the vertex group with a non-zero flow.

For the p^{th} charge window, denote the corresponding set of vertices as $\mathcal{V}_p \subset V$. Then, the index set of edges that enter $\mathcal{V}_p$ is defined as

$$\begin{aligned} \mathcal{I}_p = \{i | e_i \in E \text{ where } e_i = (v_m, v_n), \\ v_n \in \mathcal{V}_p, \text{ and } v_m \in V \setminus \mathcal{V}_p\} \end{aligned} \tag{16}$$

The constraint that a bus be charged by only a single charger when at the station can be written in summation form as

$$\sum_{i \in \mathcal{I}_p} x_i \leq 1,\ p = 1, \dots, n_g, \tag{17}$$

where n_g is the number of groups. Combined with the constraint that x_i is integer, (17) ensures that the amount of flow (i.e., number of chargers) into and out of each group (i.e., each charge window) will be either zero or one.

The definition of $\mathcal{I}_p$ can be used to write the constraint in matrix form to be more amenable to optimization routines. The matrix A_g and vector b_g are used to represent the constraint as $A_g x \leq b_g$, $b_g = \mathbb{1}_{n_g}$, where $\mathbb{1}_m$ is a column vector of m ones. Allowing a^g_{mn} to be the entry of A_g in the m^{th} row and n^{th} column, A_g can be expressed as

$$A_g = [a^g_{mn}],\ a^g_{mn} = \begin{cases} 1 & n \in \mathcal{I}_m \\ 0 & \text{otherwise.} \end{cases} \tag{18}$$

The optimization problem for a single type of charger with group constraints can be written as

$$\begin{aligned} &\min_x \ c^T x \\ &\text{s.t. } Dx = b_{f_1}, \quad A_g x \leq b_g,\ x_i \in \{0 \dots n_{c_1}\}. \end{aligned} \tag{19}$$

Continuing the Simple Example: The groups shown in Fig. 1 are now evaluated. The red vertex group is formed with vertices v_2 and v_3 and the green is formed with vertices v_3 and v_4. The edge index sets can be written as $\mathcal{I}_1 = \{1\}$ and $\mathcal{I}_2 = \{2, 5\}$. The summation and matrix forms of the constraints can be written as

$$\begin{aligned} x_1 &\leq 1 \\ x_2 + x_5 &\leq 1 \end{aligned} \text{ or } \begin{bmatrix} 1 & 0 & 0 & 0 & 0 \\ 0 & 1 & 0 & 0 & 1 \end{bmatrix} x \leq \begin{bmatrix} 1 \\ 1 \end{bmatrix}. \tag{20}$$

C. Charging Variables and Constraints

Each edge in the graph corresponds to a charger resting, transitioning to or from charging, or charging a particular bus. Recall from Section II-C that the variable $g_{j,k,l}$ is the gain for bus j using an edge starting at time k on charger type l. The mapping $\sigma(j, k, l)$ is used to map to the respective edge index, i.e., $x_{\sigma(j,k,l)}$ is the flow associated with the same edge as gain $g_{j,k,l}$. As only a single charger type is available in this section, the value $l = 1$ is used.

The case statement for the gain in (10) can be represented using Big-M notation as

$$\begin{aligned} g_{j,k,l} &\geq (\bar{a}_l - 1)s_{j,k} - \bar{b}_l M_j - M_j(1 - x_{\sigma(j,k,l)}) \\ g_{j,k,l} &\leq (\bar{a}_l - 1)s_{j,k} - \bar{b}_l M_j \\ g_{j,k,l} &\geq 0 \\ g_{j,k,l} &\leq 0 + M_j x_{\sigma(j,k,l)}, \end{aligned} \tag{21}$$

where the Big-M components are expressed in blue and $l = 1$. Note that when edge $x_{\sigma(j,k,l)}$ is used (i.e., equals 1 due to the group constraint) then the top two equations form the appropriate equality constraint for charging and the fourth equation allows the charge gain to extend up to the maximum charge. When $x_{\sigma(j,k,l)} = 0$ then the final two equations are active, forcing the gain to be zero while the first equation allows the gain to extend down to zero. Note that (21) can be written in a standard linear constraint form as

$$\begin{aligned} (\bar{a}_l - 1)s_{j,k} + M_j x_{\sigma(j,k,l)} - g_{j,k,l} &\leq M_j(\bar{b}_l + 1) \\ g_{j,k,l} - (\bar{a}_l - 1)s_{j,k} &\leq -\bar{b}_l M_j \\ -g_{j,k,l} &\leq 0 \\ g_{j,k,l} - M_j x_{\sigma(j,k,l)} &\leq 0. \end{aligned} \tag{22}$$

This can be expressed in matrix form. Denote the variables of optimization as

$$y = \begin{bmatrix} x & \text{All edge variables} \\ s & \text{All charge variables} \\ g & \text{All gain variables} \end{bmatrix}. \tag{23}$$

The mapping λ_v is used to represent the index of variable v in y. The constraints in (22) will be repeated for every possible j, k, l combination (i.e. for each time k when charging is possible for bus j and for each charger type, l). This four-row matrix is denoted as A^{jkl}_{gain} with the constraint written as $A^{jkl}_{gain} y = b^{jkl}_{gain}$. Defining A^{jkl}_{gain} element-wise as $A^{jkl}_{gain} = [a^{jkl}_{mn}]$, the elements can be expressed as

$$a^{jkl}_{1n} = \begin{cases} (\bar{a}_l - 1) & n = \lambda_{s_{j,k}} \\ M_j & n = \lambda_{x_{\sigma(j,k,l)}} \\ -1 & n = \lambda_{g_{j,k,l}} \\ 0 & \text{otherwise} \end{cases}$$

$$a^{jkl}_{2n} = \begin{cases} -(\bar{a}_l - 1) & n = \lambda_{s_{j,k}} \\ 1 & n = \lambda_{g_{j,k,l}} \\ 0 & \text{otherwise} \end{cases} \qquad b^{jkl}_{gain} = \begin{bmatrix} M_j(\bar{b}_l + 1) \\ -\bar{b}_l M_j \\ 0 \\ 0 \end{bmatrix}$$

$$a^{jkl}_{3n} = \begin{cases} -1 & n = \lambda_{g_{j,k,l}} \\ 0 & \text{otherwise} \end{cases}$$

$$a^{jkl}_{4n} = \begin{cases} 1 & n = \lambda_{g_{j,k,l}} \\ -M_j & n = \lambda_{x_{\sigma(j,k,l)}} \\ 0 & \text{otherwise} \end{cases} \tag{24}$$

The aggregate charging inequality constraint $A^{ineq}_{gain} y \leq b^{ineq}_{gain}$ is defined by stacking A^{ikl}_{gain} and b^{ikl}_{gain} for $i = 1, \ldots, n_b$, for all k such that a charging vertex is available for bus j and for each charger type l.

With the edge charge gains in hand, the charger updates in (11) and (12) can be expressed. They take the form of an equality constraint, one for each bus and time that a charging vertex appears. Recall that (12) models the change in charge after a bus has run its route and (11) models the charge while at the station. Thus, the first vertex in each group of charging vertices will use (12) and the rest will use (11). The boolean $\gamma_{j,k}$ is used to indicate starting vertices of groups, defined as

$$\gamma_{j,k} = \begin{cases} 1 & k \text{ is the time of a first group vertex for bus } j \\ 0 & \text{otherwise.} \end{cases} \tag{25}$$

The charge state dynamics equality constraint corresponding to bus j can be expressed as $A^j_c y = b^j_c$ where

$$A^j_c = [a^{c,j}_{k,n}] = \begin{cases} 1 & n = \lambda_{s_{j,k}} \\ 1 & \exists\ l \text{ s.t. } n = \lambda_{g_{j,k,l}} \\ -1 & n = \lambda_{s_{j,k+1}} \text{ and } \gamma_{j,k} = 0 \\ -1 & n = \lambda_{s_{j,\eta(j,k)}} \text{ and } \gamma_{j,k} = 1 \\ 0 & \text{otherwise} \end{cases}$$

$$b^j_c = [b^{c,j}_k] = \begin{cases} s_{j,1} & k = 1 \\ -\delta_{j,k} & \gamma_{j,k} = 1 \\ 0 & \text{otherwise.} \end{cases} \tag{26}$$

The full equality constraint, $A^{eq}_c y = b^{eq}_c$, is formed by stacking A^j_c and b^j_c for $j = 1, \ldots n_b$.

D. Including the Objective Function

To express the full optimization problem, cost variables are introduced corresponding to the charge level state variables, $c^s_{j,k}$, and charge gain variables, $c^g_{j,k,l}$. These can be stacked in the same order as the vectors s and g into the cost vectors c_s and c_g. These cost vectors are in addition to the edge costs, c_x that were previously introduced.

Each element of c_x corresponds to a charging edge, and represents a cost on charging that is independent of the energy or power used; e.g., amortized maintenance costs, energy-independent weighting against using chargers in high-demand time periods, or discouraging use of certain charger types for battery health reasons. The elements of c_s capture costs related to the battery charge level, which could be used to penalize high (or low) charge levels. The vector c_g contains any costs on the amount of charge gained (in units of energy) over a time period and are most useful for accounting for time-of-use consumption costs.

The full optimization problem can now be expressed as

$$\begin{aligned} \min_y\ & \begin{bmatrix} c_x^T & c_s^T & c_g^T \end{bmatrix} y \\ \text{s.t. } & Dx = b_{f_1},\ A_g x \leq b_g \\ & A^{ineq}_c y \leq b^{ineq}_c,\ A^{eq}_c y = b^{eq}_c \\ & x_i \in \{0 \ldots n_{c_1}\},\ s_{j,k} \geq s_{j,min} \\ & y = [x^T, d^T, g^T]^T, \end{aligned} \tag{27}$$

where $s_{j,min}$ is the minimum charge allowed.

IV. Extensions for Multiple Charger Types and Numbers of Chargers

The optimization problem presented in the previous section considered a single charger type with a fixed number of chargers. These two assumptions will be relaxed in the following developments.

A. Multiple Charger Types

Consider the scenario of a station with multiple types of chargers, each type having a potentially different charging rate, cost of usage, and quantity. As before, when a bus arrives at the station it can only visit a single charger prior to departing. The optimization must now include the ability to select which type of charger is used. Changes in the flow constraint, the group constraint, and the charge constraint are now addressed.

1) Updated Flow Constraint: A separate graph of charging availability can be designed for each charger type. Given n_c different types of chargers, the aggregate charging graph would be a set of disjoint subgraphs. Each subgraph would have a defined starting and end vertex with the l^{th} charger type incidence matrix being denoted as D_l. The aggregate incidence matrix would be the block diagonal matrix

$$D = \begin{bmatrix} D_1 & 0 & \dots & 0 \\ 0 & \ddots & \ddots & \vdots \\ \vdots & \ddots & \ddots & 0 \\ 0 & \dots & 0 & D_{n_c} \end{bmatrix}. \tag{28}$$

The right-hand side of the flow constraint can be formed by stacking b_{f_l} for $l = 1, \dots, n_c$ as

$$b_f = \begin{bmatrix} b_{f_1}^T & \dots & b_{f_{n_c}}^T \end{bmatrix}^T. \tag{29}$$

The flow constraint is defined similar to before as $Dx = b_f$.

2) Updated Group Constraint: The form of the group constraint does not change, only that vertices in a group will now span the disjoint sub-graphs for each charger type. As before, a group consists of a set of vertices $\mathcal{V}_p$ defined by all of the vertices corresponding to a particular visit by a bus to the station. The set $\mathcal{V}_p$ now contains the vertices across the various disjoint graphs that correspond to a particular visit by the bus to the station.

3) Updated Charging Constraint: Under a single type of charger, the summation in (11) included a single gain term. Under multiple types of chargers, the summation will include n_c terms. For homogeneous charger schedules, there will be n_c slack variable gains added for each possible charging edge. The charge constraint takes the same form as before with $l = 1, \dots, n_c$ instead of $l = 1$.

B. Optimizing the Number of Chargers

To choose the number of chargers, the variables of optimization are augmented with n_c additional variables as

$$y = \begin{bmatrix} x \\ s \\ g \\ [n_{c_1} \ \dots \ n_{c_{n_c}}]^T \end{bmatrix}. \tag{30}$$

The group and charge constraints are zero padded by adding an additional n_c columns of zeros to the A_g and A_c matrices. The flow constraint is updated to $\begin{bmatrix} D & 0 & A_{n_c} \end{bmatrix} y = 0$, where the 0 on the left-hand side accounts for no inclusion of s and g in the constraint and the 0 on the right-hand side is a column vector. The additional A_{n_c} matrix is an $n_v \times n_c$ matrix defined as the block diagonal

$$A_{n_c} = \begin{bmatrix} -b_{f_1} & 0 & \dots & 0 \\ 0 & \ddots & \ddots & \vdots \\ \vdots & \ddots & \ddots & 0 \\ 0 & \dots & 0 & -b_{f_{n_c}} \end{bmatrix}. \tag{31}$$

V. Example

An example is now presented to illustrate the utility of the developed planning techniques. A description of the station scenario is first presented followed by the description of the strategies used for planning. Results are then presented for three separate optimization scenarios where the planning strategies are employed.

A. Battery Electric Bus station Scenario

The bus station is required to charge 30 battery electric buses using a combination of slow and fast battery chargers. Each bus is equipped with a 388 KWh battery that is required to stay above 25% charge (97 kWh) to maintain battery health. Planning occurs over a 24 hour period where each bus is assumed to start with 90% charge (349.2 kWh). To enable repeatability in the charging scheme the next day, each bus is required to also end with at least 90% charge. Slow, low-cost charging can take several hours while fast, high-cost charging can be a fraction of an hour [4]. Thus, the low-cost charger is modeled with a value of $a_1 = 0.01$, which would charge a battery from zero charge to 90% charge in a little under four hours. The high-cost charger is modeled with a value of $a_2 = 0.1$, resulting in a 90% charge in 23 minutes.

The bus schedules are randomly generated. It is assumed that each bus route will take between 50 and 180 minutes to execute. Buses will then return to the station for a duration between 60 and 120 minutes before leaving on the same route and are assumed to be in the station for at least 120 minutes at the end of the 24 hour period. To calculate the amount of discharge along the route (i.e., $\delta_{j,k}$), it is assumed that the buses use 30 kWh of charge every hour while in route. Note that a route discharge amount is typically dependent on many more factors than the time on the route; this simplification is made to ease the random route generation process.

The planning occurs for a single 24 hour period at a ten minute resolution. The resulting randomly generated buses produce a total of 4,744 vertices, 13,248 edges, and 6,338 total charging slack variables. The optimization is performed using the Gurobi MILP solver [30] on a machine running an eight-core Intel i7-7700 3.6 GHz processor.

B. Planning Strategies

Three separate planning strategies are employed:

1) Qin-Modified: Buses are charged based on the thresholding strategy of [22]. In [22], an exhaustive search is performed to find the best battery charge threshold for charging. If a bus enters the station below that threshold (and a charger is available) then the bus is charged. We have modified the approach to be better suited for multiple charger types. First, three different charging thresholds are given: low charge (40%), medium charge (70%), and high charge (90%). Second, the day is divided into two regions: 1) the day, while buses are on routes (5 AM - 10 PM), and 2) the night, when most buses are in the station (10 PM - 5 AM). In the first region, buses below a low charge are prioritized to a fast charger if available, and a slow charger otherwise. The next priority comes to buses that are above low but below medium. These are assigned to a slow charger if available. During the day, buses above the medium threshold are not assigned to a charger.

During the night (10 PM - 5 AM), returning to high state-of-charge is prioritized. Accordingly, buses below medium are assigned first to fast chargers, followed by slow chargers if no fast charger is available. Then, buses between medium and high are assigned to slow chargers when available. Finally, buses above the high-charge level are not assigned to a charger. Once assigned a charger, the bus stays on the charger until its battery reaches 90% charge or it is time to begin its next route, whichever comes first.

This method represents a straightforward charging policy that only requires bus drivers/operators to follow simple rules to determine whether or not to charge a bus.

2) No-TOU: The MILP formulation is used with a time-invariant consumption cost of $c^g_{j,k,l} = 0.029624$ dollars per kilowatt-hour assigned for all j, k, and l. This consumption cost is the base price from the Rocky Mountain Power schedule 8 [31]. A cost on edges is used to discourage charging with the fast chargers as faster charge rates typically incur greater battery damage; formally, $c^x_{j,k,l} = 0.01$ if l corresponds to a slow-charger and $c^x_{j,k,l} = 0.2$ if l corresponds to a fast-charger. All other costs are $c_x = 0$ and $c_s = 0$. This represents an optimization-based planning strategy that does not consider the TOU consumption costs.

3) TOU: The MILP formulation is used with costs the same as the *No-TOU* strategy, but with the modification that $c^g_{j,k,l} = 0.058282$ dollars per kilowatt-hour if j is in one of two time periods: 6 AM - 9 AM or 6 PM - 10 PM. This TOU pricing corresponds to the consumption portion of the Rocky Mountain Power Schedule 8 TOU pricing [31].

C. Primary Scheduling Scenarios

Three scheduling scenarios are now considered and results discussed. The first is a scenario in which an excess of chargers exist, the second scenario considers the minimization of chargers, and the third scenario considered planning with the reduced number of chargers. The results are plotted in Figs. 3 to 5. Figures 3 and 4 plot the aggregate mean, max and min charge, as well as the charger utilization over time for each planning strategy. The zones of high-cost charging are shaded pink. Fig. 5 shows two example charge profiles for the buses under two planning strategies. Table II compares the resulting solutions in aggregate charge statistics, objective values, and charger usage.

Excess Chargers: This scenario assumes that a fixed number of chargers is available. A total of ten slow chargers and five fast chargers are used. The MILP optimizations were solved to an optimality gap of 5%.

The *Qin-Modified* strategy is able to meet charging constraints, albeit with additional cost and utilization of the chargers compared to the MILP-based approaches. Table II shows that the *TOU* MILP improves upon the *Qin-Modified* strategy by 18.7% and the *No-TOU* MILP by 15.4%. When not factoring TOU pricing into the cost, the *Qin-Modified* approach outperforms the *No-TOU* strategy by 1.4%. This is due to two factors 1) the MILP is only solved to a 5% gap and 2) the continuous (non-discrete) solution method of the *Qin-Modified*. When restricted to a 10 minute discretization, however, the *Qin-Modified* approach degrades and is 1.2% more costly than the *No-TOU* method. Fig. 3 shows that prior to the second high-cost zone, the mean, maximum, and minimum charges all increase under the *TOU* strategy to ensure that minimum charge requirements are met without charging during high-cost times. A comparison of the charger utilization plots of Fig. 3 for the *TOU* and *No-TOU* MILP results show that the *TOU* strategy uses the excess chargers to avoid costly time windows. The *TOU* strategy uses zero chargers during the high-cost time windows, which significantly reduces the TOU cost. Table II shows that to avoid the costly windows, the amount of time spent on the fast chargers is increased 4.4% over the *No-TOU* MILP.

Using the MILP strategies, the mean and minimum battery charge values are allowed to dip much lower than the Qin-Modified strategy while the max charge rarely exceeds the requisite end charge. Thus, less time is spent on unneeded charging. The *Qin-Modified* strategy uses the chargers for a much larger total time than the two MILP-based approaches, as seen in Table II and Fig. 3. Because the *Qin-Modified* does so while also not over-charging any buses at the final time, it can be inferred that, on average, the *Qin-Modified* method charges more slowly than the two MILP-based methods. In contrast, the two optimization-based approaches allow the battery charge to dip low, capitalizing on the increased charge received per unit time at lower charge levels.

Charger Minimization: Facility constraints may limit the number of chargers in a single station. The formulation in Section IV-B can be used to determine the number of required chargers. To determine the minimum number of chargers needed to satisfy requirements, all weights can be zeroed except for the weights on the number of chargers of each type. In this example, the fast charger was assigned a cost of ten times that of the slow charger to emulate the higher initial and operational costs of fast charging. Furthermore, as the possible space is constrained, the number of chargers were limited to a maximum of ten low-cost chargers and five high-cost chargers.

Optimizing over the number of chargers significantly slowed down the optimization time. While a feasible solution was rapidly found, the optimization took nearly six hours to reduce the chargers to six slow and two fast. After six additional hours, the number of chargers did not change. Accordingly, the

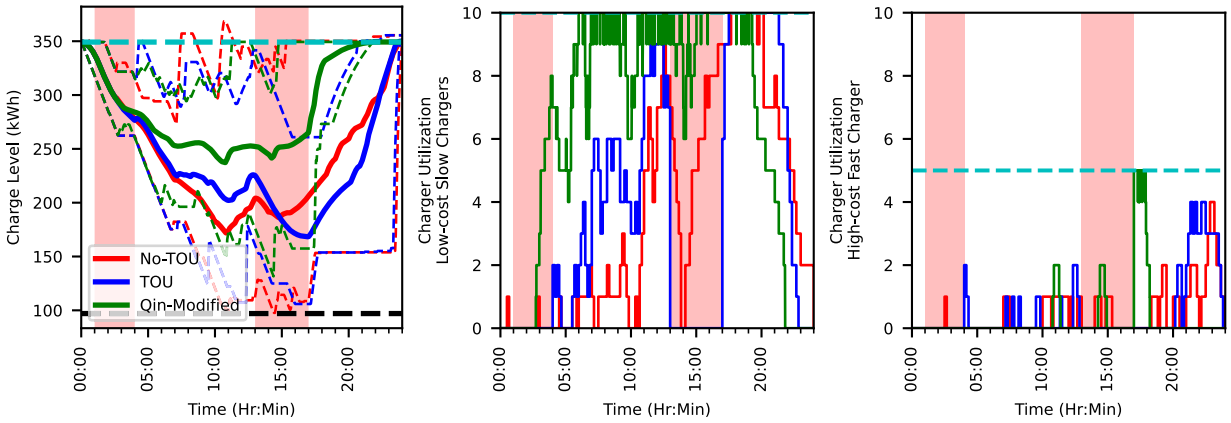

Fig. 3. Aggregate results for ten low-cost chargers and five high-cost chargers. Blue uses a MILP considering TOU pricing, red uses a MILP without considering TOU pricing, and green represents using the Qin-Modified approach. Left shows the mean charge (solid) as well as max an min charge (dotted) over time. The middle shows the slow, low-cost charger utilization and the right shows the fast, high-cost charger utilization.

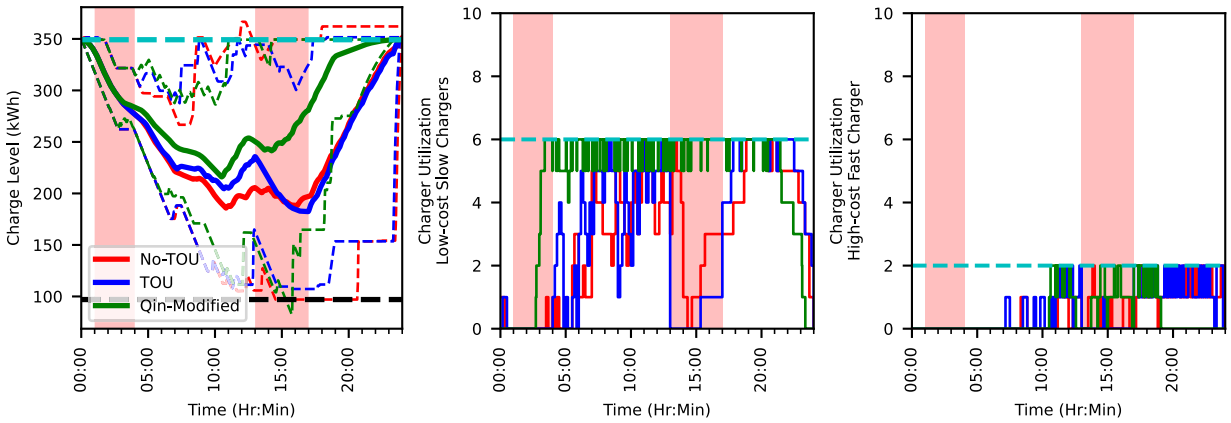

Fig. 4. Aggregate results for six low-cost chargers and two high-cost chargers. Blue uses a MILP considering TOU pricing, red uses a MILP without considering TOU pricing, and green represents using the Qin-Modified approach. Left shows the mean charge (solid) as well as max an min charge (dotted) over time. The middle shows the slow, low-cost charger utilization and the right shows the fast, high-cost charger utilization.

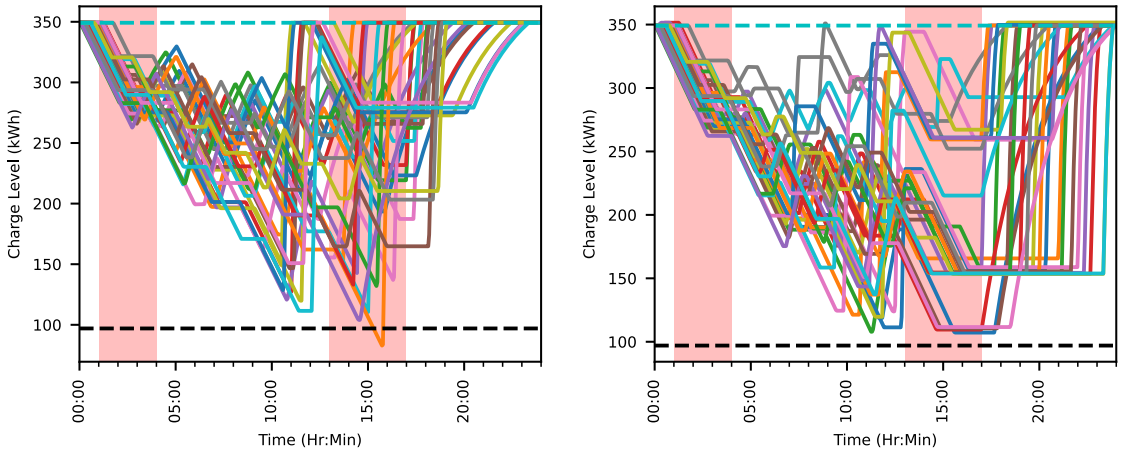

Fig. 5. Shows the charge vs time for each bus using the *Qin-Modified* strategy (left) and the *TOU* strategy (right) for the *Reduced Chargers* scenario where 6 slow and 2 fast chargers are used. The black dashed line is the minimum allowable charge and the light blue dashed line is the required final charge.

optimization was terminated early at this point. Note that this optimization duration is not prohibitive, as the question of how many chargers to install will likely not be asked frequently.

Reduced Chargers: Using the number of chargers found in the *Charger Minimization* scenario, the three planning strategies were again employed with results shown in Figs. 4 and 5 and Table II. As in the *Excess Chargers* scenario, the MILPs were solved to a 5% optimality gap. While the *Qin-Modified* approach is still able to maintain the final minimum charge constraint, it is unable to maintain the

TABLE II

THE FIRST COLUMN DESCRIBES THE CONFIGURATION OF THE STRATEGY USED TO FIND A SOLUTION. THE NUMBERS OF A CONFIGURATION NAME CORRESPOND TO THE NUMBER OF SLOW AND FAST CHARGERS, RESPECTIVELY, WHILE THE SUFFIX INDICATES THE PLANNING STRATEGY USED. COLUMNS 2 AND 3 ARE THE MEAN AND MINIMUM CHARGE OF ALL BUSES OVER TIME, COLUMN 4 IS THE MINIMUM CHARGE OF ANY BUS AT THE FINAL TIME. COLUMNS 5 AND 6 ARE THE COST OF THE SOLUTION CALCULATED WITH AND WITHOUT THE HIGHER ZONE RATES. COLUMNS 7 AND 8 ARE THE TOTAL MINUTES THAT A SLOW OR FAST CHARGER WAS USED. NOTE THAT BOLDED VALUES INDICATE THE VIOLATION OF A CONSTRAINT

Configuration	Mean Charge (kWh)	Min Charge (kWh)	Cost With TOU	Cost Without TOU	Slow Charger Utilization (Minutes)	Fast Charger Utilization (Minutes)	Solve Time (Seconds)
10-5 TOU	242	106	280.9	280.7	5,370	710	71.9
10-5 No-TOU	244	98	332.3	280.2	5,440	680	67.9
10-5 Qin-Modified	289	132	343.0	276.7	9,456	438	–
6-2 TOU	252	107	285.1	281.7	4,340	830	1728.2
6-2 No-TOU	248	97	325.0	283.1	4,170	840	592.3
6-2 Qin-Modified	285	**83**	360.3	279.6	6,951	672	–

The time to run the *Qin-Modified* approach depends primarily on the simulation environment, which can vary drastically depending on many factors. For this reason, no time is specified in the table, although for our simulation environment the time taken was no more than two seconds in all cases.

running minimum charge for a bus (Fig. 4). Additionally, when examining the costs in Table II, the *Qin-Modified* approach has a significantly degraded TOU cost (26.4% higher than the *TOU* strategy). The MILP is again able to adjust to have a lower cost when considering the zones of high-cost time, but there is less flexibility to avoid high-cost regions than with more chargers. The *TOU* strategy still utilizes chargers during zones of high cost, although it uses fewer chargers during high-cost regions than the other two strategies. Similar to the *Excess Chargers* scenario, Table II and Fig. 4 show that the *TOU* strategy again ramps up the mean charge prior to the second zone of high cost and uses the fast chargers for more time than the *No-TOU* strategy. Additionally, this scenario demonstrates that this MILP framework can reduce both charger installation and daily operational costs compared to the *Qin-Modified* method.

D. Optimizing Over Consumption Costs Only

In some cases, the direct monetary consumption costs may be the only factor so the edge costs are not necessary. This is explored for the *Excess Chargers* and *Reduced Chargers* scenarios from above, but with two modified MILP strategies. They are the same as the *TOU* and *No-TOU*, but with the edge costs, $c_x = 0$, leaving only the consumption costs in c_g. These additional strategies are denoted as *TOU-CO* and *No-TOU-CO*. This relatively minor change in the MILP structure resulted in an easier problem for the Gurobi solver to tackle, allowing the termination optimality gap to be set at a value of 0.1% (as opposed to the previous value of 5%) with similar or better solution times for the improved optimality guarantee, as seen in Table III. Additionally, while *Qin-Modified* relies much less on the fast chargers, using the MILP results in 19.7% and 23.3% lower dollar costs.

E. Exploring the Feasibility of Qin-Modified

As the results of Section V-C show, the *Qin-Modified* strategy with well-tuned thresholding behavior can perform quite well. This performance is dependent, however, on the quality of the tuning of the threshold parameters and behaviors. Additionally, one set of parameters is likely to only perform well for scenarios that are very similar. This can be seen in Table II where the *Qin-Modified* strategy breaks the minimum charge constraint in the *Reduced Chargers* scenario, as the strategy was only hand-tuned for the *Excess Chargers* scenario. To further explore this phenomenon, the same *Qin-Modified* strategy is also applied to five randomly generated bus schedules for forty buses. The *TOU-CO* strategy was also run on the same scenarios for comparison. The results of Table IV show that out of the five scenarios only once does the *Qin-Modified* maintain feasibility with the minimum charge constraint, while the *TOU-CO* demonstrates that all five scenarios are feasible. This demonstrates the flexibility that the MILP based formulation has to adapt to new scenarios or changing conditions and maintain feasibility. Additionally, the proposed method continues to outperform the *Qin-Modified* approach in terms of cost in all cases.

TABLE III

THE *Excess Chargers* AND *Reduced Chargers* SCENARIOS WERE RUN WITH THE CONSUMPTION COSTS ONLY. THE COLUMNS ARE A SUBSET OF THOSE FROM TABLE II, WITH THE DISTINCTION THAT THE COST VALUES NOW HAVE UNITS OF DOLLARS

Configuration	Min Charge (kWh)	Cost ($) With TOU	Slow Charger Utilization (Minutes)	Fast Charger Utilization (Minutes)	Solve Time (Seconds)
10-5 TOU-CO	104	260.8	730	1410	83.1
10-5 Qin-Modified	131	324.8	9,456	438	–
6-2 TOU-CO	109	260.8	3340	1210	582.3
6-2 Qin-Modified	**83**	339.9	6,951	672	–

TABLE IV

THE *Excess Chargers 40 Bus* SCENARIO INSTANCES WERE RUN WITH THE *TOU-CO* AND THE *Qin-Modified* STRATEGIES. THE COLUMNS ARE THE SAME AS IN TABLE III. THE THIRD NUMBER IN THE *Configuration* COLUMN INDICATES THE INSTANCE

Configuration (40-buses)	Min Charge (kWh)	Cost ($) With TOU	Slow Charger Utilization (Minutes)	Fast Charger Utilization (Minutes)	Solve Time (Seconds)
10-5(1) TOU-CO	105	347.5	1,740	1,780	144.3
10-5(1) Qin-Modified	**94**	420.3	9,953	855	–
10-5(2) TOU-CO	106	329.8	1,210	1,740	128.0
10-5(2) Qin-Modified	**89**	410.0	9,965	786	–
10-5(3) TOU-CO	104	337.8	1,800	1,740	185.8
10-5(3) Qin-Modified	117	418.4	10,333	746	–
10-5(4) TOU-CO	112	348.4	1,420	1,880	209.6
10-5(4) Qin-Modified	**91**	448.7	10,139	850	–
10-5(5) TOU-CO	98	345.2	1,800	1,810	226.5
10-5(5) Qin-Modified	**89**	447.1	10,318	775	–

VI. Conclusion

This work developed a scheduling framework to balance the use of slow and fast chargers assuming the bus routes and charger locations were fixed. A directed graph was used to model the available charge times for buses that routinely visit a station for charging. The incidence matrix of the graph was used to formulate a network flow constraint, group constraints were used to enforce the natural progression of the bus through the station at each visit, and charging constraints were added to model the battery charge of each bus using a first-order dynamic model. A MILP problem was formulated to enable the scheduling of BEB charging as well as determine the required number of chargers.

An example was presented that demonstrated the ability of the MILP formulation to utilize slow chargers when possible and fast chargers when needed to accommodate timing constraints and ensure a sufficient charge for route execution. The optimization was performed under three different scenarios. An excess of chargers existed in the first scenario and the scheduling framework was able to use the excess chargers to completely avoid times of high cost for an 19% reduction of cost. The second scenario demonstrated the ability of the scheduling framework to reduce the number of chargers required. With this reduced number of chargers, the third scenario again optimized over the schedule. While not completely able to avoid high-cost periods, the scheduling framework was still able to reduce costs by 21% while meeting charging threshold requirements. In each scenario the slow chargers were used significantly more than the fast chargers with increased fast charger usage when peak-time costs needed to be avoided.

Future work could explore the inclusion of additional power costs, additional charger types, multiple stations, and more rigorous battery health considerations. An additional avenue of exploration would be to extend this planning method for use in real-time operations with feedback from the real-time environment.

Acknowledgment

Any opinions, findings, and conclusion or recommendations expressed in this material are those of the authors and do not necessarily reflect the views of the National Science Foundation, the Department of Energy, or Pacificorp.

References

[1] G. De Filippo, V. Marano, and R. Sioshansi, "Simulation of an electric transportation system at the Ohio state university," *Appl. Energy*, vol. 113, pp. 1686–1691, Jan. 2014.

[2] M. Xylia and S. Silveira, "The role of charging technologies in upscaling the use of electric buses in public transport: Experiences from demonstration projects," *Transp. Res. A, Policy Pract.*, vol. 118, pp. 399–415, Dec. 2018.

[3] U. Guida and A. Abdulah. (2017). *ZeEUS eBus Report #2—An Updated Overview of Electric Buses in Europe*. International Association of Public Transport (UITP). [Online]. Available: http://zeeus.eu/uploads/publications/documents/zeeus-ebus-report-2.pdf

[4] J.-Q. Li, "Battery-electric transit bus developments and operations: A review," *Int. J. Sustain. Transp.*, vol. 10, no. 3, pp. 157–169, Mar. 2016.

[5] N. Lutsey and M. Nicholas, "Update on electric vehicle costs in the United States through 2030," Int. Council Clean Transp., Washington, DC, USA, Tech. Rep., 2019, doi: 10.13140/RG.2.2.25390.56646.

[6] S. N. Motapon, E. Lachance, L.-A. Dessaint, and K. Al-Haddad, "A generic cycle life model for lithium-ion batteries based on fatigue theory and equivalent cycle counting," *IEEE Open J. Ind. Electron. Soc.*, vol. 1, pp. 207–217, 2020.

[7] R. Wei, X. Liu, Y. Ou, and S. K. Fayyaz, "Optimizing the spatio-temporal deployment of battery electric bus system," *J. Transp. Geography*, vol. 68, pp. 160–168, Apr. 2018.

[8] M. T. Sebastiani, R. Luders, and K. V. O. Fonseca, "Evaluating electric bus operation for a real-world BRT public transportation using simulation optimization," *IEEE Trans. Intell. Transp. Syst.*, vol. 17, no. 10, pp. 2777–2786, Oct. 2016.

[9] Y. Wang, Y. Huang, J. Xu, and N. Barclay, "Optimal recharging scheduling for urban electric buses: A case study in Davis," *Transp. Res. E, Logistics Transp. Rev.*, vol. 100, pp. 115–132, Apr. 2017. [Online]. Available: https://www.sciencedirect.com/science/article/pii/S1366554516305725

[10] Y. He, Z. Liu, and Z. Song, "Optimal charging scheduling and management for a fast-charging battery electric bus system," *Transp. Res. E, Logistics Transp. Rev.*, vol. 142, Oct. 2020, Art. no. 102056.

[11] J.-Q. Li, "Transit bus scheduling with limited energy," *Transp. Sci.*, vol. 48, no. 4, pp. 521–539, Nov. 2014.

[12] X. Tang, X. Lin, and F. He, "Robust scheduling strategies of electric buses under stochastic traffic conditions," *Transp. Res. C, Emerg. Technol.*, vol. 105, pp. 163–182, Aug. 2019.

[13] G. Zhou, D. Xie, X. Zhao, and C. Lu, "Collaborative optimization of vehicle and charging scheduling for a bus fleet mixed with electric and traditional buses," *IEEE Access*, vol. 8, pp. 8056–8072, 2020.

[14] M. Rinaldi, E. Picarelli, A. D'Ariano, and F. Viti, "Mixed-fleet single-terminal bus scheduling problem: Modelling, solution scheme and potential applications," *Omega*, vol. 96, Oct. 2020, Art. no. 102070.

[15] M. Duan, G. Qi, W. Guan, C. Lu, and C. Gong, "Reforming mixed operation schedule for electric buses and traditional fuel buses by an optimal framework," *IET Intell. Transp. Syst.*, vol. 15, no. 10, pp. 1287–1303, Oct. 2021.

[16] L. Zhang, S. Wang, and X. Qu, "Optimal electric bus fleet scheduling considering battery degradation and non-linear charging profile," *Transp. Res. E, Logistics Transp. Rev.*, vol. 154, Oct. 2021, Art. no. 102445.

[17] Y. Bie, J. Ji, X. Wang, and X. Qu, "Optimization of electric bus scheduling considering stochastic volatilities in trip travel time and energy consumption," *Comput.-Aided Civil Infrastruct. Eng.*, vol. 36, no. 12, pp. 1530–1548, Dec. 2021.

[18] Y. Zhou, X. C. Liu, R. Wei, and A. Golub, "Bi-objective optimization for battery electric bus deployment considering cost and environmental equity," *IEEE Trans. Intell. Transp. Syst.*, vol. 22, no. 4, pp. 2487–2497, Apr. 2021.

[19] T. Liu and A. Ceder, "Battery-electric transit vehicle scheduling with optimal number of stationary chargers," *Transp. Res. C, Emerg. Technol.*, vol. 114, pp. 118–139, May 2020. [Online]. Available: https://www.sciencedirect.com/science/article/pii/S0968090X19304061

[20] C. Yang, W. Lou, J. Yao, and S. Xie, "On charging scheduling optimization for a wirelessly charged electric bus system," *IEEE Trans. Intell. Transp. Syst.*, vol. 19, no. 6, pp. 1814–1826, Jun. 2018.

[21] X. Wang, C. Yuen, N. U. Hassan, N. An, and W. Wu, "Electric vehicle charging station placement for urban public bus systems," *IEEE Trans. Intell. Transp. Syst.*, vol. 18, no. 1, pp. 128–139, Jan. 2017.

[22] N. Qin, A. Gusrialdi, R. P. Brooker, and A. Raissi, "Numerical analysis of electric bus fast charging strategies for demand charge reduction," *Transp. Res. A, Policy Pract.*, vol. 94, pp. 386–396, Dec. 2016. [Online]. Available: https://www.sciencedirect.com/science/article/pii/S096585641630444X

[23] R. Burkard, M. Dell'Amico, and S. Martello, *Assignment Problems: Revised Reprint*. Philadelphia, PA, USA: SIAM, 2012.

[24] D.-S. Chen, R. G. Batson, and Y. Dang, *Applied Integer Programming*. Hoboken, NJ, USA: Wiley, 2010.

[25] M. Mesbahi and M. Egerstedt, *Graph Theoretic Methods in Multiagent Networks*. Princeton, NJ, USA: Princeton Univ. Press, 2010.

[26] N. Watrin, H. Ostermann, B. Blunier, and A. Miraoui, "Multiphysical lithium-based battery model for use in state-of-charge determination," *IEEE Trans. Veh. Technol.*, vol. 61, no. 8, pp. 3420–3429, Oct. 2012.

[27] L.-R. Chen, R. C. Hsu, and C.-S. Liu, "A design of a grey-predicted Li-ion battery charge system," *IEEE Trans. Ind. Electron.*, vol. 55, no. 10, pp. 3692–3701, Oct. 2008.

[28] A. Abdollahi et al., "Optimal battery charging, Part I: Minimizing time-to-charge, energy loss, and temperature rise for OCV-resistance battery model," *J. Power Sources*, vol. 303, pp. 388–398, Jan. 2016.
[29] J. P. Hespanha, *Linear Systems Theory*. Princeton, NJ, USA: Princeton Univ. Press, 2018.
[30] Gurobi Optimization. (2021). *Gurobi Optimizer Reference Manual*. [Online]. Available: https://www.gurobi.com
[31] (Jan. 2021). *Large General Service—Rocky Moutain Power*. [Online]. Available: https://www.rockymountainpower.net/content/dam/pcorp/documents/en/rockymountainpower/rates-regulation/utah/rates/008_Large_General_Service_1_000_kW_and_Over_Distribution_Voltage.pdf

Justin Whitaker (Graduate Student Member, IEEE) received the B.S. degree in mechanical engineering from Brigham Young University in 2019. He is currently pursuing the Ph.D. degree with the Department of Electrical and Computer Engineering, Utah State University (USU). Since 2019, he has been a Graduate Research Assistant with USU. His research interests include enabling autonomous systems, intelligent coordination and planning, and optimal control. His current research interests include enabling intelligent coordination and planning for electric vehicles.

Greg Droge (Member, IEEE) received the B.S. degree (manga cum laude) from Brigham Young University in 2009 and the M.S. and Ph.D. degrees in electrical and computer engineering from the Georgia Institute of Technology in 2012 and 2014, respectively. He was a Research Engineer developing autonomous planning capabilities with the SPAWAR-PAC and USAF 309th SMXG, prior to joining USU, in 2018. He is currently an Assistant Professor with the Department of Electrical and Computer Engineering, Utah State University (USU). His research interests include planning and control techniques to coordinate multi-agent systems and is split between two major components: allocation techniques for autonomous systems with complex cross-schedule dependencies and model predictive control for distributed systems with coordination motion constraints.

Matthew Hansen (Graduate Student Member, IEEE) received the B.S. degree from Utah State University (USU) in 2020, where he is currently pursuing the Ph.D. degree in electrical engineering. His research interests include the intersection of control theory, machine learning, and wireless power transfer.

Daniel Mortensen received the B.S. and M.S. degrees in electrical engineering from Utah State University (USU), where he is currently pursuing the Ph.D. degree in electrical engineering. His interests in mathematical methods for optimization have also led him to pursue a second bachelor's degree in mathematics and statistics from the Department of Mathematics and Statistics, USU. Before the B.S. and M.S. degrees, he was a Signal Processing Engineer with the Space Dynamics Laboratory, Logan, Utah. His research focuses on mathematical methods for solving optimization problems for both model and data driven applications.

Jacob (Jake) Gunther (Senior Member, IEEE) is currently a Professor with the Department of Electrical and Computer Engineering, Utah State University (USU). His industrial work spanned an array of topics including target detection, sonar systems, satellite communications, speech recognition, acoustic echo cancellation using microphone arrays, and feedback cancellation for digital hearing aids. Since 2000, he has been with USU. His research interests include synthetic aperture radar, communication systems, radio astronomy, system identification, optimization, and machine learning.

CHAPTER 4

SCHEDULING BATTERY-ELECTRIC BUS CHARGING UNDER STOCHASTICITY USING A RECEDING-HORIZON APPROACH

Submitted to *IEEE Transactions on Intelligent Transportation Systems* [50]

Scheduling Battery-Electric Bus Charging under Stochasticity using a Receding-Horizon Approach

Justin Whitaker, *Graduate Student Member, IEEE,* Derek Redmond, *Graduate Student Member, IEEE,* Greg Droge *Member, IEEE,* Jacob Gunther *Senior Member, IEEE*

***Abstract*—A significant challenge of adopting battery electric buses into fleets lies in scheduling the charging, which in turn is complicated by considerations such as timing constraints imposed by routes, long charging times, limited numbers of chargers, and utility cost structures. This work builds on previous network-flow-based charge scheduling approaches and includes both consumption and demand time-of-use costs while accounting for uncontrolled loads on the same meter. Additionally, a variable-rate, non-linear partial charging model compatible with the mixed-integer linear program (MILP) is developed for increased charging fidelity. To respond to feedback in an uncertain environment, the resulting MILP is adapted to a hierarchical receding horizon planner that utilizes a static plan for the day as a reference to follow while reacting to stochasticity on a regular basis. This receding horizon planner is analyzed with Monte-Carlo techniques alongside two other possible planning methods. It is found to provide up to 52% cost savings compared to a non-time-of-use aware method and significant robustness benefits compared to an optimal open-loop method.**

***Index Terms*—Integer linear program, optimization, optimal scheduling, green transportation, batteries, power demand, receding horizon**

I. Introduction

With the growing interest in electric vehicles and the increasing push for greener transportation, many organizations and companies are looking to electrify significant portions of their fleet vehicles [1]. In particular, transportation agencies, like the Utah Transit Authority (UTA), are actively exploring and implementing the use of electric buses as replacements for traditional internal combustion engine (ICE) buses. A battery electric bus (BEB), however, has several difficulties compared to an ICE bus. The energy storage capacity of a BEB is usually less than an ICE bus, with significantly longer refueling time. Utility cost structures add complication with multiple components to the cost beyond the cost of energy usage or *consumption*. Charging several BEBs at once incurs *demand* costs, based on the maximum power draw, which can add significant expense [2]. Furthermore, it is common to have *time-of-use* (TOU), or time-dependent, costs. Accordingly, scheduling the charging of BEBs can make a significant impact in the day-to-day costs of using BEBs in place of ICE buses.

The stochasticity introduced into the system from real-world operations (traffic delays, discharge variations due to temperature, etc.) can also have significant adverse effect on the cost-aware scheduling of BEB charging. The complex cost structure, lower energy capacity, and slow refueling times means that BEBs often need to operate near the edge of their capabilities, which in turn amplifies the effects of the stochasticity. For example, a BEB that can normally operate with charging only at low-cost times, but that is experiencing higher than expected discharging due to temperature, traffic, etc. may require charging at inopportune times, such as during high cost TOU periods. If not properly addressed, this can even result in BEBs being at risk of violating minimum charge level constraints and being unable to continue operation. This work seeks to provide a method to mitigate the effects of stochasticity in scheduling the charging of BEB fleets while considering the complex utility pricing schedule for the fleet.

Various aspects of the problem have been addressed in the literature; of particular relevance to the proposed work are *utility costs*, *partial charging*, and *stochastice awareness*. A number of representative works are summarized with respect to these categories in Table I. As seen in Table I, nearly all works consider energy consumption costs. Fewer consider more complicated additions to the cost structure with [3], [4] considering TOU consumption costs while [5]–[7] additionally consider TOU demand costs. Despite rare consideration, these additional costs can account for a significant percentage of the overall charging costs [2], [7]

Additionally, several methods of modelling charging behavior have been explored, with the most common methods being to either assume full-charge, utilize a linear partial charge model, or to form a non-linear partial charging model. As Table I shows, many works assume a BEB always charges to full capacity when scheduled to charge, e.g., [3], [4], [8], [9]. This simplifies the problem, but also reduces fidelity and flexibility. In contrast, a partial charging model was key to [5]–[7] considering demand costs and gaining significant cost improvements. Works with partial charging use either linear [6], [7], [10] or non-linear [5], [11], [12] charging profile models. The approaches that utilize a non-linear charging profile achieve a higher fidelity model of charging behavior, typically at the cost of increased computation requirements (e.g., [11]). One exception is [5], where a linear program is formed with piecewise-linear charging profiles. This formulation, however, assumes that a charger is always available

This work was supported in part by the National Science Foundation through the Advancing Sustainability through Powered Infrastructure for Roadway Electrification (ASPIRE) Engineering Research Center under Grant EEC-1941524, in part by the Department of Energy through a Prime Award with ABB Ltd., under Grant DE-EE0009194, and in part by PacifiCorp under Contract 3590.

The authors are with the Department of Electrical and Computer Engineering, Utah State University (USU), Logan, UT 84322, USA (email: {justin.whitaker derek.redmond greg.droge jake.gunther}@usu.edu)

TABLE I
AN OVERVIEW OF THE FEATURES PRESENT IN THE LITERATURE.
An asterisk (*) indicates a limited formulation.

	Utility Costs			Partial Charging			Stochastic Awareness	
	Consumption	Demand	TOU	Linear	Non-linear	Variable-Rate	Static	Dynamic
[2]	✓	✓	-	-	✓*	-	-	-
[3]	✓	-	✓	-	-	-	-	-
[4]	✓	-	✓	-	-	-	-	-
[5]	✓	✓	✓	✓*	-	✓*	-	-
[6]	✓	✓	✓	✓	-	-	-	-
[7]	✓	✓	✓	✓	-	✓	-	-
[8]	✓	-	-	-	-	-	✓	-
[9]	✓	-	-	-	-	-	-	✓
[10]	✓	-	✓	✓	-	-	-	-
[11]	✓	-	-	-	✓	-	-	-
[12]	✓	-	✓	-	✓	-	-	-
[13]	✓	-	✓	✓	-	-	-	-
[14]	✓*	✓*	-	-	✓*	-	-	-
[15]	✓*	✓	-	-	✓*	-	-	-
[16]	✓	-	-	-	-	-	✓	-
[17]	✓	-	✓	-	-	-	-	✓
[18]	✓	-	✓	-	-	-	-	✓
Proposed	✓	✓	✓	✓	✓	✓	-	✓

when needed, which is often impractical. Another exception is our prior work in [12], where a discrete linear time-invariant dynamic system model is used, resulting in an exponential decay non-linear charge model. This exponential decay model, however, is only a rough approximation of a typical non-linear charging profile. Non-linear partial charging models that are also computationally attractive are not currently present in the literature without the aforementioned drawbacks.

Most of the works in the state-of-the-art assume the charging rate to be fixed for a charger, as Table I shows. As the charging rate directly determines power draw, it can significantly affect demand cost, making it a useful method of decreasing costs. For example, [7] uses a set of discrete charge rates with a linear model to reduce the maximum power draw, and consequently the demand cost, but is limited to a few rates. However, only [5], [7] could be found that use a variable rate charging model for BEB charge scheduling, the one limited to a few discrete rates, and the other assuming unlimited chargers.

As Table I displays, the majority of the BEB charge scheduling methods neglect the presence of real-world noise and variability. Some works, however, account for this stochasticity in both *static* [8], [16] and *dynamic* [9], [17], [18] frameworks. In [8], [9], [16], a static, *a priori* charge scheduling problem is solved to be robust to the expected sources of noise. The approach taken by [9] uses a buffer time at the end of bus routes to maintain feasibility, while [8], [16] directly incorporate the characteristics of the noise of energy consumption and route delays in a robust optimization problem. In contrast, [9], [17], [18] utilize dynamic methods that receive feedback from and react to the real-world state. In [9], the buffered, *a priori* scheduling problem is repeatedly solved with feedback from the environment, while [17], [18] use a Markov Decision Process to repeatedly solve for an optimal policy for each bus based on feedback. However, each of the methods that address stochasticity only consider TOU consumption costs and neglect TOU demand costs. To the best of our knowledge, no work that considers stochasticity also considers the full TOU consumption and demand cost structure despite the significant effects of these cost components. Furthermore, each of these works assume a BEB charges to full whenever scheduled with no partial charging, and no work could be found that included a partial charging model. Accordingly, a significant gap in the literature exists when accounting for the intrinsic stochasticity of the real-world.

In light of this state of the art, this work seeks to address gaps in the literature by providing two primary contributions.

1) A novel discrete, time-invariant, piecewise linear formulation is developed to model a non-linear constant-current/constant-voltage charging profile while considering variable-rate charging.
2) A novel two-stage dynamic receding horizon planning hierarchy is developed to react to feedback from the environment and to fully account for TOU consumption and demand costs.

These contributions are demonstrated within an extensive Monte Carlo simulation environment, demonstrating the ability of the planning hierarchy to cope with the stochastic environment.

The remainder of the paper will proceed with the formulation of the problem as a network flow problem and mixed integer linear program from previous work in Section II. Section III continues by detailing the novel modeling of the non-linear, variable-rate charging profile. This is followed by Section IV which gives the cost formulations and the full static optimization model. Following this, Section V outlines the hierarchical dynamic planning structure, after which Section VI presents the experimental findings and their analysis. Section VII concludes with a summary of the findings and their impact.

II. A NETWORK FLOW REPRESENTATION OF THE BEB CHARGING SCHEDULE

The assignment of chargers to buses can be abstracted into a network-flow problem. This network flow problem can be converted into a mixed-integer linear program (MILP) that allows modeling additional aspects and constraints of the system, such as battery charge level dynamics and constraints, power usage and demand costs, and logistic constraints. This work follows a similar process for creating the network-flow and MILP models as [12] and then extends the model to account for TOU demand and a non-linear CC/CV charging profile. For the sake of completeness, the full models used in this work are given, with the modifications and extensions to [12] appropriately derived and noted. This section begins with a brief introduction to relevant graph and network-flow concepts in Section II-A and their relation to the BEB charge scheduling problem. Finally, Section II-B details the constraints of the MILP relating to and extending the network-flow model.

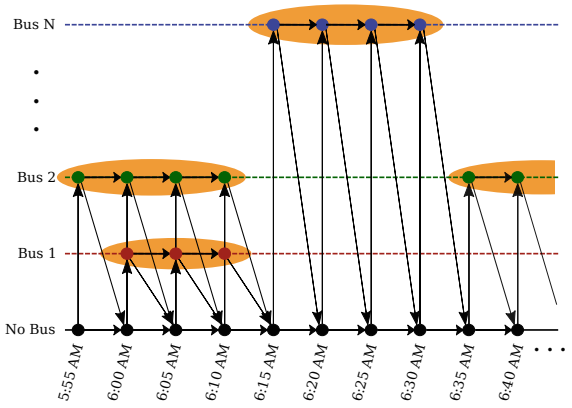

Fig. 1. A graph depicting the possible state and transitions for a single charger type over time for a simple bus charging example. The bottom row corresponds to the charger at rest while the other rows each correspond to charging a particular bus. Yellow ovals show the vertex groups that are placed around charging windows.

A. Graph and Network Flow From Previous Work [12]

A directed graph G is defined as a set of vertices, V, and edges, $E \subseteq V \times V$, i.e. $G = \{V, E\}$. Given two vertices in the graph, $v_1, v_2 \in V$, an edge from v_1 to v_2 implies that the ordered pair (v_1, v_2) is in the edge set, i.e., $(v_1, v_2) \in E$.

With the concept of *flow* along edges, a network-flow problem can be represented by a graph. For scheduling BEB charging when the BEB route schedules are known *a priori*, each vertex can be considered a state for a charger, with edges representing the action space of chargers. The amount of flow along an edge indicates the number of chargers performing the corresponding action. A *source* vertex introduces flow, or chargers, into the network, while *sink* vertices remove flow. All other vertices are *intermediary* vertices, and maintain a balance of flow in and out of the vertex. The edges in the graph correspond to one of 1) a charger transitioning to or from charging a BEB, 2) charging a BEB, or 3) doing nothing. Chargers that are in the same location and have the same characteristics are considered together as a *charger type* in a sub-graph separate from other charger types. A vertex is only present in a sub-graph when a bus will be available to charge with the corresponding charger type.

A simplified example of such a graph is shown in Fig. 1 for a single charger type; a full graph contains other similar sub-graphs for each charger type. Vertices that are grouped together (represented with an orange oval) correspond to one *visit* to the station. This grouping applies across charger types as long as they correspond to the same visit to the station.

B. Constraints from Previous Work [12]

In converting to a MILP formulation, constraints are needed to correctly model the problem. The first set of constraints maintains the relationships defined by the network flow graph. A second group of constraints is added that ensures that each bus can only be charged by one charger and each charger can only charge one bus. The final set of constraints is used to track the bus charge levels through charging and discharging.

1) Flow balance: Typical flow balance constraints ensure that the chosen path moves continuously from one vertex to another through the graph. The vector $\mathbf{x} = \begin{bmatrix} x_1 & x_2 & \cdots & x_{n_e} \end{bmatrix}^\mathsf{T}$ consists of the flow variables for each edge. Similarly, a vector $f_l = \begin{bmatrix} n_{c_l} & 0 & \cdots & 0 & -n_{c_l} \end{bmatrix}^\mathsf{T}$ contains the net flow into or out of each vertex for each charger type $l \in \mathcal{L}$. The incidence matrix, D_l, (as defined in [19]) is created for each sub-graph corresponding to a different charger type. Each row of the expression $D_l\mathbf{x}$ gives the net flow through a vertex and can be constrained as

$$D_l\mathbf{x} = f_l \qquad \forall l. \tag{1}$$

2) Vertex Grouping Constraint: Connecting a BEB to a charger typically requires coordination and time. Accordingly, it is undesirable to allow a bus to connect to a charger more than one time in a visit to a station. By grouping the vertices by each bus's visit to the station and only allowing one flow to enter the group this can be enforced. For the p^{th} visit by a bus to the station, denote the corresponding grouping of vertices as the set $\mathcal{V}_p \subset V$. Then, the index set of edges that enter $\mathcal{V}_p$ is defined as

$$\begin{aligned} \mathcal{I}_p = \{i | e_i \in E \text{ where } e_i = (v_m, v_n), \\ v_n \in \mathcal{V}_p, \text{ and } v_m \in V \setminus \mathcal{V}_p\} \end{aligned}. \tag{2}$$

The constraint that a bus be charged by at most a single charger when at the station can be written as

$$\sum_{i \in \mathcal{I}_p} x_i \leq 1 \qquad p = 1, \ldots, n_g, \tag{3}$$

where n_g is the number of groups. Combined with the constraint that x_i is integer, (3) ensures that the number of chargers assigned to a bus during a visit is at most one.

III. Non-Linear, Variable-Rate Charge Profile

A non-linear, variable-rate charging profile model allows for high-fidelity predictions of BEB charge levels, power usage, and subsequent utility costs. In [12], a discrete, linear time-invariant system was used to generate an exponential decay non-linear charging profile that loosely approximates a constant-current-constant-voltage (CC-CV) charge profile. This method is extended herein to form a discrete, piecewise linear time-invariant system that closely approximates an idealized CC-CV charging profile instead of an exponential decay model.

The formulation of the CC-CV system starts with a model in continuous-time that is exactly discretized to arrive at a discrete, piecewise linear time-invariant system in Section III-A. Section III-B adjusts the model to allow for variable rate charging with a close approximation. Finally, the model is presented in the form of MILP constraints in Section III-C

A. Modelling a CC-CV Charging Profile in Continuous Time

Forming the CC-CV model is based in a continuous-time piecewise-linear time-invariant dynamic system of the CC-CV charging profile.

Lemma 1. *The CC-CV charging profile with switching SOC of η_j for a bus, j, with battery capacity E_j can be modeled in continuous-time by the piecewise-linear time-invariant continuous dynamic system in the charge level, s_j:*

$$\dot{s}_j(t) = \begin{cases} a_l^{cc} s_j(t) + b_l^{cc} & 0 \le s_j(t) < \eta_j E_j \\ a_l^{cv} s_j(t) + b_l^{cv} & \eta_j E_j \le s_j(t) \end{cases}. \quad (4)$$

where

$$\begin{aligned} a_l^{cc} &= 0 & b_l^{cc} &= p_l^{cc} \\ a_l^{cv} &= -\alpha_{j,l} & b_l^{cv} &= \alpha_{j,l} p_l^{cc} t_{j,l}^{cc} + p_l^{cc}, \end{aligned} \quad (5)$$

and $\alpha_{j,l}$ and p_l^{cc} are parameters of the model derived from the charger characteristics.

Proof. See Appendix A □

As a linear time-invariant system, Eq. (4) can be discretized exactly for a given discretization step size of δ, as in [20]. This is stated more formally in Lemma 2.

Lemma 2. *The CC-CV charging profile can be modeled by the piecewise-linear time-invariant discrete dynamic system:*

$$s_{j,k+1} = \begin{cases} \bar{a}_l^{cc} s_{j,k} + \bar{b}_l^{cc} & 0 \le s_{j,k} < \eta_j E_j \\ \bar{a}_l^{cv} s_{j,k} + \bar{b}_l^{cv} & \eta_j E_j \le s_{j,k} \end{cases} \quad (6)$$

where

$$\begin{aligned} \bar{a}_l^{cc} &= e^{a_l^{cc}\delta} = 1 & \bar{b}_l^{cc} &= \int_0^\delta e^{a_l^{cc}\tau} d\tau b_l^{cc} = b_l^{cc}\delta \\ \bar{a}_l^{cv} &= e^{a_l^{cv}\delta} & \bar{b}_l^{cv} &= \int_0^\delta e^{a_l^{cv}\tau} d\tau b_l^{cv} = \frac{(\bar{a}_l^{cv} - 1) b_l^{cv}}{a_l^{cv}}. \end{aligned} \quad (7)$$

Proof. See Appendix B. □

B. Variable-rate Mixed Integer Charging Model

The discrete linear system (6) only holds while the bus is charging, and differs in specific parameter values between charger types. To unify the treatment of when a bus is charging and when it is not, a slack variable, $g_{j,k,l}$, is introduced. This variable represents the energy gained by bus j at charger type l from discrete time k to $k+1$ and should take on a value of zero if bus j did not charge at a charger type l from time k to $k+1$.

For notational convenience, a mapping, $\sigma(j,k,l)$, is defined that gives the edge index corresponding to bus j charging with charger type l starting at time k (i.e., the edge spans from k to $k+1$). This provides a method to easily select the edge flow that corresponds to a gain variable.

To achieve the desired behavior of the gain variable several constraints are introduced, beginning with those that enforce a value of zero if the bus is not charging,

$$\begin{aligned} g_{j,k,l} &\ge 0 \\ g_{j,k,l} &\le E_j x_{\sigma(j,k,l)} \end{aligned}. \quad (8)$$

The constraints in (8) utilize a big-M style formulation to enforce equality to zero when $x_{\sigma(j,k,l)} = 0$ but allow $g_{j,k,l}$ to take on other values when $x_{\sigma(j,k,l)} = 1$.

When $x_{\sigma(j,k,l)} = 1$ additional constraints must ensure that $g_{j,k,l}$ takes on the appropriate value. If $x_{\sigma(j,k,l)} = 1$, the gain is equivalent to $s_{j,k+1} - s_{j,k}$. Given $s_{j,k+1}$ in (6), $g_{j,k,l}$ can be written in terms of $s_{j,k}$ as

$$g_{j,k,l} = \begin{cases} (\bar{a}_l^{cc} - 1) s_{j,k} + \bar{b}_l^{cc} & 0 \le s_{j,k} < \eta_j E_j \\ (\bar{a}_l^{cv} - 1) s_{j,k} + \bar{b}_l^{cv} & \eta_j E_j \le s_{j,k} \end{cases},$$

which, since $a_l^{cc} = 1$, simplifies to

$$= \begin{cases} \bar{b}_l^{cc} & 0 \le s_{j,k} < \eta_j E_j \\ (\bar{a}_l^{cv} - 1) s_{j,k} + \bar{b}_l^{cv} & \eta_j E_j \le s_{j,k} \end{cases}. \quad (9)$$

This gives a piecewise linear equality constraint to enforce the value of $g_{j,k,l}$.

While it would be possible to formulate this piecewise linear constraint using specially ordered sets of type two[1], this would introduce many additional binary variables. Additionally, in many cases it is desirable to allow the charging rate to vary within the capabilities of the charger. Variable rate charging allows reducing the power draw and energy usage to only what is strictly necessary, potentially resulting in additional cost reductions.

Accordingly, by only constraining $g_{j,k,l}$ to be bounded above by (9), instead of maintaining strict equality, the effective charge rate is allowed to vary. This results in the ideal constraint

$$g_{j,k,l} \le \begin{cases} \bar{b}_l^{cc} & 0 \le s_{j,k} < \eta_j E_j \\ (\bar{a}_l^{cv} - 1) s_{j,k} + \bar{b}_l^{cv} & \eta_j E_j \le s_{j,k} \end{cases}. \quad (10)$$

Enforcing this constraint exactly, however, would still require the use of a specially ordered set of type two and additional binary variables to model the switching point of the inequality.

This can be overcome by using a conservative concave approximation of (10) that relaxes the switching point of the two lines of (10). This is more formally stated in Lemma 3.

Lemma 3. *The inequality* (10) *is conservatively approximated by*

$$\begin{aligned} g_{j,k,l} &\le \bar{b}_l^{cc} \\ g_{j,k,l} &\le (\bar{a}_l^{cv} - 1) s_{j,k} + \bar{b}_l^{cv}. \end{aligned} \quad (11)$$

Furthermore, for a given desired approximation error, ϵ_d, there exists a discretization step size, δ, for which the approximation error of (11)*, ϵ, is bounded by ϵ_d (i.e., $|\epsilon| \le \epsilon_d$).*

Proof. See Appendix C □

C. Formulating the Charging Profile Model for Optimization

To fully specify the charge level constraints, several useful sets are defined. For this purpose, an indicator function, $\gamma(j,k,l)$, is first introduced

$$\gamma(j,k,l) = \begin{cases} 1 & \text{if charging bus } j \text{ with charger type } l \\ & \text{from time } k \text{ to } k+1 \text{ is possible} \\ 0 & \text{otherwise} \end{cases}.$$

Two parameterized sets are defined: $\mathcal{L}(j,k)$ represents the charger types available for a bus j at a given time k, and

[1] See [21] for an introduction to specially ordered sets and their application to constraint modelling.

$\mathcal{K}(j,l)$ represents the times when bus j is able to charge with charger type l. These are defined as follows

$$\begin{aligned}\mathcal{L}(j,k) &= \{l \mid \gamma(j,k,l) = 1\} \\ \mathcal{K}(j,l) &= \{k \mid \gamma(j,k,l) = 1\}\end{aligned}.$$

Additionally, for notational convenience, the quantity $g(j,k)$ represents all of the charge gained by bus j at time k:

$$g(j,k) = \sum_{l \in \mathcal{L}(j,k)} g_{j,k,l}.$$

The parameter $d_{j,k}$ is also introduced to represent the discharge of bus j from k to $k+1$ while on route. Then, the charge level constraints can be fully specified

$$s_{j,k+1} = \begin{cases} s_{j,k} + g(j,k) & \text{if } \exists l \text{ s.t.} \\ & \gamma(j,k,l) = 1 \\ s_{j,k} - d_{j,k} & \text{otherwise} \end{cases} \quad \forall j, \forall k \tag{12}$$

with $g_{j,k,l}$ defined through a combination of Eq. (8) and Eq. (11)

$$\left.\begin{aligned} & g_{j,k,l} \le b_l^{cc} \\ & g_{j,k,l} \le (\bar{a}_l^{cv} - 1)s_{j,k} + \bar{b}_l^{cv} \\ & g_{j,k,l} \le 0 + E_j x_{\sigma(j,k,l)} \\ & g_{j,k,l} \ge 0 \end{aligned}\right\} \quad \begin{aligned} & \forall j, \forall l, \\ & \forall k \in \mathcal{K}(j,l) \end{aligned}. \tag{13}$$

IV. Minimization of Utility Costs

A significant source of operational costs for electric buses comes from charging the batteries and is governed by the electricity utility costs. Electricity utility costs often consist of two components: a "consumption" portion, based on the energy consumed over the billing period, and a "demand" portion based on the peak or maximum power draw that occurs within the billing period, e.g., [22]. It is also common for both of these components to have time-dependent rates, typically termed time-of-use (TOU) pricing, where the rate for consumption and/or demand cost changes based on the time of day[2]. The following formulation for the cost in the optimization problem, therefore, seeks to support both consumption and demand costs with TOU pricing for each.

A. Consumption Cost

The energy cost is a charge per kilowatt-hour (kWh) of energy consumed. There are different rates for high- and low-demand times. Because the gain variables, $g_{j,k,l}$, already represent the energy in kilowatt-hours used during each discrete time period, this cost is a linear combination of the $g_{j,k,l}$. Accordingly, the total energy cost can be calculated as

$$\sum_{k \in \mathcal{K}} c_{c,k} \sum_{j \in \mathcal{J}} g(j,k)$$

where each $c_{c,k}$ is a time-dependent cost on the energy consumed in the corresponding time step and, thus, encapsulates the TOU consumption pricing.

[2]For example, the Rocky Mountain Power company's Utah rate schedule eight includes both consumption and demand costs with both on- and off-peak TOU pricing for consumption and demand [22].

B. Baseline Demand Cost

In its simplest form, the demand cost might be based purely on the maximum power draw. However, it is common for utility costs to include an averaging component to smooth near-instantaneous behavior. The model herein is based on a 15-minute moving window demand cost from the Rocky Mountain Power Schedule 8 [22]. In other words, the cost is

$$c_b \max_t (p_{15}(t))$$

where c_b is the baseline demand cost multiplier and $p_{15}(t)$ is the average power over the 15 minutes ending at time t. For the sake of generalization, an arbitrary-sized time period, Δ, is considered for averaging instead of a 15-minute period. The average power over a time period Δ ending at time t can be calculated as

$$p_\Delta(t) = \frac{1}{\Delta} \int_{t-\Delta}^{t} p(\tau) d\tau.$$

Defining $e_\Delta(t) \triangleq \int_{t-\Delta}^{t} p(\tau) d\tau$ as the energy over the time period Δ ending at t, the average power is

$$p_\Delta(t) = \frac{e_\Delta(t)}{\Delta}.$$

To relate this to the gain variables of the MILP we recall that the gain variable $g_{j,k,l}$ is the energy used by bus j, with charger type l over the time period from k to $k+1$. Thus, the total energy used by charging buses over a discretization step, δ (from k to $k+1$), is

$$e_{\delta,k}^{buses} = \sum_{j \in \mathcal{J}} g(j,k). \tag{14}$$

However, there may be additional, uncontrolled loads that also contribute to the average power draw. A prediction of these uncontrolled loads can be incorporated to discourage charging buses during times of high draw from these uncontrolled loads. It is assumed that a prediction of the discrete-time energy usage of these uncontrolled loads can be obtained as $e_{\delta,k}^{load}$. The total energy used over a discretization step is

$$e_{\delta,k} = e_{\delta,k}^{load} + e_{\delta,k}^{buses}. \tag{15}$$

Accordingly, a discrete average power can be calculated

$$p_{\Delta,k} = \frac{\sum_{k'=k-m}^{k-1} {e_{\delta,k'}}^3}{\Delta} \tag{16}$$

with $m = \frac{\Delta}{\delta}$. The maximum of (16) over all time instances (over all k) is used for the baseline demand cost, i.e.,

$$c_b \max_k p_{\Delta,k}.$$

This $\max_k p_{\Delta,k}$ can be calculated in the MILP by introducing a slack variable, p_{max}, with the constraints

$$p_{max} \ge p_{\Delta,k}, \forall k.$$

[3]The discretization step size δ may not evenly divide Δ. In this case, $m = \left\lfloor \frac{\Delta}{\delta} \right\rfloor$ and the numerator would be

$$\sum_{k'=k-m}^{k-1} e_{\delta,k'} + \frac{\Delta \mod \delta}{\delta} e_{\delta,k-m-1}. \tag{17}$$

Together, these constraints ensure that p_{max} is at least as large as the largest $p_{\Delta,k}$, and the minimization of the baseline demand cost will drive p_{max} to equal the largest of the $p_{\Delta,k}$.

This allows the baseline demand cost to be written as

$$c_b p_{max}.$$

C. TOU Demand Cost

The TOU demand cost is an additional cost on the maximum average power used during high-demand times of the day. It is very similar to the baseline demand charge except that the TOU demand cost is calculated only for the k corresponding to the high-demand times (e.g., 6–9 AM and 6–10 PM). Defining $\mathcal{K}_{TOU}$ as the set of k that are within the high-demand times $p_{max,TOU}$ is introduced as another slack variable to the MILP,

$$p_{max,TOU} \geq p_{\Delta,k}, \quad k \in \mathcal{K}_{TOU},$$

that, similar to (IV-B), will be forced to equality through the cost minimization. The TOU demand cost can be expressed as

$$c_{TOU} p_{max,TOU}.$$

D. Base Model

For notational convenience, several variables are introduced

$$\begin{aligned} x &= \{x_i \forall i \in \mathcal{I}\} \\ s &= \{s_{j,k} \forall j \in \mathcal{J}, k \in \mathcal{K}\} \\ g &= \{g_{j,k,l} \forall j \in \mathcal{J}, k \in \mathcal{K}, l \in \mathcal{L}\} \\ e_\delta &= \{e_{\delta,k} \forall k \in \mathcal{K}\} \\ e_\Delta &= \{e_{\Delta,k} \forall k \in \mathcal{K}\} \\ p_\Delta &= \{p_{\Delta,k} \forall k \in \mathcal{K}\} \end{aligned}$$

Combining the constraints and costs as previously described, the base MILP for a static plan is written as follows:

$$\min_{\substack{x,s,g,\\ e_\delta,e_\Delta,p_\Delta,\\ p_{max},\\ p_{max,TOU}}} \quad \sum_{k\in\mathcal{K}} c_{c,k} \sum_{j\in\mathcal{J}} g(j,k) + c_b p_{max} + c_{TOU} p_{max,TOU} \tag{18a}$$

s.t.

$$D_l \mathbf{x} = f_l, \qquad \forall l \in \mathcal{L} \tag{18b}$$

$$\sum_{i\in\mathcal{I}_p} x_i \leq 1, \qquad \forall p \in \mathcal{P} \tag{18c}$$

$$s_{j,k+1} = \begin{cases} s_{j,k} + g(j,k) & \text{if } \exists l \text{ s.t. } \gamma(j,k,l) = 1 \\ s_{j,k} - d_j & \text{otherwise} \end{cases}, \quad \begin{matrix} \forall j \in \mathcal{J} \\ \forall k \in \mathcal{K} \end{matrix} \tag{18d}$$

$$\begin{aligned} &g_{j,k,l} \leq b_l^{cc} \\ &g_{j,k,l} \leq (\bar{a}_l^{cv} - 1) s_{j,k} + \bar{b}_l^{cv} \\ &g_{j,k,l} \leq 0 + E_j x_{\sigma(j,k,l)} \\ &g_{j,k,l} \geq 0 \end{aligned} \quad \begin{matrix} \forall j \in \mathcal{J} \\ \forall l \in \mathcal{L} \\ \forall k \in \mathcal{K}(j,l) \end{matrix} \tag{18e}$$

$$e_{\delta,k} = e_{\delta,k}^{load} + \sum_{j\in\mathcal{J}} g(j,k), \qquad \forall k \in \mathcal{K} \tag{18f}$$

$$p_{\Delta,k} = \frac{\sum_{k'=k-m}^{k-1} e_{\delta,k'}}{\Delta}, \qquad \forall k \in \mathcal{K} \tag{18g}$$

$$p_{max} \geq p_{\Delta,k}, \qquad \forall k \in \mathcal{K} \tag{18h}$$

$$p_{max,TOU} \geq p_{\Delta,k}, \qquad \forall k \in \mathcal{K}_{TOU} \tag{18i}$$

V. Receding Horizon Formulation

The base model of Eq. (18) is able to generate optimal plans for a given discretization. These plans, however, are static, or open-loop, meaning that there is no way to react to noise or model mismatches. However, as the noise is assumed to be zero-mean, the base-model plan is expected to still be a near-optimal reference to attempt to follow, on average. This suggests a two-level hierarchical approach, as visualized in Fig. 2, that is the proposed method of this work. The top-level of the hierarchy consists of the base-model forming a long-term static plan. The top-layer plan uses a coarser resolution to be able to form a plan for the whole day that captures long-term behaviors and constraints. The bottom-layer is a planner that takes as input the long-term static plan as a reference and feedback from the environment. The bottom-layer planner regularly outputs a plan with finer resolution than the static planner, allowing rapidly reacting to the environment [23].

In this work a *receding horizon* controller is used as the bottom-level planner. The receding horizon controller uses the current state of the buses to plan over a relatively short time horizon. A single time step of this plan is executed, after which feedback from the environment is collected (e.g., current BEB charge levels). The controller continues by forming a plan over a new horizon, which has "receded" one time step beyond the previous horizon. Receding horizon approaches typically use an optimization model with a "running" cost (objective) that scores the state and control trajectory, and a "terminal" cost (objective) that scores the state at the end of the horizon. The terminal cost drives the system toward a set of desired states while the running cost affects the transient behavior. The dynamics and other state and control constraints are enforced in the optimization model. It is important to stress that despite using optimization to form a plan for each horizon, there is no general guarantee of optimality with a receding horizon approach.

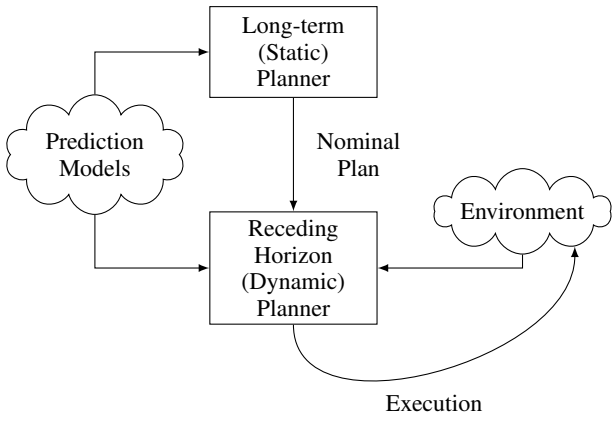

Fig. 2. The two-level hierarchical planning method and its interactions with the environment

To obtain the model to use in the receding horizon planner for this problem, the existing optimization model is modified to fit the receding horizon paradigm. Accordingly, the following adjustments are made to the base model (18)

- A terminal cost is added to the objective function to drive the controller toward the charge levels given by the top-layer reference plan.
- Constraints are added that continue to ensure that a bus charges at most once during a visit to the station.

The terminal cost is formed using a penalty on the difference between a bus's terminal charge level in the receding horizon plan and its charge level predicted by the top-level plan. To add this to the MILP, a slack variable, $s_{j,err}$, is introduced as

$$s_{j,err} \geq \begin{cases} s_{j,T,des} - s_{j,T} \\ s_{j,T} - s_{j,T,des} \end{cases}, \tag{19}$$

where T is the terminal time of the horizon, $s_{j,T}$ is the receding horizon terminal charge level for bus j, and $s_{j,T,des}$ is the predicted charge level of the bus at T. Each $s_{j,err}$ is added to the cost function, and consequentially (19) is equivalent to the 1-norm of the error between $s_{j,T}$ and $s_{j,T,des}$.

Ensuring a bus only charges at most once during a visit to the station involves tracking whether a bus has already charged in a visit or not. By tracking these variables separate from the receding horizon iterations, each receding horizon optimization problem can be constrained to disallow further charging by any bus that has already charged in a station visit.

VI. Results

An empirical analysis of the characteristics of this method is presented to demonstrate the capabilities of this approach. The general scheduling scenario is presented first, followed by an outline of the noise sources and characteristics. Finally, Monte-Carlo experiments are performed to characterize the behavior and performance of the receding horizon planning.

A. Bus Charging Scenario

Three bus charging scenarios are used to analyze the methodology, each based in the deployment scenarios of the Utah Transit Authority (UTA). In the near future UTA plans to have 18 BEBs running in the Salt Lake City (SLC), Utah area and 10 BEBs in the Ogden, Utah area running the 2, 209, 220, 509, 602, and 603X UTA routes. As an example, the 18 SLC schedules are visualized in Fig. 3. The experiments in this work utilize the schedules from these two locations as the basis for two of the situations to run in the Monte-Carlo simulations for each location.

The third scenario is one that is randomly generated with 30 buses using a generation method resulting in similar routes to those in the UTA schedules. This method randomly selects a route length, an amount of time in the station, and a nominal on-route power draw for each bus. Then, a schedule is formed by alternating on-route and in-station times through the day until the evening (23:00 in this work) when the bus returns to the depot. The route lengths are selected uniformly from 45 to 150 minutes, the time in station from 20 to 45 minutes, and a nominal power draw over the route from 28 to 36 kW.

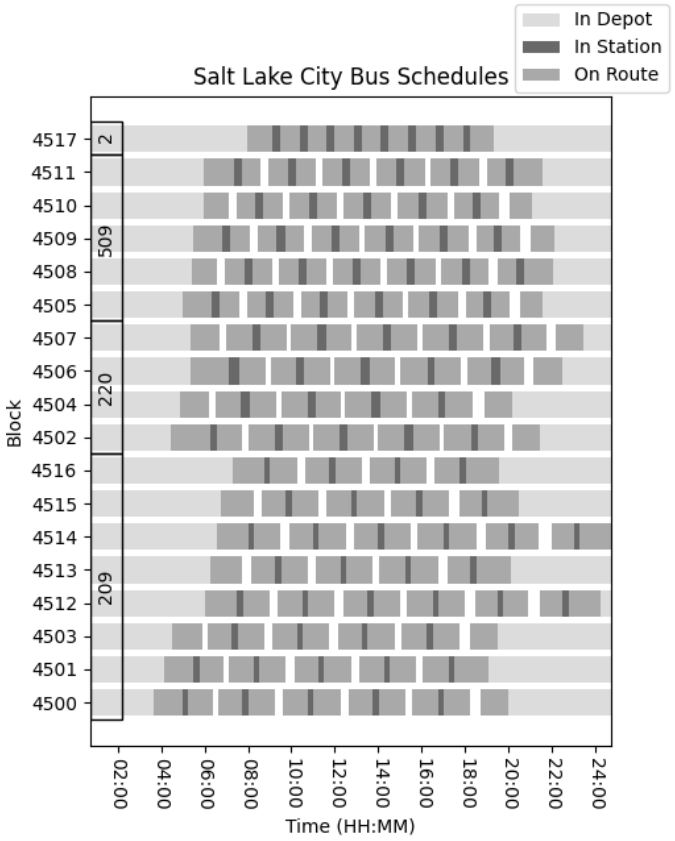

Fig. 3. The schedules for buses in the Salt Lake City, Utah area that serve routes 2, 209, 220, and 509.

The cost structure used in the following experiments is derived from the Rocky Mountain Power (RMP) Schedule 8 [22] rate schedule for the winter months. This rate schedule includes both consumption and demand costs, with a TOU component to each. The $c_{c,k}$ is set to \$0.051577 for the time k in the peak times of 06:00–09:00 and 18:00–22:00 and set to \$0.026216 in the off-peak times. The set $\mathcal{K}_{high\text{-}demand}$ is defined to match these same peak times. The off-peak demand rate, c_b, is set to \$4.81 with the on-peak rate, c_{TOU}, set to \$13.92 These rates are used for both the reference day plan and the receding horizon planner.

B. Planning parameters

As described in Section V, a static long-term plan is generated by solving the MILP in (18). For this work a 24-hour period is used in this static plan as it is naturally repeatable. A discretization step size of 5 minutes is used as it was found to adequately balance computational complexity and solution resolution. To mitigate the possibility that the upper and lower charge level constraints are violated when noise is introduced in the Monte-Carlo simulations, the static day plan uses a 5% SOC lower/higher buffer on the upper/lower bound constraints. To encourage staying near the middle of the battery capacity range, which is better for battery health [24], the initial SOC for all buses is set to 70%. The buses are required to end the day at the same 70% SOC to ensure that the generated

TABLE II
VARIABLE-RATE VS FIXED-RATE COST AND COMPUTATION

	Day Cost		Optimality Gap at 600 s (Solve Time to Optimality)	
	Variable-rate	Fixed-rate	Variable-rate	Fixed-rate
SLC	\$648.57	\$666.10	(5.76 s)	9.92%
Ogden	\$255.46	\$292.52	(9.92 s)	32.62%
Random	\$329.34	\$339.52	3.16%	10.85%

schedule is repeatable. This problem is solved using the off-the-shelf Gurobi solver [25] limited in solve time to 6 hours.

Similarly, the receding horizon method needs the discretization step size, horizon length and the optimization solve time limit to be determined. A horizon length of 1 hour with discretization of 3 minutes are used in this work. These parameters were found to allow sufficient predictive capabilities, while maintaining a relatively short optimization time limit of 10 seconds. This short time limit is important for performing many Monte Carlo runs within a reasonable time. In practice, a larger horizon and/or finer discretization could be used.

C. Benefits of variable-rate charging

To validate the benefits of variable-rate charging, the Random, Ogden, and SLC scenarios were compared in both costs and solve complexity under both a fixed-rate and variable-rate formulation. A linear charging profile was used in both cases, with the variable-rate formulation achieving this by using η_j equal to or greater than the maximum SOC. Table II show the resulting single-day costs, and the optimality gap (or solve time if solved to optimality) at the end of a 600 second (10 minute) solve time limit used for this comparison. As seen in Table II, the variable-rate charging results in both lower costs and better computation characteristics compared to the same formulation using fixed-rate charging.

D. Noise types and characteristics

To demonstrate the capability of the proposed receding horizon method to cope with noise, a Monte Carlo analysis is performed. For this, truth models that include noise sources in bus discharging, bus charging, and the station arrival times of each bus are developed. These truth models and the associated noise characteristics are considered to be not available to the planning methods considered herein.

For the discharging dynamics, a nominal discharge rate is given a random constant bias combined with white noise. This can be modeled as a discrete linear system for bus j

$$\tilde{s}_{j,k+1} = \tilde{s}_{j,k} - d_{j,k} + \beta_j^d + \nu_{j,k}^d, \tag{20}$$

where k denotes discrete time, $\nu_{j,k}^d \sim \mathcal{N}(0, \sigma_\nu^d)$ is the random variable for the added white noise, and $\beta_j^d \sim \mathcal{N}(0, \sigma_\beta^d)$ is the random constant bias.

Similarly, the charging dynamics are given a random constant bias and white noise to result in the following system for bus j

$$\tilde{s}_{j,k+1} = \tilde{s}_{j,k} + g(j,k) + \sum_{l \in \mathcal{L}} \left(\beta_l^c + \nu_{l,k}^c\right) x_{\sigma(j,k,l)} \tag{21}$$

TABLE III
NOISE PARAMETERS

σ_ν^d $\left(\frac{\text{kWh}}{\sqrt{s}}\right)$	$\sigma_{j,\beta}^d$ (kW)	$\sigma_{l,\nu}^c$ $\left(\frac{\text{kWh}}{\sqrt{s}}\right)$		$\sigma_{l,\beta}^c$ (kW)		σ^a (sec)
		slow	fast	slow	fast	
0.05	1.2	0.04167	0.0833	1.2	2.4	120

where $\nu_{l,k}^c \sim \mathcal{N}(0, \sigma_{l,\nu}^c)$ is the added white noise and $\beta_l^c \sim \mathcal{N}(0, \sigma_{l,\beta}^c)$ the random constant bias, varying depending on the charger type l. The summation over the charger types uses $x_{\sigma(j,k,l)}$ to select the bias and noise that apply to the charger type that the bus uses in the time step k to $k+1$.

The arrival time variations are achieved by perturbing a nominal arrival time, t_a by white noise such that the new arrival time, t_a', for a Monte Carlo run is

$$t_a' = t_a + \nu^a \tag{22}$$

with $\nu^a \sim \mathcal{N}(0, \sigma^a)$ being the random variable for the added white noise. It should be noted that the choice of a normal distribution is used primarily due to its ubiquity, and it is left to future work to explore additional distributions.

The noise parameter values used in this work are given in Table III. The charging and discharging values are based in data gathered over the months of June-September on the UTA SLC and Ogden routes previously mentioned. The arrival time variations are based in data from [26].

E. Monte Carlo experiments

The noise sources on the discharging, charging, and arrival times are used in a simulation environment to generate Monte Carlo runs. The Monte Carlo runs are used to analyze the performance of the receding horizon planning method.

To generate one simulation run, each bus is initialized at its nominal initial charge level, without any noise. The simulation then follows the schedules of the buses with the addition of noise on the arrival time, charge rates, and route discharge.

In each run, the decisions of when to charge, with what charger type, and for how long are made using one of three strategies: the *Qin* strategy is a thresholding strategy based on the work in [2] which also approximates a typical bus operator charging strategy; the *Open-Loop* strategy follows the top-level full-day plan as closely as possible[4]; and the *Hierarchical* strategy as presented in this work. For the Qin strategy, the decision to charge or not is made upon arrival at the station, depending on if the SOC is below the threshold (70% in this work). A bus stops charging when it reaches the maximum charge level or must leave to continue on its route, whichever comes first. The Open-Loop method will only charge if the nominal plan indicates to do so, regardless of any stochasticity. This means the Open-Loop strategy cannot charge more time than the nominal plan indicates, but may charge for less time when buses arrive late. The Hierarchical strategy, on the other hand, accounts for discrepancies from the nominal plan that it encounters.

[4]The Open-Loop strategy honors charge rates and charge stopping times. However, it cannot always start on time due to the bus arriving late.

TABLE IV
STRATEGY AND SCENARIO DAILY COST

	Qin	Open-Loop	Hierarchical
SLC	$698.10	$315.14	$384.49
Ogden	$261.26	$116.54	$134.87
Random	$1,369.26	$552.10	$650.96

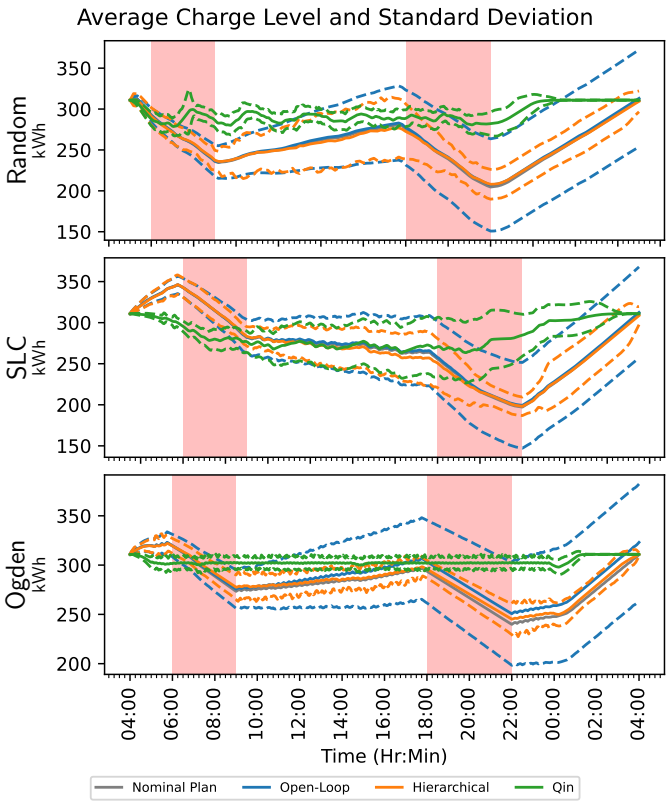

Fig. 4. The solid lines are the average charge levels (kWh) across Monte-Carlo runs and buses for each scenario. The dotted lines denote the three-σ variation across Monte-Carlo runs and buses (with each bus's charge level zeroed to its mean across Monte-Carlo runs) Note that the Qin strategy deviates from the nominal plan significantly during the day (as expected). Significantly, the three-σ variations of the Open-Loop strategy continue to grow over time, while the variations of the other two strategies do not.

A comparison of these charging strategies is made over 50 Monte Carlo runs for each combination of strategy (Qin, Open-Loop, and Hierarchical) and scenario (SLC, Ogden, Random), resulting in a total of 450 runs.

The primary points of comparison across the strategies are the performance (the resulting electric utility costs), and the feasibility and repeatability for each strategy. Analyzing the feasibility and repeatability balances the desire to reduce costs with the possibility of buses having service interruptions.

As seen in Table IV, the resulting costs of both optimization-based methods (Open-Loop and Hierarchical) are significantly better than the Qin method, which is similar to charging strategies often used in practice. While the Open-Loop strategy does provide the best costs, this is primarily due to its lack of feedback and the "lost" charging from the instances when a bus arrived late to the station and so could not charge for part of the time for which it was scheduled to charge.

Examining Fig. 4 shows the average charge level over time of each combination of scenario and strategy. These averages are taken across both the Monte-Carlo runs and the buses simultaneously. Also shown are the three-σ variations calculated across Monte-Carlo runs and buses zeroed to their individual mean across those Monte-Carlo runs (this zeroing of the mean for each bus removes the effects of inherent differences between routes from the standard deviation, σ, calculation). It is first noted that the Open-Loop and Hierarchical methods both average nearly the same as the average of the nominal plan. This aligns with expectations as all noise sources are zero-mean. The Qin strategy, however, deviates significantly from the nominal plan as this strategy makes no reference to the nominal in its execution.

Significantly, Fig. 4 demonstrates that the three-σ variations of the Open-Loop strategy grow over time in each scenario. Due to this, the Open-Loop strategy results in much larger terminal variations than the Qin and Hierarchical strategies, especially at the end of the day. These larger bound values demonstrate a greater sensitivity to the noise for the Open-Loop strategy, which is more likely to result in violations of constraints during operation. Demonstrating this higher probability of constraint violation, the Open-Loop strategy violated the minimum charge level constraint in 45 of its 150 runs (30%). On the other hand, the Hierarchical strategy only dipped below the minimum charge level constraint for one run ($< 1\%$). Furthermore, that run was able to satisfy all running and terminal constraints with the minimum charge level constraint allowed only an additional 1%.

The continual spreading of the variations for the Open-Loop strategy is due to the lack of any feedback mechanism to correct the charge levels of each bus back to the nominal values as they drift from nominal over time due to noise. This underlying drifting of the bus charge levels warns of the possibility of future infeasibility being induced if the Open-Loop strategy is used over multiple days in a row. To investigate this possibility, a Monte-Carlo analysis was performed over seven days on the Open-Loop and Hierarchical strategies to determine the multi-day feasibility of each strategy. This multi-day analysis was performed such that the beginning charge levels of each bus for a day were set to that bus's average ending charge from the previous day's Monte-Carlo runs. A new nominal plan was generated for that day, and then 50 Monte-Carlo runs were performed for each of the two strategies for that day. On the seventh day of the Random scenario the Open-Loop strategy resulted in a situation where no nominal plan could be created (the problem was infeasible) due to the significant drift of the bus charge levels over time. It should be noted that creating a new nominal plan did provide some corrective behaviors, but these were not enough to prevent the decay into infeasibility for the Open-Loop strategy. In contrast, the Hierarchical strategy was capable of continuing to run on the seventh day with no indication that performance or feasibility was degrading. The significant cost reduction compared to the Qin strategy combined with the much better feasibility characteristics compared to the Open-Loop strategy highlight the strengths of the proposed solution for scheduling the charging of BEBs within uncertain environments.

VII. Conclusion

Charging BEBs cost-effectively is a difficult problem due to the complex cost structure, the limiting battery capacity and charge rate factors, and the need to react to stochasticity in operations. This work addresses these difficulties with a receding-horizon control strategy that responds to feedback from the environment. Utilizing an optimization scheme that accounts for both consumption and demand TOU costs, and that references a non-linear, variable-rate partial charging model allows for costs to be optimized with a high degree of fidelity and flexibility. This results in a significant cost reduction over a method capable of reacting to the environment (up to 52%), and a more robust solution method compared to one that does not receive feedback.

Acknowledgements

Special thanks go to the Utah Transit Authority and Rocky Mountain Power for providing some data used to produce the results of this work.

Appendix A
Proof of Lemma 1

The CC-CV charging scheme consists of charging at a constant current until reaching the switching voltage. Then, the voltage is held constant while the current decays from the previous current level to zero. In [27], a model of the CC-CV charging profile was developed as a piecewise function of power draw with constant power p_l^{cc} during the CC phase and exponentially decaying power during the CV phase.

Following [27], the time for a bus j to reach the switching point between the CC and CV phases from zero charge with charger type l is $t_{j,l}^{cc}$. This value is based on p_l^{cc}, the bus battery's capacity, E_j, and the desired switching point (as a percentage of charge level), η_j, according to $t_{j,l}^{cc} = \frac{\eta_j E_j}{p_l^{cc}} + t_0$. Assuming, without loss of generality, that the starting time $t_0 = 0$, from [27] the power draw over time, $p_j(t)$, is

$$p_j(t) = \begin{cases} p_l^{cc} & 0 \le t < t_{j,l}^{cc} \\ p_l^{cc} e^{-\alpha_{j,l}(t - t_{j,l}^{cc})} & t_{j,l}^{cc} \le t \end{cases} \tag{23}$$

with the exponential rate, $\alpha_{j,l} > 0$, being a parameter of the underlying charging system and battery.

Going beyond [27] to form a linear dynamic system model begins with determining the bus battery charge level over time, $s_j(t)$, by integrating the power, $p_j(t)$,

$$s_j(t) = \begin{cases} \int_0^t p_j(\tau) d\tau & 0 \le t < t_{j,l}^{cc} \\ \int_0^{t_{j,l}^{cc}} p_j(\tau) d\tau + \int_{t_{j,l}^{cc}}^t p_j(\tau) & t_{j,l}^{cc} \le t \end{cases}.$$

With the appropriate substitutions from (23), this becomes

$$= \begin{cases} \int_0^t p_l^{cc} d\tau & 0 \le t < t_{j,l}^{cc} \\ \int_0^{t_{j,l}^{cc}} p_l^{cc} d\tau + \int_{t_{j,l}^{cc}}^t p_l^{cc} e^{-\alpha_{j,l}(\tau - t_{j,l}^{cc})} d\tau & t_{j,l}^{cc} \le t \end{cases}.$$

Performing the integration yields a closed-form solution

$$s_j(t) = \begin{cases} p_l^{cc} t & 0 \le t < t_{j,l}^{cc} \\ p_l^{cc} t_{j,l}^{cc} - \frac{p_l^{cc}}{\alpha_{j,l}} \left(e^{-\alpha_{j,l}(t - t_{j,l}^{cc})} - 1 \right) & t_{j,l}^{cc} \le t \end{cases}. \tag{24}$$

Equation (24) can be written as a function of $p_j(t)$. Focusing on the second case,

$$s_j(t) = p_l^{cc} t_{j,l}^{cc} - \frac{1}{\alpha_{j,l}} \left(\underbrace{p_l^{cc} e^{-\alpha_{j,l}(t - t_{j,l}^{cc})}}_{p_j(t)} - p_l^{cc} \right) \quad t_{j,l}^{cc} \le t. \tag{25}$$

Solving (25) for $p_j(t)$ allows power to be represented as a function of the charge level. Note that $\dot{s}_j(t) = p_j(t)$. Combining the solution of $p_j(t)$ in terms of $s_j(t)$ with (23), a linear dynamic system representation of $s_j(t)$ can be written as

$$\dot{s}_j(t) = \begin{cases} p_l^{cc} & 0 \le t < t_{j,l}^{cc} \\ -\alpha_{j,l} s_j(t) + \alpha_{j,l} p_l^{cc} t_{j,l}^{cc} + p_l^{cc} & t_{j,l}^{cc} \le t \end{cases}.$$

As $s_j(t)$ is the only time-dependent element, the switching conditions can be written in terms of $s_j(t)$, recalling that $s_j(0) = 0$ and $s_j(t_{j,l}^{cc}) = \eta_j E_j$,

$$\dot{s}_j(t) = \begin{cases} p_l^{cc} & 0 \le s_j(t) < \eta_j E_j \\ -\alpha_{j,l} s_j(t) + \alpha_{j,l} p_l^{cc} t_{j,l}^{cc} + p_l^{cc} & \eta_j E_j \le s_j(t) \end{cases}. \tag{26}$$

The substitutions of (5) in (26) gives the dynamics in (4).

Appendix B
Proof of Lemma 2

A continuous linear time-invariant system, $\dot{x}(t) = Ax(t) + Bu(t)$, can be exactly modeled in discrete time (if the $u(t)$ is constant over a discrete step) as

$$x_{k+1} = \bar{A} x_k + \bar{B} u_k$$

with

$$\bar{A} = e^{A\delta} \qquad \bar{B} = \int_0^\delta e^{A\tau} d\tau B \\ = A^{-1}(\bar{A} - I)B \quad (A \text{ non-singular})$$

as given in [28, 4.2.1]. These relations hold even if $u(t) = 1$ is constant: i.e., the case in (4). Applying these relations to (4) produces the discrete system in (6).

Appendix C
Proof of Lemma 3

The upper bound (10) is composed of two linear functions as visualized in Fig. 5. Equation (10) can be approximated by the concave function formed by using the intersection point of the two lines as the switching point. Concave piecewise-linear functions can be represented exactly by the minimum of all the linear functions (i.e., $f(x) = \min(f_1(x), f_2(x), \ldots, f_n(x))$). Accordingly, the concave approximation can be written as

$$g_{j,k,l} \le \min\left(\bar{b}_l^{cc}, (\bar{a}_l^{cv} - 1) s_{j,k} + \bar{b}_l^{cv} \right)$$

or, equivalently,

$$g_{j,k,l} \le \bar{b}_l^{cc}$$
$$g_{j,k,l} \le (\bar{a}_l^{cv} - 1) s_{j,k} + \bar{b}_l^{cv}.$$

The quality of this approximation depends on how close the intersection point, $s_{j,k,l}^{\times}$, is to the true switching point, $\eta_j E_j$.

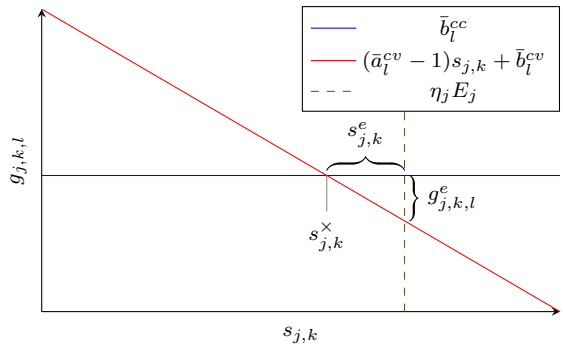

Fig. 5. A visualization of the two parts of the approximate gain upper bound constraint (not to scale). The blue constant line corresponds to the linear portion of the CC/CV charging profile, while the red corresponds to the exponential portion. The intersection point of the two lines is the switching point for the approximation, while the vertical dashed line is the true switching point. Thus, the approximation introduces error in between the intersection point and the true switching point, with the most error occurring in the limit approaching the true switching point.

Note that $\bar{b}_l^{cc}$ is a constant and $(\bar{a}_l^{cv}-1)s_{j,k}+\bar{b}_l^{cv}$ is linear in $s_{j,k}$ with $-1<\bar{a}_l^{cv}-1<0$ (i.e., the slope is negative), as Fig. 5 demonstrates. Thus, when $s_{j,k}<s^\times_{j,k}$, $g_{j,k,l}\leq \bar{b}_l^{cc}<(\bar{a}_l^{cv}-1)s_{j,k}+\bar{b}_l^{cv}$ and when $s_{j,k}>s^\times_{j,k}$, $g_{j,k,l}\leq(\bar{a}_l^{cv}-1)s_{j,k}+\bar{b}_l^{cv}<\bar{b}_l^{cc}$. Therefore, this approximation matches (11) exactly when $s_{j,k}$ is not in the interval $(s^\times_{j,k},\eta_j E_j)$.

The intersection point $s^\times_{j,k}$ occurs at the $s_{j,k}$ that satisfies

$$\bar{b}_l^{cc}=(\bar{a}_l^{cv}-1)s_{j,k}+\bar{b}_l^{cv}.$$

Solving for $s_{j,k}$ yields $s^\times_{j,k}$

$$s^\times_{j,k}=\frac{\bar{b}_l^{cc}-\bar{b}_l^{cv}}{\bar{a}_l^{cv}-1},$$

substituting from (7) gives

$$=\frac{b_l^{cc}\delta-\frac{(e^{a_l^{cv}\delta}-1)b_l^{cv}}{a_l^{cv}}}{e^{a_l^{cv}\delta}-1}$$

and substituting from (5) yields

$$\begin{aligned}&=\frac{p_l^{cc}\delta-\frac{(e^{-\alpha_{j,l}\delta}-1)(\alpha_{j,l}p_l^{cc}t_{j,l}^{cc}+p_l^{cc})}{-\alpha_{j,l}}}{e^{-\alpha_{j,l}\delta}-1}\\&=\frac{p_l^{cc}\delta}{e^{-\alpha_{j,l}\delta}-1}+\frac{\alpha_{j,l}p_l^{cc}t_{j,l}^{cc}+p_l^{cc}}{\alpha_{j,l}}\\&=\frac{p_l^{cc}\delta}{e^{-\alpha_{j,l}\delta}-1}+p_l^{cc}t_{j,l}^{cc}+\frac{p_l^{cc}}{\alpha_{j,l}}.\end{aligned}\tag{27}$$

Calculating the error, $s^e_{j,k}$, between (27) and the ideal switching point, $\eta_j E_j$, is done as

$$\begin{aligned}s^e_{j,k}&=\eta_j E_j-s^\times_{j,k}\\&=\eta_j E_j-\frac{p_l^{cc}\delta}{e^{-\alpha_{j,l}\delta}-1}-p_l^{cc}t_{j,l}^{cc}-\frac{p_l^{cc}}{\alpha_{j,l}}.\end{aligned}$$

Noting that $p_l^{cc}t_{j,l}^{cc}=\eta_j E_j$ allows cancelling terms

$$=-\frac{p_l^{cc}\delta}{e^{-\alpha_{j,l}\delta}-1}-\frac{p_l^{cc}}{\alpha_{j,l}},$$

which can be written in terms of $\bar{b}_l^{cc}$

$$=-\bar{b}_l^{cc}\left(\frac{1}{e^{-\alpha_{j,l}\delta}-1}+\frac{1}{\alpha_{j,l}\delta}\right).\tag{28}$$

Consider the function $f(z)=\frac{1}{e^{-z}-1}+\frac{1}{z}$, which is strictly decreasing[5] and bounded in range to the open interval $(-1,0)$[6]. Taking z to be $\alpha_{j,l}\delta$ indicates that $0<-s^e_{j,k}<\bar{b}_l^{cc}$, or that $s^\times_{j,k}<\eta_j E_j$, but by no more than $\bar{b}_l^{cc}$.

The maximum gain error, $g^e_{j,k,l}$, between the approximated gain and the ideal value of $\bar{b}_l^{cc}$ is related to the error in the switch condition, $s^e_{j,k}$ by

$$g^e_{j,k,l}=(\bar{a}_l^{cv}-1)s^e_{j,k}$$

as $\bar{a}_l^{cv}-1$ is the slope of the second term of the upper bound (the red line in Fig. 5). Substituting from (5), (7) and (28) gives

$$\begin{aligned}&=-(e^{-\alpha_{j,l}\delta}-1)\left(\frac{1}{e^{-\alpha_{j,l}\delta}-1}+\frac{1}{\alpha_{j,l}\delta}\right)\bar{b}_l^{cc}\\&=-\left(1-\frac{1-e^{-\alpha_{j,l}\delta}}{\alpha_{j,l}\delta}\right)\bar{b}_l^{cc}\end{aligned}$$

As both $\alpha_{j,l}$ and δ are positive, their product must also be positive. The positivity of the product $\alpha_{j,l}\delta$ ensures that the coefficient of $\bar{b}_l^{cc}$ is strictly negative with magnitude strictly less than 1, as $0<\frac{1-e^{-z}}{z}<1$ for $z>0$. Therefore, the maximum gain error, $g^e_{j,k,l}$, is directly governed by the $\frac{1-e^{-\alpha_{j,l}\delta}}{\alpha_{j,l}\delta}$ term. Since $\lim_{z\to 0}\frac{1-e^{-z}}{z}=1$, an acceptable level of error can be chosen with the selection of δ to be sufficiently small. In other words, for a given desired error, ϵ_d, a value of δ can be chosen sufficiently small according to

$$\left(1-\frac{1-e^{-\alpha_{j,l}\delta}}{\alpha_{j,l}\delta}\right)\bar{b}_l^{cc}\leq\epsilon_d$$

ensuring that the actual error $\epsilon\leq|g^e_{j,k,l}|\leq\epsilon_d$. To complete the proof it is noted that when $s^\times_{j,k}<s_{j,k}<\eta_j E_j$ (i.e., when error is introduced in $g_{j,k,l}$), the approximate upper bound to $g_{j,k,l}$ results in a *lower* value than the ideal upper bound. In other words, (11) is a conservative approximation of (10).

References

[1] S. Khan and H. Maoh, "Investigating attitudes towards fleet electrification – an exploratory analysis approach," *Transportation Research Part A: Policy and Practice*, vol. 162, pp. 188–205, 8 2022.

[2] N. Qin, A. Gusrialdi, R. Paul Brooker, and A. T-Raissi, "Numerical analysis of electric bus fast charging strategies for demand charge reduction," *Transportation Research Part A: Policy and Practice*, vol. 94, pp. 386–396, 2016. [Online]. Available: https://www.sciencedirect.com/science/article/pii/S096585641630444X

[3] G. J. Zhou, D. F. Xie, X. M. Zhao, and C. Lu, "Collaborative optimization of vehicle and charging scheduling for a bus fleet mixed with electric and traditional buses," *IEEE Access*, vol. 8, pp. 8056–8072, 2020.

[4] M. Rinaldi, E. Picarelli, A. D'Ariano, and F. Viti, "Mixed-fleet single-terminal bus scheduling problem: Modelling, solution scheme and potential applications," *Omega*, vol. 96, p. 102070, 10 2020.

[5] Y. He, Z. Liu, and Z. Song, "Optimal charging scheduling and management for a fast-charging battery electric bus system," *Transportation Research Part E: Logistics and Transportation Review*, vol. 142, p. 102056, 10 2020.

[5]The derivative of $f(z)$ can be shown to be strictly negative.

[6]The limits as z approaches positive and negative infinity are -1 and 0, respectively.

[6] A. Bagherinezhad, A. D. Palomino, B. Li, and M. Parvania, "Spatio-temporal electric bus charging optimization with transit network constraints," *IEEE Transactions on Industry Applications*, vol. 56, pp. 5741–5749, 9 2020.

[7] D. Mortensen, J. Gunther, G. Droge, and J. Whitaker, "Cost minimization for charging electric bus fleets," *World Electric Vehicle Journal 2023, Vol. 14, Page 351*, vol. 14, p. 351, 12 2023. [Online]. Available: https://www.mdpi.com/2032-6653/14/12/351/htmhttps://www.mdpi.com/2032-6653/14/12/351

[8] M. Duan, G. Qi, W. Guan, C. Lu, and C. Gong, "Reforming mixed operation schedule for electric buses and traditional fuel buses by an optimal framework," *IET Intelligent Transport Systems*, vol. 15, pp. 1287–1303, 10 2021.

[9] X. Tang, X. Lin, and F. He, "Robust scheduling strategies of electric buses under stochastic traffic conditions," *Transportation Research Part C: Emerging Technologies*, vol. 105, pp. 163–182, 8 2019.

[10] H. Chen, Z. Hu, Z. Xu, J. Li, H. Zhang, X. Xia, K. Ning, and M. Peng, "Coordinated charging strategies for electric bus fast charging stations," vol. 2016-December. IEEE Computer Society, 12 2016, pp. 1174–1179.

[11] L. Zhang, S. Wang, and X. Qu, "Optimal electric bus fleet scheduling considering battery degradation and non-linear charging profile," *Transportation Research Part E: Logistics and Transportation Review*, vol. 154, p. 102445, 10 2021.

[12] J. Whitaker, G. Droge, M. Hansen, D. Mortensen, and J. Gunther, "A network flow approach to battery electric bus scheduling," *IEEE Transactions on Intelligent Transportation Systems*, pp. 1–12, 2023.

[13] Y. Zhou, X. C. Liu, R. Wei, and A. Golub, "Bi-objective optimization for battery electric bus deployment considering cost and environmental equity," *IEEE Transactions on Intelligent Transportation Systems*, vol. 22, no. 4, pp. 2487–2497, 2020.

[14] O. Frendo, N. Gaertner, and H. Stuckenschmidt, "Open source algorithm for smart charging of electric vehicle fleets," *IEEE Transactions on Industrial Informatics*, vol. 17, pp. 6014–6022, 9 2021.

[15] A. Jahic, M. Eskander, and D. Schulz, "Preemptive vs. non-preemptive charging schedule for large-scale electric bus depots." Institute of Electrical and Electronics Engineers Inc., 9 2019.

[16] Y. Bie, J. Ji, X. Wang, and X. Qu, "Optimization of electric bus scheduling considering stochastic volatilities in trip travel time and energy consumption," *Computer-Aided Civil and Infrastructure Engineering*, vol. 36, pp. 1530–1548, 12 2021. [Online]. Available: https://onlinelibrary.wiley.com/doi/full/10.1111/mice.12684https://onlinelibrary.wiley.com/doi/abs/10.1111/mice.12684https://onlinelibrary.wiley.com/doi/10.1111/mice.12684

[17] G. Wang, X. Xie, F. Zhang, Y. Liu, and D. Zhang, "Bcharge: Data-driven real-time charging scheduling for large-scale electric bus fleets," vol. 2018-December. Institute of Electrical and Electronics Engineers Inc., 1 2019, pp. 45–55.

[18] G. Wang, Z. Fang, X. Xie, S. Wang, H. Sun, F. Zhang, Y. Liu, and D. Zhang, "Pricing-aware real-time charging scheduling and charging station expansion for large-scale electric buses," *ACM Transactions on Intelligent Systems and Technology*, vol. 12, pp. 1–26, 2 2021. [Online]. Available: https://dl.acm.org/doi/10.1145/3428080

[19] M. Mesbahi and M. Egerstedt, *Graph theoretic methods in multiagent networks*. Princeton Univ Pr, 2010.

[20] J. P. Hespanha, *Linear systems theory*. Princeton university press, 2018.

[21] D.-S. Chen, R. G. Batson, and Y. Dang, *Applied integer programming: modeling and solution*. John Wiley & Sons, 2011.

[22] "Large general service - rocky moutain power," Jan 2021. [Online]. Available: https://www.rockymountainpower.net/content/dam/pcorp/documents/en/rockymountainpower/rates-regulation/utah/rates/008_Large_General_Service_1_000_kW_and_Over_Distribution_Voltage.pdf

[23] J. S. Albus, "Four-dimensional/rcs reference model architecture for unmanned ground vehicles," in *Proceedings SPIE*, G. R. Gerhart, R. W. Gunderson, and C. M. Shoemaker, Eds., vol. 3693. International Society for Optics and Photonics, 7 1999, pp. 11–20. [Online]. Available: http://proceedings.spiedigitallibrary.org/proceeding.aspx?articleid=986270

[24] M. Woody, M. Arbabzadeh, G. M. Lewis, G. A. Keoleian, and A. Stefanopoulou, "Strategies to limit degradation and maximize li-ion battery service lifetime - critical review and guidance for stakeholders," *Journal of Energy Storage*, vol. 28, p. 101231, 2020. [Online]. Available: https://www.sciencedirect.com/science/article/pii/S2352152X19314227

[25] Gurobi Optimization, LLC, "Gurobi Optimizer Reference Manual," 2021. [Online]. Available: https://www.gurobi.com

[26] A. Comi, A. Nuzzolo, S. Brinchi, and R. Verghini, "Bus travel time variability: some experimental evidences," *Transportation Research Procedia*, vol. 27, pp. 101–108, 2017, 20th EURO Working Group on Transportation Meeting, EWGT 2017, 4-6 September 2017, Budapest, Hungary. [Online]. Available: https://www.sciencedirect.com/science/article/pii/S2352146517309699

[27] H. Wu, G. K. H. Pang, and X. Li, "A realistic and non-linear charging process model for parking lot's decision on electric vehicles recharging schedule." Institute of Electrical and Electronics Engineers Inc., 6 2020, pp. 2–7.

[28] C.-T. Chen, *Linear system theory and design*. Saunders college publishing, 1984.

Justin Whitaker (Graduate Student Member, IEEE) received a B. S. degree in mechanical engineering from Brigham Young University in2019. He is currently pursuing a Ph.D.degree with the Department of Electrical and Computer Engineering, Utah State University (USU). Since 2019, he has been a Graduate Research Assistant with USU. His research interests include enabling autonomous systems, intelligent coordination and planning, and optimal control. His current research interests include enabling intelligent coordination and planning for electric vehicles.

Derek Redmond (Graduate Student Member, IEEE) received his Associate of Pre-Engineering degree at Snow College in 2021 and his Bachelor of Science degree in Electrical Engineering at Utah State University in 2023. His research interests include planning and control techniques for coordinating multi-agent systems.

Greg Droge (Member, IEEE) received a B. S. degree (manga cum laude) from Brigham Young University in 2009 and a M. S. and Ph. D. degrees in electrical and computer engineering from Georgia Institute of Technology in 2012 and 2014, respectively. He was a Research Engineer developing autonomous planning capabilities with SPAWAR-PAC and the USAF 309th SMXG, prior to joining USU, in 2018. He is currently an Assistant Professor with the Department of Electrical and Computer Engineering, Utah State University (USU). His research interests include multi-agent planning and control techniques, split between two major components: allocation techniques for autonomous systems with complex cross-schedule dependencies and model predictive control for distributed systems with coordination motion constraints.

Jacob (Jake) Gunther is a Professor in the Department of Electrical and Computer Engineering at Utah State University. His industrial work spanned an array of topics including target detection, sonar systems, satellite communications, speech recognition, acoustic echo cancellation using microphone arrays, and feedback cancellation for digital hearing aids. Since joining USU in 2000, Dr. Gunther's research has included synthetic aperture radar, communication systems, radio astronomy, system identification, optimization, and machine learning.

CHAPTER 5

SCHEDULING THE CHARGING OF BATTERY-ELECTRIC VEHICLES UNDER HETEROGENEOUS SCHEDULING CONSTRAINTS

Submitted to *IEEE Transactions on Intelligent Transportation Systems* [51]

Scheduling the Charging of Battery-Electric Vehicles under Heterogeneous Scheduling Constraints

Justin Whitaker, *Graduate Student Member, IEEE,* Greg Droge, *Member, IEEE*

***Abstract*—A significant challenge to adopting battery electric vehicles for vehicle fleets is the need to schedule the charging of the vehicles. The problem of scheduling the charging for fleets of electric vehicles is complicated by the complex cost structure, the limiting battery capacity, and competition for charging resources. While problems with schedules known in advance have seen recent developments to address these complexities, problems that simultaneously schedule the routes and charging of vehicles neither address the full cost structure nor use high-fidelity charging models. Additionally, no work has been found that investigates considering both vehicles with known schedules and vehicles requiring concurrently scheduling routes and charging. This work addresses these deficiencies by extending the formulation for scheduling routes and charging in [1] to include TOU demand costs and a non-linear, variable-rate charging model, based in the previous work for scheduling charging with known schedules in [2]. The benefits of the proposed method are demonstrated by comparing it to the methods in [1] and [2], as well as across varying fleet compositions, with results showing 89% and 24% cost reductions over [1], [2], respectively. Across varying fleet compositions of vehicles with fixed schedules and vehicles with routes to be scheduled, the proposed method shows a trade-off between cost and computational complexity, demonstrating benefits to considering both types of vehicles together.**

***Index Terms*—electric vehicles, scheduling, charging, optimization, demand costs, variable-rate charging, mixed integer programming**

I. Introduction

Electric vehicles are quickly gaining widespread use. Reduced energy and maintenance costs [3] provide motivation to vehicle fleet operators to adopt electric vehicles. The additional environmental and societal benefits of electric vehicles [4] provide further motivation for some fleet operators, such as transportation agencies. However, several factors complicate and hinder the widespread adoption of electric vehicles into vehicle fleets. For example, electric vehicles typically have lower ranges than comparable internal combustion engine vehicles, and often take much longer to refuel/charge [5]. These, and other complexities, typically require scheduling the charging of the vehicles to ensure that they continue to operate and to achieve improved costs [5].

Scheduling the charging of a fleet of electric vehicles is more complex than simply pulling in to charge when the battery charge level is low. Charging infrastructure is expensive, typically leading to fewer charging resources than vehicles. The limited number of chargers leads to competition over these chargers, and significantly higher costs or interruptions to service if not managed properly. Additionally, energy and power utility rate structures often are multi-faceted, with utilities charging for both energy used, or *consumption*, and the maximum power drawn, or *demand*. Further complicating these costs are time-dependent *time-of-use* (TOU) rates for both consumption and demand. The prediction of these costs is also impacted by the presence of any *uncontrolled* electrical loads on the same meter as the chargers. These factors add to the complex problem of scheduling the charging for a fleet of electric vehicles. Accordingly, this work proposes a method to schedule the charging of a fleet of electric vehicles to minimize the operational costs of charging while accounting for the charging and cost structure complexities.

In the literature, there are two variations of the electric vehicle scheduling and charging problem; one where the vehicle route schedules are known in advance (e.g., [2], [6]–[11]), termed *fixed-schedule* problems herein, and one where the vehicle route schedules are to be determined as part of the scheduling problem (e.g., [1], [12]–[16]), termed *flexible-schedule* problems herein. The fixed-schedule problem has seen recent advances that consider TOU costs for both consumption and demand costs, e.g., [6]–[8]. Additionally, others have included higher fidelity charging models, some with non-linear charging profiles, like [9]–[11], or variable-rate charging, like [6], [7]. The previous work, [2], builds on previous literature by adding a non-linear, variable-rate charging model to the formulation in [11] combined with the full TOU consumption and demand costs of [6] to schedule charging for fixed-schedule vehicles.

The flexible-schedule problem has also seen recent advances, but does not consider TOU demand costs, although TOU consumption costs are often considered, e.g., [1]. Additionally, it is common to see the flexible-schedule problem solved with a simplified charging model. In particular, the simplification that a vehicle always charges to full capacity within a time step is particularly common, e.g., [1], [12]–[16], with no exceptions found among the approaches that consider the flexible-schedule problem. Due to these simplifications, most flexible-schedule formulations are not amenable to including the TOU demand costs and higher-fidelity charging models. The work in [1], however, presents a method for scheduling mixed fleets of electric vehicles and conventional combustion engine vehicles using a formulation based in bin-packing models that is more readily capable of including a

Email: justinwhtkr@gmail.com, greg.droge@usu.edu Department of Electrical and Computer Engineering, Utah State University, Logan, UT 84322, USA.

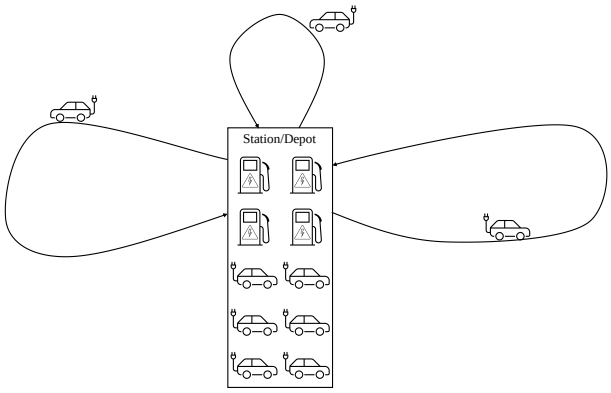

Fig. 1. Illustration of the scenario for the flexible-schedule electric vehicle scheduling and charging problem. Electric vehicles are assigned to perform routes from a central station or depot and scheduled to charge as needed to minimize operational costs.

partial-charging model, and therefore the TOU demand costs.

Accordingly, this work builds on the previous work in [2], as well as the work in [1], to provide a method for scheduling the routes and charging of a fleet of electric vehicles simultaneously, while considering the full TOU costs and using a non-linear, variable-rate charging model. This is accomplished by extending the formulation in [1] with the TOU consumption and demand, and the non-linear, variable-rate charging model from [2], with adjustments to the formulation to be compatible with the flexible-schedule problem. Accordingly, to the best of our knowledge, this work will be the first to consider the TOU demand costs and a non-linear, variable-rate charging model for the flexible-schedule electric vehicle scheduling and charging problem. The proposed method is then compared to the method in [1] to demonstrate the benefits of including the TOU demand costs and the non-linear, variable-rate charging model, and to [2] to highlight some benefits of a flexible-schedule formulation over a fixed-schedule formulation. Additionally, an analysis across varying ratios of mixed fixed- and flexible-schedule vehicles is performed showcasing the trade-offs associated with varying fleet compositions

The remainder of this work is organized as follows. Section II presents the formulation for the flexible-schedule electric vehicle scheduling and charging problem. Following this, Section III presents the results of the proposed method and compares them to the methods in [1], [2], as well as across varying fleet compositions. Finally, Section IV provides a summary of the work.

II. Flexible-Schedule Electric Vehicle Scheduling and Charging

The base formulation for flexible-schedule vehicles is based on the work in [1], with the additions of supporting TOU Demand costs, uncontrolled loads, and a variable-rate, non-linear CC-CV charging profile based in the work from [2]. The formulation primarily addresses the scheduling of routes and charging for a fleet of electric vehicles operating out of a single central station or depot, as illustrated in Fig. 1. The relevant formulation from [1] is re-stated herein for completeness, albeit with adjustments to notation to facilitate the additions of this work. Any adjustments to the formulation from [1], and the aforementioned additions from [2] will be explicitly noted for clarity.

The formulation starts by defining $\mathcal{I}$, $\mathcal{J}$, $\mathcal{K}$, and $\mathcal{L}$ to be sets that index the vehicles, routes, time and charger types, respectively. In other words, $i \in \mathcal{I}$ denotes the i^{th} vehicle, $j \in \mathcal{J}$ the j^{th} route, $k \in \mathcal{K}$ denotes the discrete time step from the beginning of the planning horizon,0, to the end of the horizon, T, $l \in \mathcal{L}$ denotes the l^{th} charger type. The decision variables of the optimization problem are $x_{il}^k \in \{0,1\}$ with $x = 1$ indicating vehicle i charges with charger l at time k, $y_{ij}^k \in \{0,1\}$ with $y = 1$ indicating vehicle i starts route j at time k, $s_i^k \in \mathbb{R}$, which denotes the charge level of vehicle i at time k, and $g_{il}^k \in \mathbb{R}$, which denotes the charge gained by vehicle i from charger type l over the time step from k to $k+1$. The variables x_{il}^k, y_{ij}^k, and s_i^k are original to [1], while g_{il}^k is newly introduced. Note that the charge level s_i^k denotes the energy contained in the vehicle's battery and is measured in kilowatt-hours. Accordingly, the charge gained g_{il}^k is also measured in kilowatt-hours and corresponds to the energy added to the vehicle's battery. Additionally, the following are parameters of the optimization problem. For route j, let δ_j^k and δ_j^s be the number of time steps and the energy required to complete the route, respectively, with $k_{j,d}$ being the desired start time of route j. Also, let $\mathcal{K}_j(k) = \{k' | k \leq k' \leq k + \delta_j\}$ be a mapping for route j from a start time to the set of times that the route would occupy a vehicle if started at the start time k. For vehicle i, let the battery energy capacity be E_i, the minimum allowed charge level be $E_{i,min}$, the desired starting charge level be $s_{i,d}^0$, and the desired ending charge level be $s_{i,d}^T$.

As visualized in Fig. 2, this formulation can be considered as a discrete bin-packing problem where each vehicle is a "bin" and the routes and charging sessions are "packed" into the vehicle bins. Each route occupies δ_j^k "slots", or time steps, in a vehicle's bin, while each charging session occupies one time step.

A. Costs

As g_{il}^k represents the same quantity as in the previous work, [2], (energy gained in kilowatt-hours), the cost functions for TOU consumption and demand can be used from that work. Additionally, the costs associated with starting a route not at the desired start time $(k_{j,d})$ are also reused from [1]. For completeness, these cost formulations are re-stated herein.

From [2], the TOU consumption cost is calculated as

$$\sum_{k \in \mathcal{K}} c_c^k \sum_{i \in \mathcal{I}} \sum_{l \in \mathcal{L}} g_{il}^k$$

where each c_c^k is a time-dependent cost on the energy consumed in the corresponding time step.

The demand cost from [2] has two parts, the *baseline* demand, which consists of a rate applied the maximum power draw averaged over a time period Δ (typically 15 or 30 minutes), with the maximum being taken over the whole planning period. The second part is the *TOU* demand, which

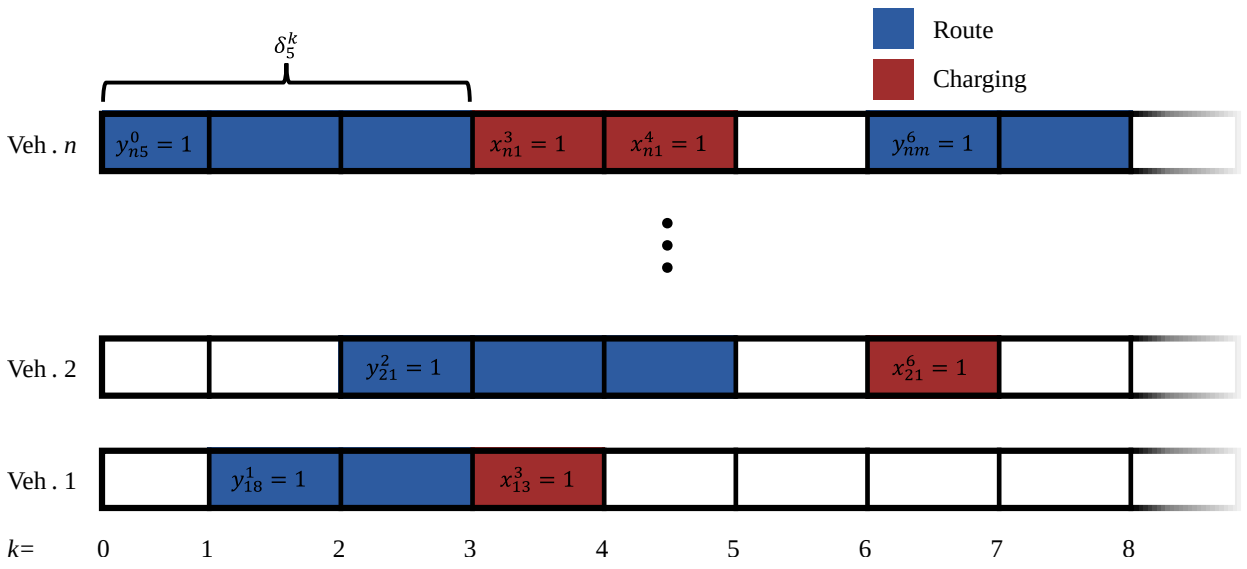

Fig. 2. Example of the bin-packing aspects of scheduling the routes and charging for a fleet of electric vehicles.

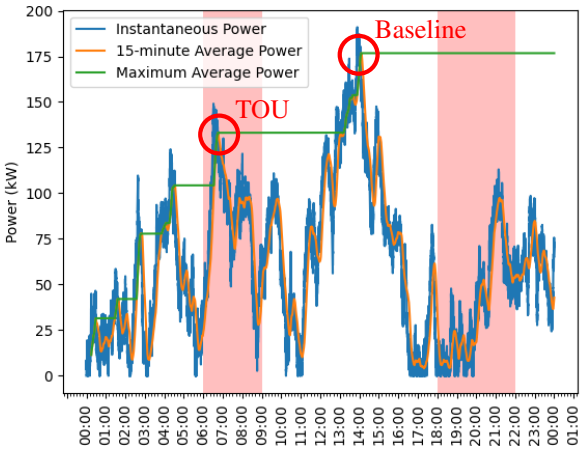

Fig. 3. The relationship between the instantaneous power draw, the averaged power draw, and the baseline and TOU demand costs. The pink indicates time windows of high-cost. The red circles indicate the average power value used in the calculation of the demand cost for the baseline and TOU rates.

applies a second rate to the maximum averaged power draw (with the same Δ), but only takes the maximum over a subset of times, referred to as *peak times*, defined by the set $\mathcal{K}_{TOU}$. These parts and their relation to the instantaneous and averaged power draw values is illustrated in Fig. 3. Given these maximum averaged power draw values for the baseline and TOU demand costs, p_{max} and $p_{max,TOU}$ respectively, the total demand cost can be written as

$$c_d p_{max} + c_{d,TOU} p_{max,TOU}$$

with c_d and $c_{d,TOU}$ being the baseline and TOU rates, respectively. Within the optimization, p_{max} and $p_{max,TOU}$ are calculated as slack variables from the following constraints

$$p_{max} \geq p_\Delta^k \ \forall k \in \mathcal{K},$$
$$p_{max,TOU} \geq p_\Delta^k \ \forall k \in \mathcal{K}_{TOU},$$
$$p_\Delta^k = \frac{1}{\Delta} \sum_{k'=k-m}^{k-1} e_\delta^{k'}, \ \forall k \in \mathcal{K},$$

and

$$e_\delta^k = e_\delta^{k,load} + \sum_{i \in \mathcal{I}} \sum_{l \in \mathcal{L}} g_{il}^k, \ \forall k \in \mathcal{K}$$

where δ is the discretization size of the optimization, $m = \frac{\Delta}{\delta}$, p_Δ^k is the power usage at time-step k averaged over the previous time window Δ, and e_δ^k and $e_\delta^{k,load}$ correspond to the energy used in time-step k by the vehicles and by uncontrolled loads, respectively.

The start-time costs from [1] use a cost, c_j^k, on the difference between the actual start time and the desired start time $k_{j,d}$ for route j to form the cost as

$$\sum_{k \in \mathcal{K}} \sum_{j \in \mathcal{J}} c_j^k |k - k_{j,d}| y_{ij}^k.$$

Note that the k and $k_{j,d}$ variables in this equation are not variables of optimization, thus maintaining the linearity of the cost.

B. Constraints

The constraints for the bin-packing-based routing and charging scheduling problem for flexible-schedule vehicles are divided into two groups. The first group of constraints ensures proper scheduling of route and vehicle-to-charger assignments. The second group defines the dynamic and other constraints on the charge level and gain variables.

The first group starts by constraining each vehicle i to be assigned to at most one charger or route at time k. Formally,

$$\sum_j y_{ij}^k + \sum_l x_{il}^k \leq 1 \quad \forall i, k. \tag{1}$$

As well, each route must be assigned to a vehicle and can only be performed during the route's allowed times. To accomplish this, two sets are defined: a set of times at which route j is allowed to start, $\mathcal{K}_j^+$, and a set of times at which route j is not allowed to start, $\mathcal{K}_j^\times$. These two sets partition the full index set of time, i.e. $\mathcal{K}_j^+ \cup \mathcal{K}_j^\times = \mathcal{K}$ and $\mathcal{K}_j^+ \cap \mathcal{K}_j^\times = \emptyset$. Then, the constraints

$$\sum_i \sum_{k \in \mathcal{K}_j^+} y_{ij}^k = 1 \quad \forall j \tag{2}$$

and

$$\sum_i \sum_{k \in \mathcal{K}_j^\times} y_{ij}^k = 0 \quad \forall j \tag{3}$$

enforce that each route is assigned to exactly one vehicle across the allowed start times and no vehicles across the disallowed start times. Note that these two constraints are a generalization of those found in [1] to allow for greater flexibility in the allowed and disallowed start times of each route.

Additionally, the vehicle must be restricted from performing any other route or charging during the times it is on route. The variable y_{ij}^k takes the value of 1 at the time the vehicle *starts* the route (if assigned), but effects the variables for charging and other routes for the $\delta_j^k - 1$ time steps following the selected start time. To account for these interactions a constraint is formed as follows,

$$\begin{aligned} \sum_{k' \in \mathcal{K}_j(k)} \left(\sum_{j' \neq j, j' \in \mathcal{J}} y_{ij'}^{k'} + \sum_{l \in \mathcal{L}} x_{il}^{k'} \right) \\ \leq (\delta_j^k - 1)(1 - y_{ij}^k) \end{aligned} \quad \forall i, j, k \in \mathcal{K}_j^+. \tag{4}$$

The outer sum of the left-hand side sums over all the $\delta_j^k - 1$ time steps following the start time k. The inner two summations are over the assignments of other routes $y_{ij'}^{k'}$ and the assignment of charging $x_{il}^{k'}$. In other words, the left-hand side counts the number of assignments other than route j that are made during the time that route j would be performed by vehicle i. Then the right-hand side is a big-M formulation with $M = \delta_j^k - 1$. Thus, if $y_{ij}^k = 0$ (route j is not assigned to start at time k) the constraint is trivially satisfied. This is due to (1), which allows at most one assignment to be made per time step and therefore at most $\delta_j^k - 1$ tasks may be assigned over the $\delta_j^k - 1$ time steps. However, if route j is assigned to start at time k, i.e., $y_{ij}^k = 1$, the right-hand side collapses to zero, disallowing vehicle i from being assigned to charge or go on route while the vehicle is performing route j for the following $\delta_j^k - 1$ time steps.

As the final scheduling constraint, a route may not be scheduled with a vehicle if it does not have sufficient charge level to complete the route. That is,

$$y_{ij}^k \leq \frac{s_i^k}{\delta_j^s + E_{min,i}} \quad \forall i, j, k \in \mathcal{K}_j^+, \tag{5}$$

or equivalently,

$$(\delta_j^s + E_{min,i}) y_{ij}^k \leq s_i^k \quad \forall i, j, k \in \mathcal{K}_j^+. \tag{6}$$

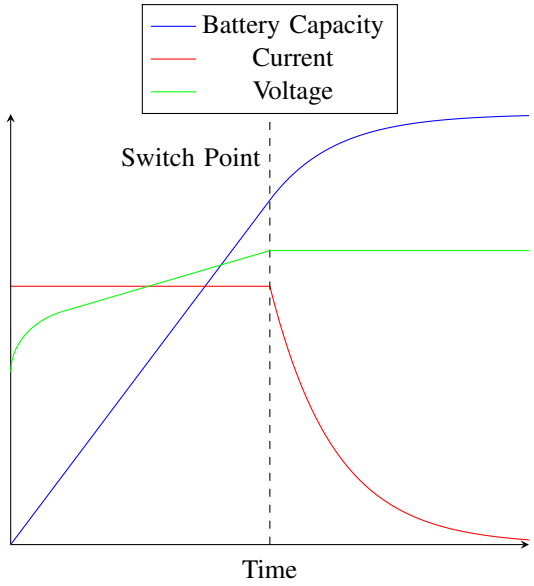

Fig. 4. An intuitive representation of the CC-CV charging profile. The current is held constant until the voltage reaches a threshold, then the current is allowed to decay as the voltage is held constant.

Now we consider the constraints that govern the charge level. The first constraint is the dynamic constraint

$$s_i^{k+1} = s_i^k + \sum_{l \in \mathcal{L}} g_{il}^k - \sum_j \delta_j^s y_{ij}^k \quad \forall i, k, \tag{7}$$

which is modified from [1]. In [1], the dynamic constraint only allows for charging the vehicle to full capacity over a time step using their own parameters and slack variables in place of the $\sum_{l \in \mathcal{L}} g_{il}^k$ term. In contrast, the formulation in this work allows for partial charging over a time step, with the charge gained, g_{il}^k, being a decision variable

In addition to the constraints in [1], the gain g_{il}^k is constrained with the following inequalities as developed in [2],

$$\begin{aligned} g_{il}^k &\leq \bar{b}_l^{cc} x_{il}^k \\ g_{il}^k &\leq (\bar{a}_l^{cv} - 1) s_i^k + \bar{b}_l^{cv} \quad \forall i, l, k. \\ g_{il}^k &\geq 0 \end{aligned} \tag{8}$$

This allows variable rate charging with a CC-CV non-linear charging profile where $\bar{b}_l^{cc}$ is the dynamic system parameters associated with the constant-current (CC) portion of the charging profile, and $\bar{a}_l^{cv}, \bar{b}_l^{cv}$ are the dynamic system parameters associated with the constant-voltage (CV) portion of the charging profile. An intuitive representation of the CC-CV charging profile is shown in Fig. 4 demonstrating the characteristic constant current followed by a constant voltage, and the associated battery capacity over time.

Finally, as in [1], the initial and final charge levels are constrained to the desired values according to

$$s_i^0 = s_{i,d}^0 \quad \forall i \tag{9}$$

$$s_i^T \geq s_{i,d}^T \quad \forall i. \tag{10}$$

C. Optimization Problem

To more concisely state the optimization problem, the following notation is introduced:

$$\begin{aligned} x &= \{x_{il}^k \ \forall i \in \mathcal{I}, l \in \mathcal{L}, k \in \mathcal{K}\} \\ y &= \{y_{ij}^k \ \forall i \in \mathcal{I}, j \in \mathcal{J}, k \in \mathcal{K}\} \\ s &= \{s_i^k \ \forall i \in \mathcal{I}, k \in \mathcal{K}\} \\ g &= \{g_{il}^k \ \forall i \in \mathcal{I}, l \in \mathcal{L}, k \in \mathcal{K}\} \\ e_\delta &= \{e_\delta^k \ \forall k \in \mathcal{K}\} \\ p_\Delta &= \{p_\Delta^k \ \forall k \in \mathcal{K}\}. \end{aligned}$$

Combining the constraints and costs as previously described, the mixed-integer linear program is written as:

$$\min_{\substack{x,y,s,g,\\ e_\delta,p_\Delta,\\ p_{max},\\ p_{max,TOU}}} \quad \left(\begin{array}{l} \displaystyle\sum_{k\in\mathcal{K}} c_c^k \sum_{i\in\mathcal{I}} \sum_{l\in\mathcal{L}} g_{il}^k \\ \quad + c_d p_{max} + c_{d,TOU} p_{max,TOU} \\ \quad + \displaystyle\sum_{k\in\mathcal{K}} \sum_{j\in\mathcal{J}} c_j^k |k - k_{j,d}| y_{ij}^k \end{array} \right) \tag{11a}$$

s.t.

$$\sum_{j\in\mathcal{J}} y_{ij}^k + \sum_{l\in\mathcal{L}} x_{il}^k \le 1 \qquad \begin{array}{l}\forall i \in \mathcal{I} \\ k \in \mathcal{K}\end{array} \tag{11b}$$

$$\left(\begin{array}{c} \displaystyle\sum_{k'\in\mathcal{K}_j(k)} \left(\sum_{j'\in\mathcal{J}\neq j} y_{ij'}^{k'} + \sum_{l\in\mathcal{L}} x_{il}^{k'} \right) \\ - (\delta_j^k - 1)(1 - y_{ij}^k) \end{array} \right) \le 0 \qquad \begin{array}{l}\forall i \in \mathcal{I} \\ j \in \mathcal{J} \\ k \in \mathcal{K}_j^+\end{array} \tag{11c}$$

$$\sum_{i\in\mathcal{I}} \sum_{k\in\mathcal{K}_j^+} y_{ij}^k = 1 \qquad \forall j \in \mathcal{J} \tag{11d}$$

$$\sum_{i\in\mathcal{I}} \sum_{k\in\mathcal{K}_j^\times} y_{ij}^k = 0 \qquad \forall j \in \mathcal{J} \tag{11e}$$

$$\left(\delta_j^s + E_{min,i}\right) y_{ij}^k \le s_i^k \qquad \begin{array}{l}\forall i \in \mathcal{I} \\ j \in \mathcal{J} \\ k \in \mathcal{K}_j^+\end{array} \tag{11f}$$

$$s_i^{k+1} = s_i^k + \sum_{l\in\mathcal{L}} g_{il}^k - \sum_{j\in\mathcal{J}} \delta_j^s y_{ij}^k \qquad \begin{array}{l}\forall i \in \mathcal{I} \\ k \in \mathcal{K}\end{array} \tag{11g}$$

$$\begin{array}{ll} g_{il}^k \le \bar{b}_l^{cc} x_{il}^k & \forall i \in \mathcal{I} \\ g_{il}^k \le (\bar{a}_l^{cv} - 1) s_i^k + \bar{b}_l^{cv} & l \in \mathcal{L} \\ g_{il}^k \ge 0 & k \in \mathcal{K} \end{array} \tag{11h}$$

$$s_i^0 = s_{i,d}^0 \qquad \forall i \in \mathcal{I} \tag{11i}$$

$$s_i^T \ge s_{i,d}^T \qquad \forall i \in \mathcal{I} \tag{11j}$$

$$e_\delta^k = e_{\delta,k}^{load} + \sum_{j\in\mathcal{J}} g(j,k), \qquad \forall k \in \mathcal{K} \tag{11k}$$

$$p_\Delta^k = \frac{1}{\Delta} \sum_{k'=k-m}^{k-1} e_{\delta,k'}, \qquad \forall k \in \mathcal{K} \tag{11l}$$

$$p_{max} \ge p_\Delta^k, \qquad \forall k \in \mathcal{K} \tag{11m}$$

$$p_{max,TOU} \ge p_\Delta^k \qquad \forall k \in \mathcal{K}_{TOU} \tag{11n}$$

III. Results and Analysis

The method presented in this manuscript is analyzed under three scenarios: flexible-schedule vehicles only, fixed-schedule vehicles only, and a mix of fixed- and flexible-schedule vehicles. In analyzing the flexible-schedule only scenario, the method is compared to that in [1]. In studying the fixed-schedule only scenario, the method is compared to that in [2]. Finally, the method is analyzed under a scenario with varying ratios of fixed- to flexible-schedule vehicles to demonstrate the trade-offs associated with varying fleet compositions.

To maintain similarity across these scenarios, the same number of vehicles, battery capacities, charger types, and cost structures were used in each scenario, except where noted otherwise. The vehicles used are based on battery-electric buses that might be used in public transportation, with a battery capacity of 388 kWh. This capacity is chosen to be in line with typical battery capacities of electric buses [17], and matches the capacity of buses in use by the Utah Transit Authority (UTA). In all cases, the buses are required to start the day at 90% battery capacity and return to this level by the end of the day. Additionally, the buses are constrained to operate with the battery charge level between 20% and 95% capacity to ensure a margin of operational robustness, and to reduce battery wear experienced at the extremes of charge level. A fleet of 32 buses is used across all scenarios.

The chargers used are a mix of depot chargers and station chargers, with the depot chargers capable of charging up to 50 kW and the station chargers capable of charging up to 300 kW. These chargers are assumed to be under the same metering, and therefore subject to the same TOU power and demand rates. These rates are taken from the winter rates of the Rocky Mountain Power Schedule 8 rate schedule [18], which has TOU for both power and demand, and has peak hours from 6AM–9AM and 6PM–10PM. The route timing costs c_j^k are set to \$0.06 per minute of deviation from the desired start time for all routes in all scenarios.

A. Flexible-Schedule Vehicles Only

The two main modifications of [1] presented in Section II allow considering TOU consumption and demand costs, and enable non-linear, variable-rate charging of the batteries. To analyze the effects of these modifications, a comparison is made between four methods, referred to as:

- *Rinaldi*: The method presented in [1]
- *TOU Costs*: The method from [1] with the modifications for considering TOU costs
- *Variable-Rate*: The method from [1] with the modifications to allow non-linear, variable-rate charging
- *VR-TOU*: The method proposed in this manuscript that considers both TOU costs and allows non-linear, variable-rate charging.

For this scenario, 80 randomized routes are generated each with a random duration between 30–225 minutes and a power draw randomly selected between 28–36 kW. On average, these parameters result each individual route using 18% of the battery capacity of a bus. At the longest duration and highest power draw, a route would use 35% of the battery capacity.

TABLE I
DAILY OPERATING COSTS
All values are the average across 10 random runs.

	Consumption		Demand			
	Off-Peak	On-Peak	Off-Peak	On-Peak	Timing	Total
Rinaldi	\$91.45	\$0.36	\$803.15	\$160.74	**\$17.83**	\$1073.53
TOU Costs	\$53.59	**\$0**	\$54.72	**\$0**	\$19.81	\$128.12
Variable-Rate	\$69.18	\$0.27	\$184.08	\$179.30	**\$17.83**	\$450.66
VR-TOU	**\$53.11**	**\$0**	**\$47.11**	**\$0**	**\$17.83**	**\$118.05**

TABLE II
COMPUTATION CHARACTERISTICS
Tests performed on a computer with 32 GB RAM and an Intel Core i7-7700 CPU.
The Gurobi optimization solver was used with a 600-second time limit.
All values are the average across 10 random runs.

	Optimality Gap	Time (s)
Rinaldi	0%	121.53
TOU Costs	12.8%	600
Variable-Rate	0%	117.93
VR-TOU	0%	121.43

The allowed times for each of these routes, $\mathcal{K}_j^+$, is restricted to the hours of 5AM-10PM. Additionally, each route has a 50% probability of having a fixed start time, so that there is a mix of routes that have a fixed start time and routes that have a flexible start time. In all cases, however, each route is still able to be assigned to any vehicle.

For the *Rinaldi* and *TOU Costs* methods, the chargers that are used are not differentiated based on their capabilities (e.g., fast vs. slow) as [1] does not consider partial charging, nor the charging capabilities of a charger. This differs from the general scenario as described previously, but reflects the method in [1]. For the *Variable-Rate* and *VR-TOU* methods the ability to consider partial charging is added, and consequently the ability to consider a charger's capabilities is also included. Therefore, for the *Variable-Rate* and *VR-TOU* methods, the number and types of the chargers is as specified in the general scenario.

1) Flexible-Schedule Results: The main points of comparison are the resulting cost, and the computational tractability. Additionally, it is important to note the maximum power draw requirements imposed by each solution method. The results for this analysis utilize 10 randomly generated runs. Each random run is held constant across the four methods to maintain comparability. Results for each of the four methods are averaged across the 10 random runs.

The resulting costs for each method are compared in Table I where the costs are broken down into the on- and off-peak components of consumption and demand, as well as the timing cost. From this cost analysis, the best overall cost is from the *VR-TOU* method at an 89% reduction over the cost of the *Rinaldi* method. This drastic reduction can be seen to be primarily due to the much improved demand cost in both on- and off-peak times. The *TOU Costs* method also shows a significant decrease in costs over the *Rinaldi* method as it does directly consider the utility costs, but the inability to consider partial charging leads to higher costs than the *VR-TOU* method. Interestingly, the *Variable-Rate* method is also able to significantly reduce costs compared to *Rinaldi* due to the reduction in power draw.

The computational results of the methods are shown in Table II with both the time spent optimizing and the final optimality gap at the end of the optimization time. From these results, the complexity of the demand cost structure increases the computation time significantly, evidenced by the results for the *TOU Costs* method. On the other hand, the inclusion of the variable-rate, partial charging structure, with the additional flexibility it provides, significantly reduces the computational complexity that the demand cost formulation adds, as the *VR-TOU* method has a similar computation time to the *Rinaldi* and *Variable-Rate* methods.

The implications of the various methods on the charging infrastructure needed to implement their charging schedules warrant attention. The *Rinaldi* and *TOU Costs* methods always charge a vehicle to full capacity within one time step. This simplifies the model of vehicle battery charge level but necessitates a charger with high charging capabilities. For instance, to charge one of the buses from the minimum charge level of 20% to the maximum of 95% (291 kWh) within the discretization step size of 10 minutes equates to a charging rate of 1,726 kW. The *Rinaldi* and *TOU Costs* solutions exhibit charging rates of 1,534 kW and 410 kW, respectively, averaged across these scenarios. There are chargers capable of supplying the 410 kW required by the *TOU Costs* method (e.g., [19]), but they usually entail significant up-front costs [20]. A charger capable of supplying the 1,534 kW required by the *Rinaldi* method is, to our knowledge, not yet available.

In contrast, the *Variable-Rate* and *VR-TOU* methods allow charging to a level less than full charge, and can respect the limits of the chargers and/or vehicles. In the experiments performed these two methods averaged 300 kW and 265 kW, respectively. As demand costs heavily depend on the charging rates used in the charging schedule, this substantial reduction in charge rates leads to a significant decrease in demand costs, in addition to the expected reduction in up-front costs for both chargers and vehicles.

B. Fixed-Schedule Vehicles Only

While [1] and other similar work focus on flexible-schedule vehicles, they are capable of handling fixed-schedule vehicles as a special case. Consequently, the method presented in this manuscript can be used to solve the fixed-schedule problem as well. Accordingly, the method is compared to the fixed-schedule formulation in [2].

To more closely match the analysis done in [2], the route for each bus is generated with similar parameters to those used in [2]. The routes for these buses are generated on a per-bus basis. For each bus, a route is generated with a random duration between 30–120 minutes, with a random duration for time in the station selected between 20–30 minutes. The average power draw for the route is randomly selected between 28–36 kW. Each bus starts the day at 5AM at the depot and stays there for its selected station duration time. After this duration the bus starts its route and alternating between the

TABLE III
FIXED-SCHEDULE SCENARIO RESULTS
Tests performed on a computer with 32 GB RAM and an Intel Core i7-7700 CPU.
The Gurobi optimization solver was used with a 1-hr time limit.
All values are the average across 10 random runs.

	Cost ($ per day)	Optimality Gap (at 1 hr)	Time to Initial Solution (s)
[2]	$672.92	6.25%	56.3
Proposed	$512.33	1.73%	9.4

route and the station until it can no longer complete a full route before 10PM, at which point it returns to the depot. In this scenario, the depot chargers are limited in availability to the hours of 10PM–6AM, while the station chargers are available from the hours of 6AM–10PM to simulate the different locations for the depot and station chargers. This restriction on charger availability is done to more closely match the analysis scenario in [2].

1) Fixed-Schedule Results: The main points of comparison in the fixed-schedule scenario are again the resulting cost and the computational tractability. Related drawbacks and benefits of the two methods are also discussed. This analysis utilized 10 randomly generated runs, with each run held constant across the two methods to maintain comparability. All results are averaged across the 10 random runs.

The costs and computational results for the fixed-schedule scenario are shown in Table III. In comparing the costs, the proposed method has a 24% lower cost than [2]. This difference in cost is likely due to the graph structure of [2] requiring a transition time between charging one bus and another with the same charger, thus restricting some solutions in that formulation. Looking at the computational results, the proposed method also achieves an improved optimality gap, and finds an initial feasible solution much faster than [2], as seen in Table III.

C. Concurrent Fixed- and Flexible-Schedule Analysis

To analyze the effects of considering fixed- and flexible-schedule vehicles together, the proposed method is tested on scenarios that include both fixed- and flexible-schedule vehicles in varying ratios. These scenarios differ from the general scenario by only using 5 depot chargers, and 2 station chargers instead of the 10 and 5, respectively, from the general scenario. These values are near the lowest possible number of chargers of both types that can feasibly charge all vehicles in the scenarios considered, resulting in a challenging charging scenario. This is done to help demonstrate the kinds of trade-offs that can arise when considering both fixed- and flexible-schedule vehicles together. The routes for the vehicles are generated in the same manner as the fixed-schedule scenario, with the same power draw and duration limits. Therefore, the base scenario for this analysis is a fixed-schedule scenario with 32 vehicles.

The series of scenarios consists of varying ratios of fixed- to flexible-schedule vehicles, with the percentage of flexible-schedule vehicles being 0%, 25%, 50%, 75%, and 100%. For each percentage level, the corresponding number of vehicles and their associated routes are converted to flexible-schedule vehicles and routes. For example, in the 25% flexible-schedule scenario, 8 vehicles are converted from fixed- to flexible-schedule vehicles, and their routes are converted to flexible-schedule routes. It is important to note that the number of constraints of the problem (and consequently memory requirements) drastically increases with the number of flexible-schedule routes, particularly when not limited in the available start times. Accordingly, when converting a fixed-schedule route to a flexible-schedule route, the available start times are limited to a two-hour window centered around the original start time of the route.

When solving these scenarios, the optimization time limit was set to 4 hours. As the 0% scenario has the most constraints, it is expected to have the solution with the highest cost. The solution for this problem is then used as a warm-start for the other scenarios so that at least one feasible solution is found within the time limit in the other scenarios.

1) Concurrent Fixed- and Flexible-Schedule Results: The results for the two series of scenarios are both shown in Table IV. The results for each test scenario are broken down into the cost per day, the model characteristics (number of variables, constraints, etc.) before and after the solver pre-solve routine, the final optimality gap, and the time required to first reach a solution within 2% of the final solution.

The model characteristics are shown before and after the Gurobi solver's internal pre-solve routine to show the size of the model as formulated, and the size of the model that goes through the solution process. The drastic difference in model size before and after the pre-solve routine indicates the potential for a more compact or efficient formulation, which could be explored in future work.

From the cost results in Table IV, including more flexible-schedule vehicles in the fleet results in a decrease in the daily operating cost compared to a fully fixed-schedule fleet. The decreases in cost from 0% to 25% and 25% to 50% seem to indicate that the cost decreases as the percentage of flexible-schedule vehicles increases. Expectation dictates that a scenario with greater flexibility, as a relaxation of the lower flexibility scenarios, would result in a lower cost, matching these first examples. However, the 75% and 100% scenarios show a slight increase in cost compared to the 50% and 75% scenarios, respectively, breaking the expectation of increased flexibility leading to decreased cost. It is posited, as discussed in further detail next, that the increased flexibility in these scenarios results in a significant increase in computational complexity, which may be the cause of the increased cost.

Inspecting the computational results, as the percentage of flexible-schedule vehicles increases, the computational complexity increases significantly, evidenced in the number of constraints and variables, the optimality gap at the end of the time limit, and most clearly in settling time. This increased computational complexity appears to affect the resulting cost of the solutions as well, with the 75% and 100% solutions having higher costs than the 50% solution, despite the increased flexibility. The increased computational difficulty seems to hinder the speed of finding a near-optimal solution, which then

TABLE IV
CONCURRENT FIXED- AND FLEXIBLE-SCHEDULE SCENARIO RESULTS
Tests performed on a computer with 32 GB RAM and an Intel Core i7-7700 CPU.
The Gurobi optimization solver was used with a 4-hr time limit.

	Cost ($ per day)	Before Pre-solve		After Pre-solve		Optimality Gap (at 4 hr)	Settling Time (s)
		Num. Constraints	Num. Variables	Num. Constraints	Num. Variables		
0%	$367.46	1,168,789	1,145,954	12,655	10,122	3.32%	66
25%	$354.79	1,190,165	1,145,954	28,956	18,301	5.96%	363
50%	$348.73	1,205,031	1,145,954	57,831	33,582	3.60%	1956
75%	$349.09	1,212,113	1,145,954	75,022	42,614	3.96%	4319
100%	$350.26	1,219,993	1,145,954	96,113	53,762	5.57%	6298

degrades the quality of the solutions found within a given time limit.

The significant differences in cost and computation time across the full-flexibility scenarios suggest that there is a clear trade-off between the potential cost savings and the increased computational complexity of considering flexible-schedule vehicles. In this particular scenario, 50% flexibility provides good balance between cost savings and computational complexity, providing a 5% decrease in cost with less computational burden than the more flexible 75% and 100% scenarios.

It is worth reiterating, however, that the scenarios considered here are particularly challenging due to the low number of chargers available, and the high density of routes. This likely leaves less room for the timing and assignment flexibility to provide cost savings than in a less constrained scenario.

IV. CONCLUSION

Scheduling the charging for fleets of electric vehicles is a complex problem due to the complex cost structure, the limiting battery capacity, and competition for charging resources. While problems with schedules known in advance have seen recent developments to address these complexities, problems that simultaneously schedule the routes and charging of vehicles neither address the full cost structure nor use high-fidelity charging models. This work addresses these deficiencies by extending the formulation for scheduling routes and charging in [1] to include TOU demand costs and a non-linear, variable-rate charging model, based in the previous work for scheduling charging with known schedules in [2]. The benefits of the proposed method are demonstrated by comparing it to the methods in [1] and [2], as well as across varying fleet compositions. In comparison to the previous works, the proposed method demonstrates improved charging costs with 89% and 24% cost reductions over the methods in [1], [2], respectively. Additionally, the proposed method shows no increase in time to solve over the method in [1], and improves the computational characteristics over the method in [2] both in time to an initial solution and the optimality gap at the end of the solve time.

Across varying fleet compositions of vehicles with fixed schedules and vehicles with routes to be scheduled, the proposed method shows a trade-off between cost and computational complexity. The analysis shows that for the scenario and fleet compositions considered, a 50/50 split between vehicles with fixed schedules and vehicles with routes to be scheduled balances the cost reduction and computational complexity.

REFERENCES

[1] M. Rinaldi, E. Picarelli, A. D'Ariano, and F. Viti, "Mixed-fleet single-terminal bus scheduling problem: Modelling, solution scheme and potential applications," *Omega*, vol. 96, p. 102070, 10 2020.

[2] J. Whitaker, D. Redmond, J. Gunther, and G. Droge, "Scheduling battery-electric bus charging under stochasticity using a receding-horizon approach," *IEEE Transactions on Intelligent Transportation Systems*, 2024, Under Review.

[3] N. Lutsey and M. Nicholas, "Update on electric vehicle costs in the United States through 2030," *The International Council on Clean Transportation*, vol. 2, 2019.

[4] I. Malmgren, "Quantifying the societal benefits of electric vehicles," *World Electric Vehicle Journal*, vol. 8, no. 4, pp. 996–1007, 2016.

[5] J. C. Mukherjee and A. Gupta, "A review of charge scheduling of electric vehicles in smart grid," *IEEE Systems Journal*, vol. 9, pp. 1541–1553, 12 2015.

[6] D. Mortensen, J. Gunther, G. Droge, and J. Whitaker, "Cost minimization for charging electric bus fleets," *World Electric Vehicle Journal 2023, Vol. 14, Page 351*, vol. 14, p. 351, 12 2023. [Online]. Available: https://www.mdpi.com/2032-6653/14/12/351

[7] Y. He, Z. Liu, and Z. Song, "Optimal charging scheduling and management for a fast-charging battery electric bus system," *Transportation Research Part E: Logistics and Transportation Review*, vol. 142, p. 102056, 10 2020.

[8] A. Bagherinezhad, A. D. Palomino, B. Li, and M. Parvania, "Spatio-temporal electric bus charging optimization with transit network constraints," *IEEE Transactions on Industry Applications*, vol. 56, pp. 5741–5749, 9 2020.

[9] N. Qin, A. Gusrialdi, R. Paul Brooker, and A. T-Raissi, "Numerical analysis of electric bus fast charging strategies for demand charge reduction," *Transportation Research Part A: Policy and Practice*, vol. 94, pp. 386–396, 2016. [Online]. Available: https://www.sciencedirect.com/science/article/pii/S096585641630444X

[10] L. Zhang, S. Wang, and X. Qu, "Optimal electric bus fleet scheduling considering battery degradation and non-linear charging profile," *Transportation Research Part E: Logistics and Transportation Review*, vol. 154, p. 102445, 10 2021.

[11] J. Whitaker, G. Droge, M. Hansen, D. Mortensen, and J. Gunther, "A network flow approach to battery electric bus scheduling," *IEEE Transactions on Intelligent Transportation Systems*, pp. 1–12, 2023.

[12] G. J. Zhou, D. F. Xie, X. M. Zhao, and C. Lu, "Collaborative optimization of vehicle and charging scheduling for a bus fleet mixed with electric and traditional buses," *IEEE Access*, vol. 8, pp. 8056–8072, 2020.

[13] M. Duan, G. Qi, W. Guan, C. Lu, and C. Gong, "Reforming mixed operation schedule for electric buses and traditional fuel buses by an optimal framework," *IET Intelligent Transport Systems*, vol. 15, pp. 1287–1303, 10 2021.

[14] Y. Bie, J. Ji, X. Wang, and X. Qu, "Optimization of electric bus scheduling considering stochastic volatilities in trip travel time and energy consumption," *Computer-Aided Civil and Infrastructure Engineering*, vol. 36, pp. 1530–1548, 12 2021. [Online]. Available: https://onlinelibrary.wiley.com/doi/10.1111/mice.12684

[15] G. Wang, X. Xie, F. Zhang, Y. Liu, and D. Zhang, "Bcharge: Data-driven real-time charging scheduling for large-scale electric bus fleets," vol. 2018-December. Institute of Electrical and Electronics Engineers Inc., 1 2019, pp. 45–55.

[16] G. Wang, Z. Fang, X. Xie, S. Wang, H. Sun, F. Zhang, Y. Liu, and D. Zhang, "Pricing-aware real-time charging scheduling and charging station expansion for large-scale electric buses," *ACM Transactions on Intelligent Systems and Technology*, vol. 12, pp. 1–26, 2 2021. [Online]. Available: https://dl.acm.org/doi/10.1145/3428080
[17] IEA. (2023) Global EV Outlook 2023. [Online]. Available: https://www.iea.org/reports/global-ev-outlook-2023
[18] "Large general service - rocky moutain power," Jan 2021. [Online]. Available: https://www.rockymountainpower.net/content/dam/pcorp/documents/en/rockymountainpower/rates-regulation/utah/rates/008_Large_General_Service_1_000_kW_and_Over_Distribution_Voltage.pdf
[19] ABB. (2024) Pantograph down for electric buses. [Online]. Available: https://new.abb.com/ev-charging/pantograph-down
[20] M. Nicholas, "Estimating electric vehicle charging infrastructure costs across major us metropolitan areas." ICCT Washington, DC, USA, 2019.

Justin Whitaker (Graduate Student Member, IEEE) received a B. S. degree in mechanical engineering from Brigham Young University in2019. He is currently pursuing a Ph.D.degree with the Department of Electrical and Computer Engineering, Utah State University (USU). Since 2019, he has been a Graduate Research Assistant with USU. His research interests include enabling autonomous systems, intelligent coordination and planning, and optimal control. His current research interests include enabling intelligent coordination and planning for electric vehicles.

Greg Droge (Member, IEEE) received a B. S. degree (manga cum laude) from Brigham Young University in 2009 and a M. S. and Ph. D. degrees in electrical and computer engineering from Georgia Institute of Technology in 2012 and 2014, respectively. He was a Research Engineer developing autonomous planning capabilities with SPAWAR-PAC and the USAF 309th SMXG, prior to joining USU, in 2018. He is currently an Assistant Professor with the Department of Electrical and Computer Engineering, Utah State University (USU). His research interests include multi-agent planning and control techniques, split between two major components: allocation techniques for autonomous systems with complex cross-schedule dependencies and model predictive control for distributed systems with coordination motion constraints.

CHAPTER 6

CONCLUSION

To enable the use of electric vehicles in fleets, methods to schedule the charging for the vehicles that are tractable, cost-effective, and robust are needed. As electric vehicles continue to find their way into vehicle fleets, the need to consider the complex charging costs with high-fidelity models while accounting for stochasticity and uncontrolled loads across multiple types of vehicle scheduling constraints will become increasingly important. While this is a challenging problem, the work presented in this dissertation has made significant progress towards addressing these challenges. Namely, the contributions and accomplishments of this dissertation are as follows:

1. Developed a mathematical model for scheduling the charging of fixed-schedule electric vehicles with uncontrolled loads that accounts for both TOU consumption and TOU demand costs.
    (a) Developed a network-flow-based mixed integer linear program for scheduling the charging of fixed-schedule electric vehicles.
    (b) Developed a high-fidelity non-linear charging profile that closely approximates the CCCV charging profile and is compatible with a mixed-integer linear program.
    (c) Formulated the TOU consumption and TOU demand costs, and the associated constraints, to allow for consideration within mixed-integer linear formulations of the charge scheduling problem.
2. Extended an existing flexible-schedule electric vehicle charging scheduling method ([14]) to consider complex costs, high-fidelity models, and uncontrolled loads.

   (a) Adjusted the bin-packing-based mixed-integer linear program formulation of [14] to include the non-linear charging profile, uncontrolled loads, and the TOU consumption and TOU demand costs from the fixed-schedule formulation.

   (b) Analyzed the impact of considering fixed- and flexible-schedule vehicles simultaneously on the problem solution and computational complexity.

3. Demonstrated a receding horizon technique to schedule the charging of electric vehicles that accounts for stochasticity in vehicle arrival, charging, and discharging times and provides a balance between robustness and cost savings benefits.

4. Demonstrated a technique to scale the high-fidelity, cost-effective scheduling of electric vehicle charging to hundreds of vehicles and routes inspired by the market-based methods in [52].

These developments and accomplishments are significant steps towards addressing the challenges of scheduling the charging of electric vehicles in fleets. They enable significantly improved cost savings over existing methods, and provide techniques for robustness and scalability that make significant strides toward enabling real-world use of electric vehicles in fleets. Additional insights into the effects of fleet compositions on the problem and its solution are provided, allowing for better decisions to be made when considering the adoption of electric vehicles in fleets. These contributions can be leveraged across a wide range of applications, from public transit to delivery services, to enable the cost-effective and robust use of electric vehicles in fleets.

While the work presented in this dissertation is a significant step towards addressing the challenges of scheduling the charging of electric vehicles in fleets, there are several areas for future work. An immediate area for future work is to further develop the receding-horizon and the semi-distributed techniques to apply to the scheduling of both fixed- and flexible-schedule vehicles. Additionally, the scalability of the semi-distributed market-based techniques presented in this dissertation could be further improved by developing fully distributed algorithms for the scheduling of electric vehicle charging. Finally, the techniques

presented in this dissertation could be extended to consider the open-schedule vehicle charging problem, which would allow for the consideration of a wider range of vehicle scheduling constraints.

REFERENCES

[1] N. Lutsey and M. Nicholas, "Update on electric vehicle costs in the United States through 2030," *The International Council on Clean Transportation*, vol. 2, 2019.

[2] I. Malmgren, "Quantifying the societal benefits of electric vehicles," *World Electric Vehicle Journal*, vol. 8, no. 4, pp. 996–1007, 2016.

[3] J. C. Mukherjee and A. Gupta, "A review of charge scheduling of electric vehicles in smart grid," *IEEE Systems Journal*, vol. 9, pp. 1541–1553, 12 2015.

[4] R. Wei, X. Liu, Y. Ou, and S. K. Fayyaz, "Optimizing the spatio-temporal deployment of battery electric bus system," *Journal of Transport Geography*, vol. 68, pp. 160–168, 4 2018.

[5] "Large general service - rocky moutain power," Jan 2021. [Online]. Available: https://www.rockymountainpower.net/content/dam/pcorp/documents/en/rockymountainpower/rates-regulation/utah/rates/008_Large_General_Service_1_000_kW_and_Over_Distribution_Voltage.pdf

[6] I. Kucukoglu, R. Dewil, and D. Cattrysse, "The electric vehicle routing problem and its variations: A literature review," *Computers & Industrial Engineering*, vol. 161, p. 107650, 11 2021.

[7] T. Erdelic, T. Carić, and E. Lalla-Ruiz, "A survey on the electric vehicle routing problem: Variants and solution approaches," *Journal of Advanced Transportation*, vol. 2019, 2019.

[8] C. Ye, W. He, and H. Chen, "Electric vehicle routing models and solution algorithms in logistics distribution: A systematic review," *Environmental Science and Pollution Research*, vol. 29, pp. 57 067–57 090, 8 2022. [Online]. Available: https://link.springer.com/article/10.1007/s11356-022-21559-2

[9] A. Froger, J. E. Mendoza, O. Jabali, and G. Laporte, "A matheuristic for the electric vehicle routing problem with capacitated charging stations," Centre interuniversitaire de recherche sur les reseaux d'entreprise, la logistique et le transport (CIRRELT), Tech. Rep., 6 2017. [Online]. Available: https://hal.science/hal-01559524https://hal.science/hal-01559524/document

[10] N. M. Moghaddam, "The partially rechargeable electric vehicle routing problem with time windows and capacitated charging stations," Master's thesis, Clemson University, 8 2015. [Online]. Available: https://tigerprints.clemson.edu/all_theses/2205

[11] Y. He, Z. Liu, and Z. Song, "Optimal charging scheduling and management for a fast-charging battery electric bus system," *Transportation Research Part E: Logistics and Transportation Review*, vol. 142, p. 102056, 10 2020.

[12] J. Barco, A. Guerra, L. Muñoz, and N. Quijano, "Optimal routing and scheduling of charge for electric vehicles: A case study," *Mathematical Problems in Engineering*, vol. 2017, 2017.

[13] O. Sassi, W. R. Cherif, A. Oulamara, and W. R. Cherif-Khettaf, "Vehicle routing problem with mixed fleet of conventional and heterogenous electric vehicles and time dependent charging costs," 10 2014, working paper or preprint. [Online]. Available: https://hal.science/hal-01083966https://hal.science/hal-01083966/document

[14] M. Rinaldi, E. Picarelli, A. D'Ariano, and F. Viti, "Mixed-fleet single-terminal bus scheduling problem: Modelling, solution scheme and potential applications," *Omega*, vol. 96, p. 102070, 10 2020.

[15] G. J. Zhou, D. F. Xie, X. M. Zhao, and C. Lu, "Collaborative optimization of vehicle and charging scheduling for a bus fleet mixed with electric and traditional buses," *IEEE Access*, vol. 8, pp. 8056–8072, 2020.

[16] L. Zhang, S. Wang, and X. Qu, "Optimal electric bus fleet scheduling considering battery degradation and non-linear charging profile," *Transportation Research Part E: Logistics and Transportation Review*, vol. 154, p. 102445, 10 2021.

[17] A. Bagherinezhad, A. D. Palomino, B. Li, and M. Parvania, "Spatio-temporal electric bus charging optimization with transit network constraints," *IEEE Transactions on Industry Applications*, vol. 56, pp. 5741–5749, 9 2020.

[18] H. Chen, Z. Hu, Z. Xu, J. Li, H. Zhang, X. Xia, K. Ning, and M. Peng, "Coordinated charging strategies for electric bus fast charging stations," in *2016 IEEE PES Asia-Pacific Power and Energy Engineering Conference (APPEEC)*, vol. 2016-December. IEEE Computer Society, 12 2016, pp. 1174–1179.

[19] D. Mortensen, J. Gunther, G. Droge, and J. Whitaker, "Cost minimization for charging electric bus fleets," *World Electric Vehicle Journal*, vol. 14, no. 12, 2023. [Online]. Available: https://www.mdpi.com/2032-6653/14/12/351

[20] D. Mortensen, J. Gunther, and G. Droge, "A bin packing approach to minimize charging cost for electric bus fleets," *IEEE Transactions on Intelligent Transportation Systems*, vol. 25, no. 7, pp. 7818–7831, 2024.

[21] D. Mortensen and J. Gunther, "A scalable approach to minimize charging costs for electric bus fleets," *World Electric Vehicle Journal*, vol. 15, no. 4, 2024. [Online]. Available: https://www.mdpi.com/2032-6653/15/4/161

[22] X. Tang, X. Lin, and F. He, "Robust scheduling strategies of electric buses under stochastic traffic conditions," *Transportation Research Part C: Emerging Technologies*, vol. 105, pp. 163–182, 8 2019.

[23] G. Wang, X. Xie, F. Zhang, Y. Liu, and D. Zhang, "Bcharge: Data-driven real-time charging scheduling for large-scale electric bus fleets," in *2018 IEEE Real-Time Systems Symposium (RTSS)*, vol. 2018-December. Institute of Electrical and Electronics Engineers Inc., 1 2019, pp. 45–55.

[24] G. Wang, Z. Fang, X. Xie, S. Wang, H. Sun, F. Zhang, Y. Liu, and D. Zhang, "Pricing-aware real-time charging scheduling and charging station expansion for large-scale electric buses," *ACM Transactions on Intelligent Systems and Technology*, vol. 12, pp. 1–26, 2 2021. [Online]. Available: https://dl.acm.org/doi/10.1145/3428080

[25] M. Duan, G. Qi, W. Guan, C. Lu, and C. Gong, "Reforming mixed operation schedule for electric buses and traditional fuel buses by an optimal framework," *IET Intelligent Transport Systems*, vol. 15, pp. 1287–1303, 10 2021.

[26] Y. Bie, J. Ji, X. Wang, and X. Qu, "Optimization of electric bus scheduling considering stochastic volatilities in trip travel time and energy consumption," *Computer-Aided Civil and Infrastructure Engineering*, vol. 36, pp. 1530–1548, 12 2021. [Online]. Available: https://onlinelibrary.wiley.com/doi/full/10.1111/mice.12684https://onlinelibrary.wiley.com/doi/abs/10.1111/mice.12684https://onlinelibrary.wiley.com/doi/10.1111/mice.12684

[27] O. Sassi and A. Oulamara, "Electric vehicle scheduling and optimal charging problem: complexity, exact and heuristic approaches," *https://doi.org/10.1080/00207543.2016.1192695*, vol. 55, pp. 519–535, 1 2016. [Online]. Available: https://www.tandfonline.com/doi/abs/10.1080/00207543.2016.1192695

[28] J. Varga, G. R. Raidl, and S. Limmer, "Computational methods for scheduling the charging and assignment of an on-site shared electric vehicle fleet," *IEEE Access*, vol. 10, pp. 105 786–105 806, 2022.

[29] J. Q. Li, "Transit bus scheduling with limited energy," *Transportation Science*, vol. 48, pp. 521–539, 6 2014. [Online]. Available: https://pubsonline.informs.org/doi/abs/10.1287/trsc.2013.0468https://www.jstor.org/stable/pdf/43666940.pdf

[30] M. Alonso, H. Amaris, J. G. Germain, and J. M. Galan, "Optimal charging scheduling of electric vehicles in smart grids by heuristic algorithms," *Energies 2014, Vol. 7, Pages 2449-2475*, vol. 7, pp. 2449–2475, 4 2014. [Online]. Available: https://www.mdpi.com/1996-1073/7/4/2449/htmhttps://www.mdpi.com/1996-1073/7/4/2449

[31] M. Wen, E. Linde, S. Ropke, P. Mirchandani, and A. Larsen, "An adaptive large neighborhood search heuristic for the electric vehicle scheduling problem," *Computers & Operations Research*, vol. 76, pp. 73–83, 12 2016.

[32] O. Sassi, W. R. Cherif-Khettaf, and A. Oulamara, "Iterated tabu search for the mix fleet vehicle routing problem with heterogenous electric vehicles," *Advances in Intelligent Systems and Computing*, vol. 359, pp. 57–68, 2015. [Online]. Available: https://link.springer.com/chapter/10.1007/978-3-319-18161-5_6

[33] N. Qin, A. Gusrialdi, R. Paul Brooker, and A. T-Raissi, "Numerical analysis of electric bus fast charging strategies for demand charge reduction," *Transportation Research Part A: Policy and Practice*, vol. 94, pp. 386–396, 2016. [Online]. Available: https://www.sciencedirect.com/science/article/pii/S096585641630444X

[34] A. Jahic, M. Eskander, and D. Schulz, "Preemptive vs. non-preemptive charging schedule for large-scale electric bus depots," in *2019 IEEE PES Innovative Smart Grid Technologies Europe (ISGT-Europe)*. Institute of Electrical and Electronics Engineers Inc., 9 2019.

[35] O. Frendo, N. Gaertner, and H. Stuckenschmidt, "Open source algorithm for smart charging of electric vehicle fleets," *IEEE Transactions on Industrial Informatics*, vol. 17, pp. 6014–6022, 9 2021.

[36] P. Toth and D. Vigo, *Vehicle routing: problems, methods, and applications*. SIAM, 2014.

[37] Z. H. Ahmed, A. S. Hameed, and M. L. Mutar, "Hybrid genetic algorithms for the asymmetric distance-constrained vehicle routing problem," *Mathematical Problems in Engineering*, vol. 2022, 2022.

[38] H. Preis, S. Frank, and K. Nachtigall, "Energy-optimized routing of electric vehicles in urban delivery systems," in *Operations Research Proceedings 2012*, S. Helber, M. Breitner, D. Rösch, C. Schön, J.-M. Graf von der Schulenburg, P. Sibbertsen, M. Steinbach, S. Weber, and A. Wolter, Eds. Cham: Springer International Publishing, 2014, pp. 583–588.

[39] S. Ropke and D. Pisinger, "An adaptive large neighborhood search heuristic for the pickup and delivery problem with time windows," *Transportation Science*, vol. 40, no. 4, pp. 455–472, 2006. [Online]. Available: http://www.jstor.org/stable/25769321

[40] U. D. of Transportation. (2023) Electric bus basics. [Online]. Available: https://www.transportation.gov/urban-e-mobility-toolkit/e-mobility-basics/bus#:~:text=Larger%20batteries%20typical%20of%20BEBs,solutions%20available%20for%20transit%20vehicles.

[41] M. J. Hansen, "Techniques to overcome energy storage limitations in electric vehicles," Ph.D. dissertation, Utah State University, 5 2024. [Online]. Available: https://digitalcommons.usu.edu/etd2023/168

[42] R. Basso, B. Kulcsár, I. Sanchez-Diaz, and X. Qu, "Dynamic stochastic electric vehicle routing with safe reinforcement learning," *Transportation Research Part E: Logistics and Transportation Review*, vol. 157, p. 102496, 1 2022.

[43] G. You, "Sustainable vehicle routing problem on real-time roads: the restrictive inheritance-based heuristic algorithm," *Sustainable Cities and Society*, vol. 79, p. 103682, 4 2022.

[44] M. . Herrera, E. M. . Neroni, M. . Juan, A. A. . Faulin, J. Wikarek, M. Ammouriova, E. M. Herrera, M. Neroni, A. A. Juan, and J. Faulin, "Solving vehicle routing problems under uncertainty and in dynamic scenarios: From simheuristics to agile optimization," *Applied Sciences 2023, Vol. 13, Page 101*, vol. 13, p. 101, 12 2022. [Online]. Available: https://www.mdpi.com/2076-3417/13/1/101/htmhttps://www.mdpi.com/2076-3417/13/1/101

[45] F. Alesiani and N. Maslekar, "Optimization of charging stops for fleet of electric vehicles: A genetic approach," *IEEE Intelligent Transportation Systems Magazine*, vol. 6, no. 3, pp. 10–21, 2014.

[46] M. Schneider, A. Stenger, and D. Goeke, "The electric vehicle-routing problem with time windows and recharging stations," *Transportation Science*, vol. 48, no. 4, pp. 500–520, 2014. [Online]. Available: http://www.jstor.org/stable/43666939

[47] D. Pisinger and S. Ropke, "A general heuristic for vehicle routing problems," *Computers & Operations Research*, vol. 34, no. 8, pp. 2403–2435, 2007. [Online]. Available: https://www.sciencedirect.com/science/article/pii/S0305054805003023

[48] N. Tucker, B. Turan, and M. Alizadeh, "Online charge scheduling for electric vehicles in autonomous mobility on demand fleets," *2019 IEEE Intelligent Transportation Systems Conference, ITSC 2019*, pp. 226–231, 10 2019.

[49] J. Whitaker, G. Droge, M. Hansen, D. Mortensen, and J. Gunther, "A network flow approach to battery electric bus scheduling," *IEEE Transactions on Intelligent Transportation Systems*, vol. 24, no. 9, pp. 9098–9109, 2023.

[50] J. Whitaker, D. Redmond, G. Droge, and J. Gunther, "Scheduling battery-electric bus charging under stochasticity using a receding-horizon approach," *IEEE Transactions on Intelligent Transportation Systems*, 2024, Under Review.

[51] J. Whitaker and G. Droge, "Scheduling the charging of battery-electric vehicles under heterogeneous scheduling constraints," *IEEE Transactions on Intelligent Transportation Systems*, 2024, Under Review.

[52] H. L. Choi, L. Brunet, and J. P. How, "Consensus-based decentralized auctions for robust task allocation," *IEEE Transactions on Robotics*, vol. 25, pp. 912–926, 2009.

CURRICULUM VITAE

Justin Whitaker

Published Journal Articles

- Scheduling the Charging of Battery-Electric Vehicles under Heterogeneous Scheduling Constraints, Justin Whitaker, and Greg Droge, *IEEE Transactions on Intelligent Transportation Systems*, *Under Review.*
- Scheduling Battery-Electric Bus Charging Under Stochasticity Using a Receding-Horizon Approach, Justin Whitaker, Derek Redmond, Greg Droge, and Jacob Gunther, *IEEE Transactions on Intelligent Transportation Systems*, *Under Review.*
- Cost Minimization for charging Electric Bus Fleets, Daniel Mortensen, Jacob Gunther, Greg Droge, and Justin Whitaker, *World Electric Vehicle Journal*, vol. 14, 2023.
- A Network Flow Approach to Battery Electric Bus Scheduling, Justin Whitaker, Greg Droge, Matthew Hansen, Daniel Mortensen, and Jacob Gunther, *IEEE Transactions on Intelligent Transportation Systems*, vol. 24, pp. 9098-9109, 2023.

Published Conference Papers

- Differentially Flat Model Predictive Trajectory Tracking for Mobile Robots, Justin Whitaker, and Greg Droge, in *Proc. Intermountain Engineering, Technology, and Computing Conference (IETC)*, 2024.
- Optimal Path Smoothing while Maintaining a Region of Safe Operation, Justin Whitaker, and Greg Droge, in *Proc. American Control Conference (ACC)*, 2021.

- Global Localization of Ground Vehicles Using Self-Describing Fiducials Coupled with IMU Data, Justin Whitaker, Randall Christensen, and Greg Droge, in *Proc. IEEE/ION Position, Localization and Navigation Symposium (PLANS)*, 2020.

- Adaptive Control of Large-ScaleSoft Robot Manipulators With Unknown Payloads, Jonathan Terry, Justin Whitaker, Randal Beard, and Marc Killpack, in *Proc. Dynamic Systems and Control Conference (DSCC)*, 2019.